

Copyright

By

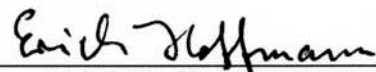
Santhana Gowri Thangavelu Devaraj

2009

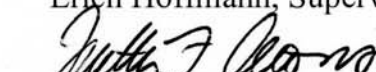
**The Dissertation Committee for Santhana Gowri Thangavelu Devaraj Certifies that  
this is the approved version of the following dissertation:**

**MOLECULAR INSIGHTS INTO MODULATION OF HOST INNATE  
IMMUNE RESPONSE BY VIRAL PROTEINS OF RNA VIRUSES  
*SARS-COV, HCV AND INFLUENZA VIRUS***

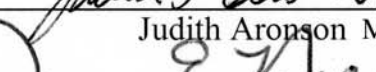
**Committee:**



Erich Hoffmann, Supervisor, Ph.D.



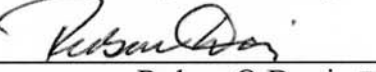
Judith Aronson M.D., Ph.D.



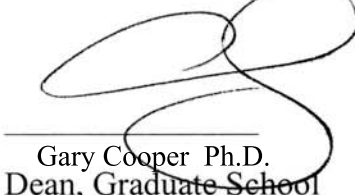
Joan Nichols Ph.D.



Janice Endsley Ph.D.



Ruben O Donis D.V.M., Ph.D.

  
Gary Cooper Ph.D.  
Dean, Graduate School

**Molecular insights into modulation of host innate immune response by  
viral proteins of RNA viruses *SARS-CoV*, *HCV* and *Influenza virus***

**By**

Santhana Gowri Thangavelu Devaraj M. S.

**Dissertation**

Presented to the Faculty of the Graduate School of  
The University of Texas Medical Branch  
In Partial Fulfillment  
Of the Requirements  
For the Degree of

**Doctor of Philosophy**

**The University of Texas Medical Branch  
Galveston, Texas  
August, 2009**

**To**

*My Family and Teachers*

*Where the mind is without fear and the head is held high;  
Where knowledge is free;  
Where words come out from the depth of truth;  
Where tireless striving stretches its arms towards perfection;  
Where the clear stream of reason has not lost its way into the dreary desert sand of dead habit;  
Into the heaven of freedom;  
Let me awake; Let me awake;*  
**(Gitanjali by Rabindranath Tagore)**

*There is a square; there is an oblong;  
The players take the square and place it upon the oblong;  
They place it very accurately; they make a perfect dwelling place;  
Very little is left outside; the structure is now visible;  
What is inchoate is here stated; we are not so various or so mean;  
We have made oblongs and stood them upon squares;  
This is our triumph; this is our consolation;*  
**(The Waves by Virginia Wolf)**

## **Acknowledgements**

First and foremost, I would like to thank Dr. Erich Hoffmann for being my mentor on a short notice. He welcomed me to his lab and allowed me to pursue the same line of research on influenza virus that I started with other positive strand RNA virus. He has been a constant source of encouragement during graduate studies at UTMB.

Special thanks to Dr. Judith Aronson and Dr. Janice Endsley for serving on my qualifer's committee and for all the critical inputs they have provided me for my research. Special thanks for Dr. Joan Nichols for sharing her knowledge on influenza virus and providing me *Influenza* strains for my research project in Dr. Hoffmann's lab. I thank Dr. Rubin O Donis from CDC for serving on my graduate committee and for his guidance.

I would like to thank Dr. Kui Li for his guidance during my SARS Corona virus and Hepatitis C virus projects. I thank Dr. Stanley Lemon for his interest and support in my research work. I thank Dr. Andres Oberhauser for help and support.

I would like to thank Dr. Robert Davey for his great help in resolving issues during troubled times. Thanks are due to Drs. Rolf König, Thomas Hughes, Gary Cooper and Dorian Coppenhaver. Special thanks to ever welcoming and friendly, Martha Lewis our program coordinator and to all graduate school staff for their help during my school days.

I would like to thank my best friends Drs. David McGivern, Krishna Naryanan, Huang Chen, Kumari Lokugamage for making 4<sup>th</sup> floor MRB such a fun filled, wonderful place to work and for all their help and encouragement during my experiments. I would like to thank my fellow graduate students and friends for the useful discussions at times.

I would like to thank Dr. Lokesh Rao, for his constant encouragement, support and keen interest in my research and for being a patient listener to my everyday success and failures as student. Finally, I would like to thank my parents who have always encouraged me in all my endeavors. Of course, last but not least my special thanks and love to Pinto who always cheers me on all occasions.

**Molecular insights into modulation of host innate immune response by  
viral proteins of RNA viruses *SARS-CoV*, *HCV* and *Influenza virus***

Publication No. \_\_\_\_\_

Santhana Gowri Thangavelu Devaraj, Ph.D.

The University of Texas Medical Branch Graduate School of Biomedical Sciences, 2009

Supervisor: Erich Hoffmann

One of the first and fast line of defense launched by mammalian hosts to counter virus infection is production of type I interferon (IFN), an innate immune response that generates antiviral state to prevent virus replication and spread by expressing several IFN-stimulated genes. Type I interferon response depends on a set of germ-line encoded receptors called pattern recognition receptors (PRRs) that initiate antiviral signaling upon recognizing distinct pathogen associated molecular patterns (PAMPs). TLR3, RIG-I and MDA5, trigger complex intertwined signaling pathways in response to viral dsRNA leading to the activation of interferon regulatory transcription factors IRF3, IRF7 and NF- $\kappa$ B. These transcription factors mediate inflammatory process to clear virus infection. Viruses can evade host antiviral defenses by using several strategies. SARS coronavirus (SARS-CoV), a highly contagious causative agent of severe acute respiratory syndrome does not induce interferon response suggesting an unknown immune evasive mechanism. My experiments demonstrate that papain-like protease (PLpro) encoded by SARS-CoV is a potent interferon antagonist that functions independent of its protease activity. PLpro directly interacts with IRF-3 preventing its phosphorylation, dimerization, nuclear translocation and thus inhibits type I interferon response triggered by TLR3/RIG-I pathways. Hepatitis C virus is a major blood borne pathogen responsible for 100,000 deaths worldwide annually due to chronic liver cirrhosis. In cell culture normal human hepatocytes are not permissive to HCV replication due to intact TLR3/RIG-I/MDA5 antiviral signaling pathways. However, human hepatoma cells defective in antiviral signal pathways are found to permit HCV replication. My experiments involving reconstitution of functional TLR3 signaling pathways in human hepatoma cells demonstrate that TLR3 plays a major role in HCV cellular permissiveness. Finally, my studies with influenza virus NS1 protein demonstrate that NS1 antagonizes the IFN response by blocking RIG-I activation in a strain specific manner. In conclusion, I have made an attempt to understand the complex antiviral signaling pathways at the cellular level in context to three distinct single strand RNA viruses namely, SARS-CoV, HCV and Influenza virus. Though, these viruses are detected by the same set of PRRs to trigger antiviral signaling, the mechanism by which they evade antiviral response appears to be distinct.

## Table of Contents

List of Abbreviations .....	xii
List of Tables .....	xv
List of Figures.....	xv
<b>CHAPTER 1: INNATE IMMUNE RESPONSE TO VIRUS INFECTION ...</b>	<b>1</b>
1.1 Introduction.....	1
1.2 Pattern recognition receptors .....	2
1.2.1 <i>Pathogen associated molecular patterns</i> .....	2
1.2.2 <i>RIG-I like receptors (RLRs)</i> .....	3
1.2.3 <i>Toll-like receptors (TLRs)</i> .....	4
1.2.4 <i>NOD-like receptors (NLRs)</i> .....	5
1.2.5 <i>RNase L, PKR and other cytosolic proteins in induction of interferon response</i> .....	6
1.3 Retinoic acid inducible gene-I (RIG-I).....	7
1.4 Toll-like receptor-3 (TLR3) .....	10
1.5 Pattern recognition receptor initiated antiviral signaling.....	12
1.6 Viral evasion of host antiviral defenses.....	15
<b>CHAPTER 2: SARS CORONAVIRUS .....</b>	<b>17</b>
2.1 Coronaviridae.....	17
2.1.2 <i>Virus architecture and entry</i> .....	19
2.1.3 <i>Genome organization</i> .....	21
2.1.4 <i>Viral gene products, gene expression strategy and virus replication</i> .....	22
2.1.5 <i>Virus assembly</i> .....	23
2.2 Severe Acute respiratory syndrome corona virus (SARS-CoV)...	23
2.2.1 <i>Introduction</i> .....	23
2.2.2 <i>Virus entry and pathogenesis</i> .....	24
2.2.3 <i>Genome organization and expression of functional gene products</i> .....	25

2.2.4	<i>Polyprotein processing</i> .....	26
2.2.5	<i>Papain like protease (PLpro)</i> .....	27
2.2.6	<i>Pathogenesis of SARS-CoV</i> .....	29
<b>CHAPTER 3: SARS-COV EVADES INNATE IMMUNE DEFENSES BY PLPRO MEDIATED DISRUPTION OF IRF3 ACTIVATION STEP OF ANTIVIRAL SIGNALING.....</b>		31
3.1	<b>Introduction.....</b>	31
3.1	<b>Experimental materials and methods .....</b>	34
3.2.1	<i>Plasmids.....</i>	34
3.2.1a	<i>Construction of WT and mutant PLpro-sol and PLpro-TM</i> .....	34
3.2.1b	<i>Construction of WT and mutant of pTREBla-PLpro-TM...</i>	35
3.2.2	<i>Cell lines .....</i>	36
3.2.2a	<i>Generation of stable HeLa cell line with conditional expression of SARS-CoV PLpro TM .....</i>	36
3.2.3	<i>Sendai virus infection .....</i>	37
3.2.4	<i>PolyI:C treatment.....</i>	37
3.2.5	<i>Transfection and Reporter gene assays.....</i>	38
3.2.6	<i>Indirect Immunofluorescence staining (immunostaining) ...</i>	38
3.2.7	<i>Assay for IRF3 nuclear translocation.....</i>	39
3.2.8	<i>Reverse transcription PCR (RT-PCR).....</i>	39
3.2.9	<i>Immunoblot Analysis .....</i>	41
3.2.10.	<i>Native Polyacrylamide Gel Electrophoresis (PAGE) .....</i>	42
3.2.11	<i>Immunoprecipitation .....</i>	42
3.2.12	<i>Okadaic acid treatment (Phosphatase inhibitor) .....</i>	43
3.3	<b>Results .....</b>	44
3.3.1	<i>SARS-CoV PLpro inhibits TLR3 and RIG-I induced activation of IFN-<math>\beta</math> .....</i>	44
3.3.2	<i>Inhibition of PRR stimulated IFN-<math>\beta</math> promoter activity is independent of PLpro's protease activity .....</i>	45
3.3.3	<i>PLpro inhibits transcription from IFN-<math>\beta</math> promoter by affecting the activation of transcription factor of IRF3.....</i>	47

3.3.4	<i>Conditional expression of PLpro in HeLa-Tetoff cell modulate ISG56</i> .....	49
3.3.5	<i>SARS-CoV PLpro inhibits IRF3 activation by interfering with its phosphorylation, dimerization and nuclear translocation</i> .....	51
3.3.6	<i>SARS-CoV PLpro physically interacts with IRF3</i> .....	54
3.4	Discussion .....	57
<b>CHAPTER 4: HEPATITIS C VIRUS</b> .....		61
4.1	Flaviviridae .....	61
4.1.1	<i>Classification</i> .....	61
4.2	Hepatitis C virus .....	62
4.2.1	<i>Genome organization, expression strategies and virus life cycle</i> .....	62
4.2.2	<i>HCV and Innate Immune response</i> .....	65
4.2.3	<i>HCV and its Cellular permissiveness</i> .....	67
<b>CHAPTER 5: ANTIVIRAL SIGNALING BY TLR3 RECEPTOR IS COMPARTMENTALIZED TO MEMBRANE ASSOCIATED HCV REPLICATION COMPLEX</b> .....		70
5.1	Introduction.....	70
5.2	Materials and Methods.....	72
5.2.1	<i>Cell lines</i> .....	72
5.2.2	<i>HCV virus</i> .....	72
5.2.4	<i>Determination of HCV titer by counting immunofoci</i> .....	73
5.2.5	<i>Plasmid constructs</i> .....	74
5.2.6	<i>Retrovirus mediated TLR3 expression</i> .....	74
5.2.7	<i>Poly(I:C) and Sendai virus treatments</i> .....	75
5.2.8	<i>Renilla luciferase assay to monitor HCV RNA replication</i> ... .....	75
5.2.9	<i>Confocal Immunofluorescence microscopy</i> .....	76
5.2.10	<i>Sub-cellular fractionation of HCV replication complex by sucrose density gradient ultracentrifugation</i> .....	77
5.2.11	<i>Immunoblot analysis</i> .....	77
5.2.12	<i>Immunoprecipitation</i> .....	78

<b>5.3 Results .....</b>	<b>79</b>
<b>5.3.1 Functional reconstitution of RIG-I and TLR3 in human hepatoma cell lines.....</b>	<b>79</b>
<b>5.3.2 RIG-I reconstitution limits HCV replication in Huh 7.5 cells</b>	<b>81</b>
<b>5.3.3 TLR3 limits HCV replication in Huh7 and Huh7.5 cells.....</b>	<b>82</b>
<b>5.3.4 TLR3 co localizes with HCV virus replication complex.....</b>	<b>85</b>
<b>5.3.5 TLR3 localizes to membrane fractions containing HCV replication protein .....</b>	<b>87</b>
<b>5.1 Discussion .....</b>	<b>90</b>
<b>CHAPTER 6: INFLUENZA VIRUS EVADES INNATE IMMUNE DEFENSES BY NS1 MEDIATED ANTAGONISM INVOLVING RIG-I INHIBITION .....</b>	<b>92</b>
<b>6.1 Orthomyxoviridae.....</b>	<b>92</b>
<b>6.1.1 Classification.....</b>	<b>92</b>
<b>6.1.2 Virus architecture, entry, genome organization, virus replication and pathogenesis .....</b>	<b>94</b>
<b>6.1.3 Non-structural protein (NS1) of influenza virus .....</b>	<b>98</b>
<b>6.1 Materials and Methods.....</b>	<b>101</b>
<b>6.2.1 Plasmids.....</b>	<b>101</b>
<b>6.2.2 Construction of mammalian expression plasmids expressing NS1 .....</b>	<b>101</b>
<b>6.2.3 Cloning of A/Brisbane/59/2007/H1N1, A/California/04/2009/H1N1, A/Brisbane/10/2007/H3N2 and B/Florida/04/2006 .....</b>	<b>102</b>
<b>6.2.4 Cell lines .....</b>	<b>104</b>
<b>6.2.5 Sendai virus infection .....</b>	<b>104</b>
<b>6.2.6 PolyI:C treatment.....</b>	<b>104</b>
<b>6.2.7 Transfection and Reporter gene assays.....</b>	<b>105</b>
<b>6.2.8 Rescue of PR8 strain of H1N1 A/Puerto Rico/8/34 by reverse genetics. .....</b>	<b>105</b>
<b>6.2.9 Plaque assay to determine the virus titers .....</b>	<b>106</b>
<b>6.3 Results .....</b>	<b>107</b>

<i>6.3.1 Influenza NS1 inhibits RIG-I but not TLR3 induced activation of IFN-<math>\beta</math></i> .....	107
<i>6.3.2 Influenza NS1 regulates RIG-I induced interferon blockade in strain specific manner</i> .....	110
<i>6.3.3 Cloning of A/Brisbane/59/2007/H1N1, A/California/04/2009/H1N1, A/Brisbane/10/2007/H3N2 and B/Florida/04/2006 and Rescue of PR8 strain</i> .....	112
<b>6.4 Discussion</b> .....	114
<b>CHAPTER 7: CONCLUSIONS AND FUTURE DIRECTIONS</b> .....	120
<b>REFERENCES</b> .....	124
<b>BIOSKETCH (VITA)</b> .....	151

## List of Abbreviations

-ve strand	.....	Negative strand
+ve strand	.....	Positive strand
3CLP	.....	3C-like protease
ACE2	.....	Angiotensin-converting enzyme 2
AIBV	.....	Avian infectious bronchitis virus
ATPase	.....	Adenosine triphosphatase
BDV	.....	Borna disease virus
BIRs	.....	Baculovirus inhibitor repeats
BSA	.....	Bovine serum albumin
BVDV	.....	Bovine viral diarrheal virus
CARD	.....	Caspase recruitment domain
CARDIF	.....	CARD adaptor-inducing interferon-β
CBP	.....	CREB binding protein
CCHFV	.....	Crimean-congo hemorrhagic fever virus
CSFV	.....	Classical swine fever virus
CTD	.....	C-terminal domain
DAI	.....	DNA-dependent activator of IFN-regulatory factors
dsRNA	.....	Double-stranded RNA
DUB	.....	Deubiquitination
E	.....	Envelope protein
ECD	.....	Ectodomain
eIF2- α	.....	Eukaryotic initiation factor 2-α
EMCV	.....	Encephalomyocarditis virus
ER	.....	Endoplasmic reticulum
FLU	.....	Influenza
HA	.....	Hemagglutinin
HAU	.....	Hemagglutinin units
HAUSP	.....	Herpesvirus associated ubiquitin-specific protease
HCC	.....	Hepatocellular carcinoma
HCoV	.....	Human corona virus
HCV	.....	Hepatitis C virus
HE	.....	Hemagglutinin-Esterase glycoprotein
HEK 293, 293T, 293TLR-3	..	Human embryonic kidney cells 293, 293T, 293WT TLR-3
HSV1	.....	Herpes simplex virus1
HSV2	.....	Herpes simplex virus2
HTNV	.....	Hantaan virus
Huh7	.....	Human hepatoma cell line
IFN- β	.....	Interferon β
IFNs	.....	Interferons
IPS-1	.....	IFN promoter-stimulator 1
IRES	.....	Internal ribosome entry site

IRF-3	Interferon regulatory factor3
ISGs	Interferon stimulatory genes
JEV	Japanese encephalitis virus
JFH1	Japanese fulminant hepatitis
LGP-2	Laboratory of genetics and physiology-2
LPS	Lipopolysaccharides
LRRs	Leucine rich repeats
M	Matrix
MAPK	Mitogen-activated protein kinase
MAVS	Mitochondrial antiviral signaling
MCMV	Murine cytomegalovirus
MDA5	Melanoma differentiation-associated gene 5
MDCK	Madin-Darby canine kidney cells
MHV	Murine hepatitis virus
mRNA	Messenger RNA
N	Nucleocapsids glycoprotein
NA	Neuraminidase
NCR	Non-coding region
NDV	Newcastle disease virus
NF- κB	Nuclear factor κB
NLRs	Nod-like receptors
NS	Non-structural
NSPs	Non-structural proteins
OA	Okadaic acid
ORFs	Open reading frames
PA	Polymerase acidic
PAMPs	Pathogen associated molecular patterns
PB1	Polymerase basic 1
PB2	Polymerase basic 2
PDCs	Plasmacytoid dendritic cells
PEG	Polyethylene glycol
PFU	Plaque forming units
PKR	Protein kinase R
PLP	Papain-like protease
PLpro	Papain like protease
PLpro sol	Papain like protease soluble
PLpro TM	Papain like protease transmembrane
PP	Polyprotein
PRRs	Pattern recognition receptors
PYD	Pyrin domain
R genes	Resistance genes
RD	Repressor domain
RIG-I	Retinoic acid inducible gene I

RLRs	Retinoic acid inducible gene I (RIG-I)-like receptors
RSV	Respiratory syncytial virus
RT-PCR	Reverse transcriptase polymerase chain reaction
S protein	Spike glycoprotein
SARS-CoV	Severe acute respiratory syndrome virus
SeV	Sendai virus
sgRNAs	Sub-genomic RNAs
ssDNA	Single-stranded DNA
ssRNA	Single-stranded RNA
TBEV	Tick-borne encephalitis virus
Tet	Tetracycline
TGEV	Porcine transmissible gastroenteritis virus
TIR domain	Toll/IL-1 receptor homology domain
TLR1	Toll-like receptor 1
TLR2	Toll-like receptor 2
TLR3	Toll-like receptor 3
TLR4	Toll-like receptor 4
TLR5	Toll-like receptor 5
TLR6	Toll-like receptor 6
TLR7	Toll-like receptor 7
TLR8	Toll-like receptor 8
TLR9	Toll-like receptor 9
TLRs	Toll-like receptors
TM	Trans-membrane domain
Ub	Ubiquitination
UTR	Untranslated region
VISA	Virus- induced signaling adaptor
VSV	Vesicular stomatitis virus
WNV	West Nile virus
WT	Wild type
YFV	Yellow fever virus
ZBP1	Z-DNA-binding protein 1

## List of Tables

<b>Table 2.1 List of cellular receptors used by coronaviruses to gain cellular entry ....</b>	<b>21</b>
<b>Table 3.1 List of primers used for Semi-quantitative RT-PCR.....</b>	<b>40</b>
<b>Table 6.1 Primers used for NS1 PCR amplification .....</b>	<b>102</b>
<b>Table 6.2 Primers used for RT-PCR amplification of influenza 8 segments.....</b>	<b>103</b>

## List of Figures

<b>Figure 1.1 Schematic depiction of RIG-I .....</b>	<b>8</b>
<b>Figure 1.2 Model showing dsRNA induced activation of RIG-I.....</b>	<b>9</b>
<b>Figure 1.3 Schematic depiction of Toll-like receptor.....</b>	<b>11</b>
<b>Figure 1.4 Schematic representations of signaling pathways initiated by PRRs RIG-I/MDA5/TLR3 leading to the activation of IRF3 and .....</b>	<b>14</b>
<b>Figure 2.1 Classification of Coronaviridae .....</b>	<b>18</b>
<b>Figure 2.2 Proposed model of Corona virus.....</b>	<b>19</b>
<b>Figure 2.3 Genome organization of SARS-CoV .....</b>	<b>26</b>
<b>Figure 2.4 Schematic representation of SARS-CoV PP1a and PP1ab polyprotein processing.....</b>	<b>27</b>
<b>Figure 3.1 SARS-CoV PLpro domain inhibits activation of IFN-<math>\beta</math> promoter stimulated by TLR3 or RIG-I pathways.....</b>	<b>44</b>
<b>Figure 3.2 Inhibition of PRR stimulated IFN-<math>\beta</math> promoter is independent of PLpro protease activity. ....</b>	<b>46</b>
<b>Figure 3.3 PLpro inhibits transcription from IFN-<math>\beta</math> promoter by affecting transcription factor IRF3.....</b>	<b>48</b>
<b>Figure 3.4 Conditional expression of PLpro in HeLa-Tetoff cells modulate ISG56.</b>	<b>50</b>
<b>Figure 3.6 SARS-CoV PLpro interacts with IRF3 .....</b>	<b>55</b>
<b>Figure 4.1 Classification of Flaviviridae .....</b>	<b>61</b>
<b>Figure 4.2 Schematic representation of HCV life cycle.....</b>	<b>63</b>
<b>Figure 4.3 Schematic representation of HCV genome organization.....</b>	<b>64</b>
<b>Figure 4.2 HCV NS3/4A protease inhibits host innate immune response. HCV NS3/4A protease cleaves the adapter molecules MAVS and TRIF of RIG-I and TLR3 antiviral signaling pathways. ....</b>	<b>67</b>
<b>Figure 5.1 Interferon responses in Huh7 and Huh7.5 human hepatoma cells .....</b>	<b>80</b>
<b>Figure 5.2 RIG-I inhibit HCV propagation in Huh7.5 human hepatoma cells.....</b>	<b>81</b>
<b>Figure 5.3 TLR3 inhibits HCV replication.....</b>	<b>83</b>
<b>Figure 5.4 TLR3 and its mutants H539E, N541A and P554S co localize with HCV dsRNA and NS5B .....</b>	<b>85</b>

<b>Figure 5.5 TLR3 redistributes to membrane compartments containing HCV replication complex.....</b>	88
<b>Figure 6.1 Schematic representation of influenza virion.....</b>	94
<b>Figure 6.2 Schematic representation of genomic segments of influenza A (top) and influenza B (bottom)......</b>	95
<b>Figure 6.3 Schematic representation of influenza virus life cycle.....</b>	97
<b>Figure 6.4 Schematic representations of NS1 protein and its cellular interactors....</b>	99
<b>Figure 6.5 Schematic representation of virus rescue using influenza reverse genetics system .....</b>	106
<b>Figure 6.6 Clustal W Alignment of NS1 proteins of Influenza A virus strains tested for NS1 antagonism in reporter assays.....</b>	108
<b>Figure 6.7 NS1 protein of influenza inhibits activation of IFN-<math>\beta</math> promoter stimulated by RIG-I pathway but not TLR3.....</b>	109
<b>Figure 6.8 NS1 protein of influenza regulates activation of IFN-<math>\beta</math> and NF-<math>\kappa</math>B promoter by RIG-I pathway.....</b>	111
<b>Figure 6.9 Virus rescue and plaque formation of PR8 strain.....</b>	113
<b>Figure 6.10 Schematic representation of NS1 protein involvement with PRR RIG-I.....</b>	115

## **CHAPTER 1: INNATE IMMUNE RESPONSE TO VIRUS INFECTION**

### **1.1 INTRODUCTION**

Every organism from the single-celled amoeba to the complex human being is always under threat from parasitic organisms like viruses and bacteria. To defend themselves, they have evolved complex strategies. For example, in bacteria, restriction-modification system is a simple mechanism by which bacteria counter invading nucleic acids. Plants defend themselves from harmful pathogens by several strategies that include systemic signaling mediated by salicylic acid, localized hypersensitive response leading to programmed cell death, and dsRNA mediated pathogen gene silencing. Mammals are equipped with a plethora of complex defense mechanisms that are collectively known as the immune system (Hoffmann et al., 1999). The immune system can be divided into the evolutionarily conserved rapidly responding innate immune system, and the highly specific, but temporarily delayed adaptive immune system. Though they are functionally independent, a great deal of crosstalk has been observed between the two systems at several levels with the recent discovery of toll and nod-like receptors (Akira and Takeda, 2004; Theofilopoulos et al., 2005). However the most immediate defense response to a virus infection is production of type I interferon, an innate immune mechanism which not only puts a check on the virus infection and spread, but also stimulates the generation of long lasting adaptive immune response. In sharp contrast to the adaptive immunity,

mediated by antibodies and B-cell and T-cell gene rearrangements, innate immunity depends on a set of germ-line encoded receptors expressed on a large variety of immune cells. The receptors, called pattern recognition receptors (PRRs) are involved in the recognition of conserved pathogen associated molecular patterns (PAMPs) that are distinct from self and are specific for a given class of microbes (Medzhitov and Janeway, 2000a; Medzhitov and Janeway, 2000b; Medzhitov and Janeway, 2000c; Medzhitov and Janeway, 2000d).

## 1.2 PATTERN RECOGNITION RECEPTORS

### 1.2.1 *Pathogen associated molecular patterns*

Pathogen associated molecular patterns (PAMPs) are specific molecular signatures of invading microbial pathogens that are recognized by pattern recognition receptors (PRRs). PAMPS include dsRNA, ssRNA, DNA or un-methylated DNA of microbial origin, lipopolysaccharides (LPS) and flagellin from bacterial origin (Ahmad-Nejad et al., 2002; Aliprantis et al., 1999; Hayashi et al., 2001; Latz et al., 2002; Medzhitov and Janeway, 1997; Nishiya and DeFranco, 2004; Poltorak et al., 1998; Schwandner et al., 1999; Takeuchi et al., 1999a). The PAMP recognizing PRRs fall into three main classes: Toll-like receptors (TLRs), Nod-like receptors (NLRs) and retinoic acid inducible gene I (RIG-I)-like receptors (RLRs) segregated to various cellular compartments set to function by signaling through different adaptors to activate the innate immune response.

### *1.2.2 RIG-I like receptors (RLRs)*

At present, three RLR proteins are known to recognize viral signatures in the cytosol of host cells. They are RIG-I (also known as DDX58), melanoma differentiation-associated gene 5 (MDA5) and laboratory of genetics and physiology-2 (LGP-2) (Takeuchi and Akira, 2007). RIG-I and MDA5 contain a DExD/H box helicase domain that is suggested to bind dsRNA and a pair of N-terminal caspase recruitment (CARD) domains involved in signaling (Kang et al., 2002; Kovacsics et al., 2002; Saito et al., 2007; Yoneyama et al., 2004). LGP-2 has a similar helicase domain, but lacks a CARD domain, and is suggested to function as a negative regulator (Rothenfusser et al., 2005; Venkataraman et al., 2007). Mouse knockout studies carried out to analyze *in vivo* roles of RIG-I and MDA5 reveal that RIG-I, but not MDA5, is required for activating the interferon response in conventional dendritic cells and embryonic fibroblasts against positive strand RNA viruses like Japanese encephalitis, West Nile, Dengue and Hepatitis C virus (Kato et al., 2005; Kato et al., 2006; Loo et al., 2008; Sumpter et al., 2005) and few negative strand RNA viruses such as Influenza, VSV, Sendai and Newcastle disease. However, antiviral signaling is not affected in plasmacytoid dendritic cells of RIG-I knockout mice where TLR (TLR3, TLR7, TLR9) initiated signaling through MyD88 seems to play a prominent role. MDA5 detects picornaviruses such as Encephalomyocarditis virus (EMCV), Mengo virus and Theilers Virus (Gitlin et al., 2006; Kato et al., 2006) as well as Calici viruses (McCartney et al., 2008). These viruses contain a 5'-VPg instead of 5'-triphosphate and make large amounts of dsRNA during

replication. The antiviral response initiated against paramyxovirus RNA by MDA5 is severely suppressed by viral V protein as it is specific inhibitor of MDA5(Andrejeva et al., 2004; Childs et al., 2009; Komatsu et al., 2007).

### 1.2.3 *Toll-like receptors (TLRs)*

Toll-like receptors are a family of evolutionarily conserved type I transmembrane proteins that specifically recognize a wide variety of PAMPs. There are 10 and 13 TLRs in humans and mice, respectively. They are expressed in the membranes of intracellular compartments as well as on the cell surface of several immune and non-immune cells. TLR1, TLR2, TLR4, TLR5 and TLR6 are present in immune cells and recognize bacterial PAMPs such as LPS and flagellin. (Ahmad-Nejad et al., 2002; Aliprantis et al., 1999; Hayashi et al., 2001; Latz et al., 2002; Medzhitov and Janeway, 1997; Nishiya and DeFranco, 2004; Poltorak et al., 1998; Schwandner et al., 1999; Takeuchi et al., 1999a; Takeuchi et al., 1999b). TLR3, TLR7, TLR8 and TLR9 are expressed in endoplasmic reticulum (ER), endosome and lysosomes in plasmacytoid dendritic cells (PDCs) and B cells. TLR7/9 have high sequence identity with TLR8 to a lesser extent to TLR3 (Ahmad-Nejad et al., 2002; Alexopoulou et al., 2001; Heil et al., 2003; Heil et al., 2004; Hemmi et al., 2002; Hemmi et al., 2000; Jurk et al., 2002; Latz et al., 2004a; Latz et al., 2004b; Leifer et al., 2004; Matsumoto et al., 2003; Nishiya and DeFranco, 2004; Nishiya et al., 2005). TLR3 and TLR7/8/and TLR9 are nucleotide-sensing receptors that detect dsRNA, ssRNA and un-methylated DNA respectively (Ahmad-Nejad et al., 2002; Alexopoulou et al., 2001; Heil et al., 2003; Heil et al., 2004; Hemmi et al., 2002; Hemmi

et al., 2000; Jurk et al., 2002; Latz et al., 2004a; Latz et al., 2004b; Leifer et al., 2004; Matsumoto et al., 2003; Nishiya and DeFranco, 2004; Nishiya et al., 2005; Roach et al., 2005; Wagner, 2004). TLR7 recognizes guanosine- and uridine-rich ssRNA present in viruses such as influenza and VSV (Diebold et al., 2004; Heil et al., 2004; Lund et al., 2004). TLR7/8 also responds to the synthetic imidazoquinoline compounds imiquimod and R-848 (Heil et al., 2003; Hemmi et al., 2002; Jurk et al., 2002). TLR9 recognizes unmethylated A-type CpG DNA and B-type CpG DNA of bacterial and viral origin like herpes simplex virus 1 (HSV1), HSV2 and murine cytomegalovirus (MCMV) (Hemmi et al., 2000; Krug et al., 2004a; Krug et al., 2004b; Lund et al., 2003). Structurally, TLRs have an ectodomain containing leucine-rich repeats involved in PAMP recognition, a single-pass TM domain for membrane anchorage and a cytoplasmic TIR domain responsible for signaling transduction. The TIR domain of TLRs interact with TIR domain-containing adapter proteins such as MyD88 (TRIF in case of TLR3) initiating subsequent signaling cascades resulting in the induction of pro-inflammatory cytokines and type I IFNs (Subramaniam et al., 2004; Yamamoto and Akira, 2004; Yamamoto et al., 2004).

#### *1.2.4 NOD-like receptors (NLRs)*

Nucleotide oligomerization domain (NOD)-like receptors (NLRs), first identified in plants as disease resistance (R genes) against microbial and parasitic pathogens (Chisholm et al., 2006; Hibino et al., 2006; Jones and Dangl, 2006) are evolutionarily conserved and thought to play an important role in host defense. There are 23 known

NLRs in humans and 34 in mice expressed typically in the cytosol of macrophages and neutrophils. NLRs are basically scaffolding proteins comprising of multiple functional domains. The N-terminal domain consists variable effectors region necessary for downstream signaling, consisting either of a caspase recruitment domain (CARD) or a pyrin domain (PYD), or an acidic domain, or baculovirus inhibitor repeats (BIRs) followed by a central NOD domain. NOD domains are related to the oligomerization module found in AAA+ family of adenosine triphosphatases (ATP-ases) and are necessary for NLR activation. At the C-terminus of the NLRs contain leucine-rich repeats (LRRs) that detect PAMPs (Hanson and Whiteheart, 2005). NLRs are subdivided into several families based on the N-terminal effector domain (Ting et al., 2008). CARD and PYD domains are related to death domain-fold superfamily, involved in apoptosis and inflammation mediated by homophilic interactions with other CARD and PYD containing proteins. NLRs with a BIR effector domain originally regulate apoptosis similarly to inhibitor of apoptosis proteins (IAPs). Nod1 and Nod2, upon sensing microbes, trigger signaling, resulting in activation of nuclear factor  $\kappa$ B (NF- $\kappa$ B) and MAP kinase pathway. This leads to transcriptional upregulation of a variety of proinflammatory cytokines and anti-microbial peptides (Abbott et al., 2004).

#### *1.2.5 RNase L, PKR and other cytosolic proteins in induction of interferon response*

RNase L and protein kinase R (PKR) are among the other known proteins that are involved in the innate immune response. PKR is activated in the presence of dsRNA by homodimerization to generate kinase activity leading to phosphorylation of eukaryotic

initiation factor 2- $\alpha$  (eIF2- $\alpha$ ) that inhibits translation of viral genes (Garcia et al., 2006). Small quantities of interferon, produced from antiviral responses, is capable of inducing the expression of 2'5'oligoadenylate synthetase that generates 2'5' oligoadenylate (2,5'-A,  $\text{pppA}(2'\text{p}5'\text{A})n$  where  $n=1$  to 10) from ATP. 2',5'-A activates RNase L leading to degradation of mRNA in cells shutting off protein translation and generating small dsRNAs that may have a positive feedback on interferon response. Therefore, an intricate crosstalk exists between PRRs, RNase L and PKR in response to type I IFNs, triggering a robust antiviral state in the cell in response to virus infection. There are additional cytosolic proteins like DNA-dependent activator of IFN-regulatory factors (DAI), Z-DNA-binding protein 1 (ZBP1), and DLM-1 that are thought to play a role in activating innate immune response triggered by viral DNA in the cytosol (Takaoka et al., 2007; Wang et al., 2008). A “Inflammasome” complex is proposed to recognizes viral DNA to activate caspase-1 and induce maturation of pro-IL-1 $\beta$  in macrophages (Muruve et al., 2008). It is composed of proteins containing Nacht-like, LRR, and PYD3 domains (NALP3). Innate immune response to DNA viruses was shown to be compromised in NALP3 knock out mice (Muruve et al., 2008).

### **1.3 RETINOIC ACID INDUCIBLE GENE-I (RIG-I)**

RIG-I is ~101 kDa protein, that functions in the innate immune response with N-terminal CARD domains, a central helicase domain followed by a repressor domain (RD) and a C-terminal domain (CTD) that binds PAMPs (Figure 1.1).

RIG-I preferentially recognizes polyadenylated and polyuridylated RNAs, and RNAs with 5' terminal triphosphates. Host mRNA present in the cytosol are spared from RIG-I recognition because of either the cap structure or nuclear modification of 5' triphosphates (Andrejeva et al., 2004; Fredericksen et al., 2008; Loo et al., 2008; Roth-Cross et al., 2008).



**Figure 1.1 Schematic depiction of RIG-I.** RIG-I is a cytoplasmic helicase containing two N-terminal CARD domains and a dead box helicase domain, at the C-terminus it has repressor domain and a cytoplasmic tail domain.

RIG-I knock out mice are embryonically lethal due to liver degeneration suggesting that RIG-I may play several other important functions apart from its role in innate immunity (Kato et al., 2005). However, conditional knock out strains develop colitis due to down regulation of a G protein subunit involved in T-cell activation (Wang et al., 2007). *In vitro* binding assays reveal RIG-I interact with 5'-ppp-ssRNA, dsRNA and polyI:C in an ATP independent manner, however helicase activity requires ATP and can only use a dsRNA substrate with a 3' overhang but not a blunt end or a 5' overhang. Cell based assays indicate that dsRNA that is resistant to RIG-I unwinding forms a stable complex leading to efficient interferon production while those dsRNAs susceptible to unwinding fail to make the stable complex necessary for interferon signaling. Helicase activity may be another mechanism by which RIG-I is able to distinguish between self and non-self RNAs (Takahasi et al., 2008) as cytosolic t-RNA have a 3' overhang. A 17 kDa core

domain was spared from trypsin digestion in the presence of a RNA substrate which is referred as CTD. CTD was found structurally similar to MSS4, a GDP/GTP exchange factor of Rab-GTPase having a zinc ion for stabilizing the structure. Further structural analysis revealed a cup shaped structure with a cleft lined with positively charged amino acids on the concave side responsible for RNA binding while the opposite convex side is lined with acidic amino acids (Cui et al., 2008; Takahasi et al., 2008) whose functional significance is not clear.

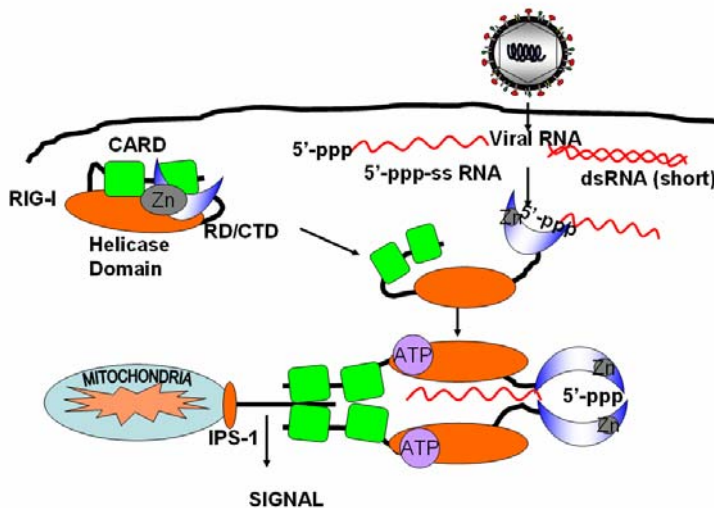


**Figure 1.2 Model showing dsRNA induced activation of RIG-I** (modified from (Yoneyama and Fujita, 2009)) In the absence of viral infection, RIG-I remains latent due to intramolecular interaction between C-terminal repressor domain (RD) and caspase recruitment domain (CARD) or linker region of helicase domain. RIG-I selectively detects non-self viral RNAs via basic cleft-like structure at C-terminal domain (CTD) and induces ATP-dependent Conformational change to form a dimer or oligomer, which allows CARD domains to interact with the downstream adapter protein MAVS.

Two mechanisms are proposed to explain the molecular basis of RIG-I activation. According to (Cui et al., 2008) the repressor domain (RD) could mediate homodimerization upon binding to 5'ppp-RNA and this dimerization may induce ATPase

activity needed for conformational change leading to RIG-I activation (Figure 1.2). Another hypothesis speculates that CARD domains of RIG are masked by repressor domain to maintain an inactive state. Binding of viral RNA to the CTD activates an intrinsic ATPase that produces a conformational change exposing the N-terminal CARD domain available for interaction with downstream adaptor molecules (Yoneyama and Fujita, 2009).

#### **1.4 TOLL-LIKE RECEPTOR-3 (TLR3)**

TLR3, expressed in myeloid DCs, intestinal epithelial cells and fibroblasts (Kadowaki et al., 2001; Kumar et al., 2006; Kumar et al., 2004; Matsumoto et al., 2002; Tohyama et al., 2005) plays an important role in defense against RNA viruses like encephalomyocarditis virus (EMCV), respiratory syncytial virus (RSV), influenza A virus, West Nile virus, murine cytomegalo virus (MCMV) and Herpes simplex virus 1 (HSV1) a dsDNA virus (Hardarson et al., 2007; Le Goffic et al., 2007; Rudd et al., 2006; Tabeta et al., 2004; Wang et al., 2004; Zhang et al., 2007). It is also shown to elicit T-helper 2 (Th2) responses in airway epithelial cells against RSV infection (Rudd et al., 2005; Rudd et al., 2006). Structurally, TLR3 is a transmembrane protein of ~120kDa in size with a single membrane spanning region. TLR3 contains an extra cellular ectodomain (ECD) having ligand binding functionality and a cytoplasmic Toll/IL-1 receptor homology domain (TIR) that harbors signaling potential (Bell et al., 2005; Choe et al., 2005). The TLR3 ECD domain has a horse-shoe shaped architecture composed of 23 canonical and 2 irregular LRRs that cap the hydrophobic surface of N and C-terminus. The molecule

appears as solenoid having remarkable curvature with concave and convex surfaces. TLR3 ECD has 15 predicted N-linked glycosylation sites that are completely glycosylated when expressed in insect cells.

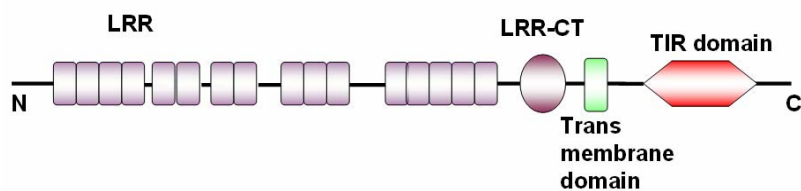


**Figure 1.3 Schematic depiction of Toll-like receptor.** TLR3 is a transmembrane protein of 120 kDa in size with a single membrane spanning region. It has an extra cellular domain which is important for ligand binding function and cytoplasmic TIR domain for signaling. TLR3 ECD structure has been solved by (Bell et al., 2006a; Bell et al., 2006b; Bell et al., 2005) has shown that it is a horse shoe shaped solenoid structure 23 canonical and 2 irregular leucine rich repeats. Signaling is initiated when two TIR domains come in close association due to TLR3 dimerization.

The glycosylation covers almost the entire concave and convex surface of the molecule except a lateral surface that is lined with several basic amino acid residues that are capable of associating with dsRNA. According to one of the proposed models of TLR3 activation, dsRNA binds to a glycan free lateral surface between two molecules to form a sandwich that brings cytosolic TIR domains in close proximity.

Signaling from TLR3 is initiated when two TIR domains come in close association due to TLR3 dimerization following dsRNA binding to the ECDs. Double stranded RNA binds directly to the TLR3 ECD under acidic conditions. TLR3 residues that are important for dsRNA binding includes H539 and N541 on the glycan free lateral face (Bell et al., 2006a; Bell et al., 2006b; Bell et al., 2005). Apart from these, conserved amino acid residues such as H39, H60 and H108 on the glycan-free surface at the N-

terminus interact with consecutive phosphate groups present on the RNA are also thought to contribute to dsRNA binding (Leonard et al., 2008; Liu et al., 2008; Pirher et al., 2008). TLR activated immune responses appear to be regulated by membrane trafficking and spatio-temporal localization of the receptor. Studies with chimeric TLR domains revealed localization of TLR3 is determined by the linker region between its TM and TIR domains, whereas localization of TLR7 and TLR9 is determined by their TM domains (Barton et al., 2006; Kajita et al., 2006; Nishiya et al., 2005). Initiation of antiviral signaling triggered by viral nucleic acid appears to be membrane associated compartmentalized event requiring multiple protein-protein interaction at the membrane interface. In that respect, UNC93B1 a 598 amino acid protein with 12 transmembrane domains specifically binds to TLR3, TLR7 and TLR9 and localizes in the ER (Brinkmann et al., 2007; Tabeta et al., 2006). The physical interaction between UNC93B1 and TLRs appear to be important for trafficking from the ER to endolysosome (Kim et al., 2008) and for proper TLR signaling.

## 1.5 PATTERN RECOGNITION RECEPTOR INITIATED ANTIVIRAL SIGNALING

The replicative intermediate dsRNA produced by viruses upon infection can be recognized by more than one PRR. These include TLR3, RIG-I, MDA5 (Kang et al., 2002; Kawai and Akira, 2006a; Kawai and Akira, 2006b; Perry et al., 2005; Yoneyama and Fujita, 2004a; Yoneyama and Fujita, 2004b) (Figure. 1.4). Upon dsRNA binding to RIG-I, a CARD-containing adaptor protein MAVS (also known as IPS-1, VISA or CARDIF) (Kawai et al., 2005; Meylan et al., 2005; Seth et al., 2005; Xu et al., 2005) is

recruited which further signals to activate downstream kinases like TBK-1 and IKK-ε (Sharma et al., 2003) that phosphorylate and activate IRF3. MAVS activation also leads to activation of I $\kappa$ B kinase that phosphorylates IKK-α/β/γ resulting in the activation of transcription factors RelA and P50. Activated IRF3 and NF-κB translocate to nucleus and associate with p300/CREB binding protein (CBP), initiating IFN-β transcription (Yang et al., 2003; Yang et al., 2004). IRF3 transcriptionally activates the promoters for IFN-β, IFN-stimulated genes ISG56 and ISG15, chemokine (RANTES), genes (Grandvaux et al., 2002; Lin et al., 1998). Signaling via TLR7/8/9 is dependent on the TIR-containing adapter protein MyD88. The activation of MyD88 leads to its further association with tumor necrosis factor receptor-associated factor 6 (TRAF6) (Gohda et al., 2004; Hacker et al., 2006). The TRAF6 complex activates TGF-β activated kinase 1 (TAK1) (Deng et al., 2000; Jefferies et al., 2003; Pisitkun et al., 2006; Sochorova et al., 2007; Suzuki et al., 2002; Wang et al., 2001; Yang et al., 2005), TAK1 activates nuclear factor-κB (NF- κB) and IRF5 to produce proinflammatory cytokines and type I IFNs (Takaoka et al., 2005). The TRAF3 complex including IL-1 receptor-associated kinase 1 activates IRF7 to produce robust type I IFNs (Honda et al., 2005a; Honda et al., 2005b; Kawai et al., 2004; Matsuzawa et al., 2008; Oganesyan et al., 2006).

TLR3 is normally localized in the endoplasmic reticulum of unstimulated cells. Stimulation and localization of dsRNA in the endosomes signals the c-Src kinase to recruit the TLR3 on the endosomes along with kinase (Johnsen et al., 2006). TLR3 is activated by virus associated dsRNA (and also by the synthetic dsRNA analog

polyI:polyC) to induce the secretion of type I IFNs through MyD88 independent signaling pathway (Alexopoulou et al., 2001).

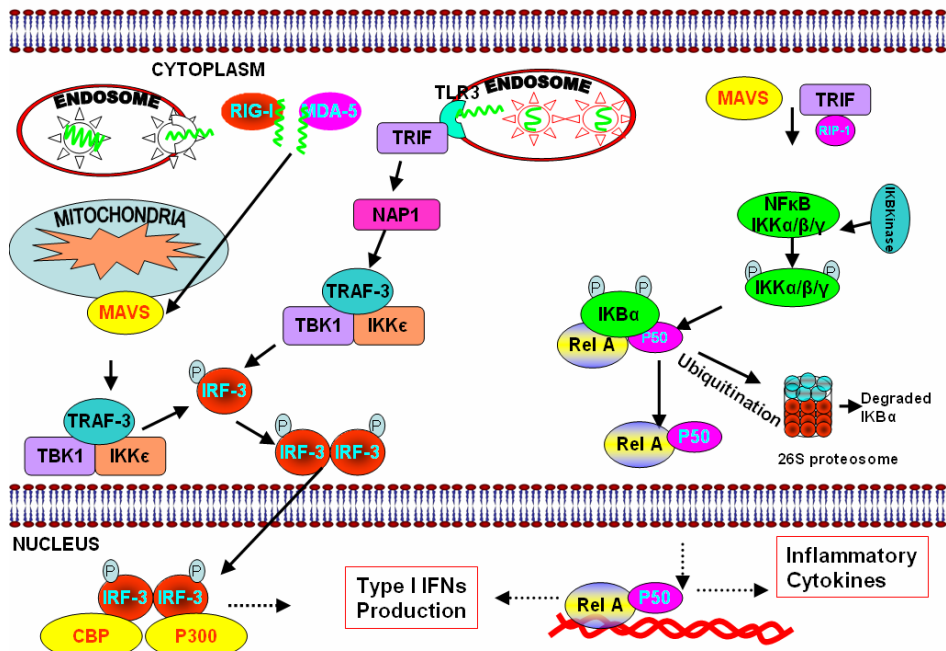


**Figure 1.4 Schematic representations of signaling pathways initiated by PRRs RIG-I/MDA5/TLR3 leading to the activation of IRF3 and NF-κB.** The cytokine transcription factors IRF3 and NF-κB are critical to the activation of innate immune response. TLR-3 dependent and independent signaling pathways converge on to activate IRF3 or NF-κB. In TLR3 dependent mechanism, the signaling pathway is initiated by the ligand induced dimerization of TLR3 upon recognizing replicative intermediate viral RNAs. This is followed by TRIF recruitment by TLR3's TIR domain leading to the activation of TBK1 and IKK $\epsilon$  which phosphorylates IRF-3. TLR-3 independent pathway depends on the initiation from RIG-I and MDA5. In this pathway RIG-I recruits MAVS (mitochondrial antiviral signaling protein also called as IPS-1, CARDIF, VISA) upon activation by 5'-triphosphate of the viral RNA. MAVS will further activate downstream kinases TBK1/IKK $\epsilon$ . Activation of kinases will leads to the activation of IRF3 (interferon regulatory factor-3) by phosphorylation. Phosphorylated IRF-3 undergoes dimerization and nuclear translocation where it interacts with transcriptional co-activators like CBP/p300 leading to the induction of interferon expression. MAVS and TRIF can also activate NF-κB pathway involving the activation of I $\kappa$ B kinase.

The dsRNA recognition triggers the initiation of a signaling cascade by interaction of the cytoplasmic TIR domains of TLR3 through the adaptor molecule TRIF or TICAM-1 (Oshiumi et al., 2003a) resulting in the activation of several kinases including PI3 and AKT that leads to phosphorylation (Sarkar et al., 2004) and nuclear translocation of IRF3. IRF3 interacts with CBP/P300 in the nucleus and acts as a potent transcription factor to turn on IFN- $\beta$  expression (Akira and Takeda, 2004; Iwasaki and Medzhitov, 2004). TLR3 is unique in the way that it recruits the adapter protein TRIF instead of MyD88 or MAVS used by other TLRs and RIG-I or MDA5 respectively. TRIF engagement is necessary to engage other downstream signaling proteins like TRAF, TBK1 and IKK- $\epsilon$  that lead to activation of IRF3 to turn on transcription from IFN- $\beta$  promoters.

## **1.6 VIRAL EVASION OF HOST ANTIVIRAL DEFENSES**

In order to successfully multiply in the host, viruses have evolved to combat host defenses by multiple strategies that can be referred as “Interferon antagonism”. These strategies include active blockade of interferon production by interfering with one or more proteins in host signaling cascades and passively, by hiding dsRNA from the PRR detection. For example, Hantaan virus (HTNV), Crimean-congo hemorrhagic fever virus (CCHFV) of family Bunyaviridae, and Borna disease virus (BDV) of family Bornaviridae do not contain 5'ppp at the 5' end and hence are not recognized by RIG-I (Habjan et al., 2008). Picornavirus evades RIG-I detection by having VPg at the 5' end (Paul et al., 2003). Paramyxoviruses such as Sendai virus encode the V protein that interacts with

MDA5 to inhibit antiviral signaling (Andrejeva et al., 2004; Childs et al., 2009). In the case of influenza A virus, the non-structural protein NS1 is thought to inhibit interferon response most probably by sequestering viral RNA away from RIG-I (Guo et al., 2007; Mibayashi et al., 2007; Opitz et al., 2007). SARS-CoV ORF 3b, ORF 6 and N proteins have been shown to inhibit the expression of interferon  $\beta$  by inhibiting the activation of IRF3. In addition, SARS-CoV nsp1 has also been shown to inhibit the interferon response by degrading the host mRNAs (Kamitani et al., 2006). These studies indicate that SARS-CoV encodes multiple proteins that are able to inhibit the interferon response (Kopecky-Bromberg et al., 2007; Kopecky-Bromberg et al., 2006). In hepatitis C virus and GBV-B, the viral serine-like protease NS3/4A plays an important role in the regulation of IRF3 mediated interferon response (Foy et al., 2003; Li et al., 2005b).

## **CHAPTER 2: SARS CORONAVIRUS**

### **2.1 CORONAVIRIDAE**

Six years ago, an epidemic outbreak of severe acute respiratory illness occurred in the Guangdong province in southern China that quickly spread to the neighboring countries infecting 8,400 people resulting in 800 deaths. The causative agent was identified as a novel coronavirus named “Severe Acute Respiratory Syndrome Corona Virus” (SARS-CoV). As the subsequent chapter describes the ability of SARS-CoV to evade host innate immune response, this chapter aims to summarize the biological background of coronaviruses. At present, there is immense interest around the world to understand virus-host interactions in context to viral pathogenesis, particularly, the mechanisms by which a virus evades the host immune defenses employing one or more strategies involving viral proteins.

#### *2.1.1 Classification*

Members of the genus Coronavirus cause respiratory and gastrointestinal diseases in humans and animals. Human coronaviruses, HCoV-HKU1 and HCoV-NL63 are shown to cause severe but non-fatal upper respiratory distress while HCoV-OC43 and HCoV229E cause common cold (Fouchier et al., 2004; van der Hoek et al., 2004; Woo et al., 2005a; Woo et al., 2005b). The genus Coronavirus along with the genus Torovirus belong to the Coronaviridae family classified under the order Nidovirales (Cavanagh,

1997; Cavanagh et al., 1993) (Figure 2.1). They are distinct from other positive strand RNA viruses in having a large genome and unique virion morphology (Cavanagh et al., 1993; Guy et al., 2000), where the viral envelope is studded with long petal shaped spikes resembling a crown and hence named “corona”. Other characteristic features of Coronaviridae are long flexible helical nucleocapsids, high sequence homology among the members and a genome organization with multiple sub genomic mRNAs with unique gene expression strategy (Cavanagh, 2008; Lai and Cavanagh, 1997).

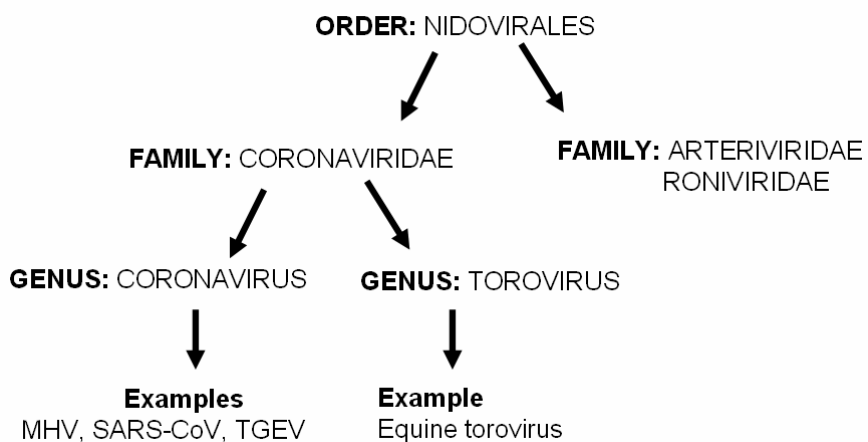


**Figure 2.1 Classification of Coronaviridae.** Coronaviridae belongs to the order Nidovirales.

Most members of the coronaviruses naturally infect only one kind of animal species or a limited number of closely related species. The genome of many coronaviruses including Human Coronavirus 229E (HCoV-229E), Severe respiratory syndrome coronavirus (SARS-CoV), Avian infectious bronchitis virus (IBV), Murine hepatitis virus (MHV) and Porcine transmissible gastroenteritis virus (TGEV) were

sequenced and found homologous (Boursnell et al., 1987a; Eleouet et al., 1995a; Herold et al., 1993a; Herold et al., 1993b; Lee et al., 1991).

### 2.1.2 Virus architecture and entry

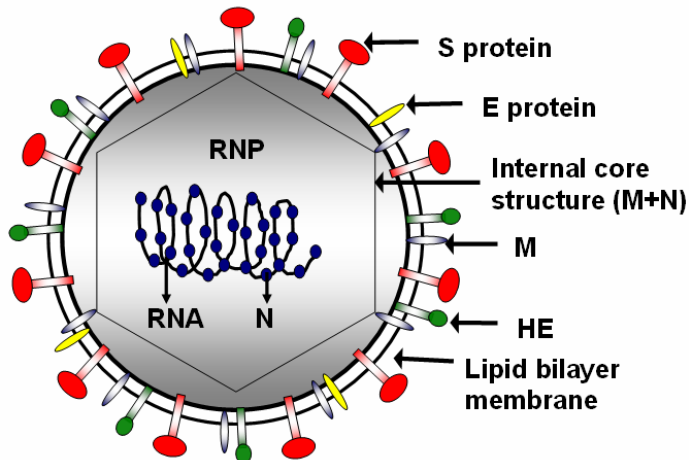


**Figure 2.2 Proposed model of Corona virus.** (Modified from Lai MMC and Holmes KV Fundamental Virology 4<sup>th</sup> edition). SARS-CoV is an enveloped positive strand RNA virus where RNA is present as nucleocapsid encased in lipid bilayer. From the lipid bilayer the virus spike proteins protrude out appearing sun's crown.

Virions in the family are spherical in structure and measure 100-120 nm in diameter surrounded by a membrane envelope. The envelope membrane is of intracellular origin obtained during virus maturation and budding from the infected cells. It is decorated with two types of spikes that radially project out from the virion. Long spikes composed of the spike glycoprotein (S) are 20 nm in length and are common feature of all the coronaviruses studied. Short spikes consisting of Hemagglutinin-Esterase glycoprotein (HE) are present in only few coronaviruses. The 150-180 kDa S glycoprotein (Fazakerley et al., 1992) plays a major role in the pathogenesis of

coronavirus infection (Gombold et al., 1993; Sturman et al., 1985). It undergoes proteolysis into S1 and S2 and the cleavage is necessary to enhance envelope membrane fusion with host cell membranes. Uncleaved S protein can also mediate membrane fusion activity but at lower efficiency (Bos et al., 1995; Stauber et al., 1993; Taguchi et al., 1993).

Inside the envelope, viral core particles measuring 65 nm in diameter composed of M glycoprotein and N protein is thought to be arranged with an icosahedral symmetry (Griffiths and Rottier, 1992; Tooze and Tooze, 1985). The M glycoprotein spans the lipid bilayer three times and along with a 9-12 kDa envelope protein (E) functions in budding of virions (Bos et al., 1996; Godet et al., 1992; Liu et al., 1991; Machamer et al., 1993; Machamer et al., 1990; Machamer and Rose, 1987; Risco et al., 1996; Vennema et al., 1996; Yu et al., 1994). The N protein is a 50-60 kDa nucleocapsid protein that has three conserved structural domains including an RNA-binding domain that interacts with viral genomic RNA to form the helical viral nucleocapsids. The N-protein has been shown to bind the leader sequence of viral RNA (Masters, 1992; Stohlman et al., 1988). It also binds to cellular membranes and phospholipids necessary for virus assembly and formation of RNA replication complexes (Anderson and Wong, 1993).

Most coronaviruses gain access to animal host through the gastrointestinal or respiratory tract. The virions enter target cells by binding to specific cell surface receptors (Table 1) (Dubois-Dalcq et al., 1982; Williams et al., 1991) involving virus membrane fusion with either the plasma or endosomal membranes. Fusion is suggested to occur at neutral or alkaline pH as opposed to the acid-mediated membrane fusion observed in

class II membrane fusion proteins of flavi or alphaviruses. Once the nucleocapsids reach the cytoplasm, they are rapidly uncoated to release the genomic RNA, which undergoes translation to produce precursor polyprotein.

VIRUS	HOST	RECEPTOR GLYCOPROTEIN
MHV	Mouse	MHVR and several additional carcino-embryonic related glycoproteins in the immunoglobulin superfamily
HCoV-229E	Human	Human aminopeptidase N, a metallo-protease
TGEV	Pig	Porcine aminopeptidase N, a metallo-protease
BCV	Cow	9-O-Acetylated neuraminic acid
SARS-CoV	Human	Angiotensin-converting enzyme 2 (ACE2)

**Table 2.1 List of cellular receptors used by coronaviruses to gain cellular entry**

### 2.1.3 *Genome organization*

In the mature virion, the viral genome is a single-stranded, positive-sense RNA of 27-32 kb in size (Boursnell et al., 1987b; Eleouet et al., 1995b; Herold et al., 1993b; Lai and Cavanagh, 1997; Lee et al., 1991) compactly organized into a long flexible helical nucleocapsid through its association with nucleocapsid phosphoprotein (N) (MacNaughton, 1978; Sturman et al., 1980). Genomic RNAs are messenger sense and is infectious (Lomniczi, 1977; Schochetman et al., 1977).

The 5' terminus of the genome is capped with 65-98 nucleotides of leader sequence, which is also present in the 5'end of the sub-genomic RNAs. The leader

sequence is followed by 200-400 nucleotides of untranslated region (UTR). Similarly, a 200-500 nucleotide UTR precedes a poly(A) tail of varying length at the 3-terminus (Lai et al., 1983; Shieh et al., 1987; Spaan et al., 1983). Many sequenced coronavirus are predicted to encode 7 to 10 putative open reading frames (ORFs) whose organization differs slightly among the members with number, order and sequence of the ORFs. Two large ORFs, ORF1a and ORF1b, spans the initial two thirds of the genome from the 5'end. The major gene product is the polymerase precursor expressed from ORF1a and ORF1b as a single polyprotein by a ribosomal frameshift mechanism. The polymerase precursor and structural genes typical of a coronavirus are organized in the following sequence order 5' pol-spike-Env-M-N-3' within which other non-structural and structural genes are interspersed. The interspersed proteins vary from virus to virus with respect to sequence, order and mechanism of expression (Lai and Cavanagh, 1997).

#### *2.1.4 Viral gene products, gene expression strategy and virus replication*

Coronavirus genomic RNA is translated by a cap-dependent ribosomal scanning mechanism. The polymerase precursor polyprotein encoded by overlapping ORF1a and 1b whose start codon appears first, may be the only viral protein synthesized initially from the freshly uncoated viral genome as it may be prerequisite for the establishment of virus infection. The polyprotein is then processed into several mature protein products either co- or post-translationally by the viral protease domains nested within the polyprotein. ORF1a encodes two such protease domains, namely papain-like cysteine protease (PLP) and chymotrypsin-picornavirus 3C-like protease (3CLP) (Gorbalenya et

al., 1989; Lee et al., 1991). Each of the structural proteins, S, M, N and HE are thought to be expressed from distinct monocistronic sub genomic RNAs that contain 5' leader sequence. These sub genomic RNA are synthesized from the genomic RNA by viral polymerase. Coronavirus replication is thought to take place in the cytoplasm of infected cells (Brayton et al., 1981; Wesley et al., 1991).

#### *2.1.5 Virus assembly*

The N protein produced at a late stage in the virus life cycle interacts with viral genomic RNA to form helical nucleocapsids. In the case of MHV, the N protein needs to specifically recognize a stretch of 61 nucleotides at the 3' end of the genomic RNA for efficient packaging of genomic RNA into virions (Fosmire et al., 1992; Masters et al., 1994; van der Most et al., 1991; Woo et al., 1997). Nucleocapsids interact with the golgi/ER membrane -anchored M protein and E protein to package themselves into virions which subsequently bud out of cell membrane (Bos et al., 1996; Dubois-Dalcq et al., 1982; Klumperman et al., 1994; Tooze et al., 1984; Vennema et al., 1996).

## **2.2 SEVERE ACUTE RESPIRATORY SYNDROME CORONA VIRUS (SARS-CoV)**

#### *2.2.1 Introduction*

At the end of 2002, a previously unknown respiratory disease suddenly emerged in Asia. The disease was a rapidly spreading influenza-like disease which quickly progressed to atypical pneumonia and fatal respiratory failure in 10% of infected cases

(Peiris et al., 2003). Extensive research led to the identification of the causative agent as a new coronavirus and it was named SARS-CoV. SARS-CoV seemed to be enzootic in animals like masked palm civets (*Paguma larvata*) that were frequently traded as food in Guangdong province in China. It is this market place, where there are dense human populations in close proximity to the animals, that is believed to be ground zero for the SARS outbreak (Guan et al., 2003; Peiris, 2003; van der Hoek et al., 2004). It may be the same region, where the virus evolved to cross the species barrier infecting humans via respiratory droplets or aerosolized virus (Seto et al., 2003; Wong and Tam, 2005; Yu et al., 2004). Infected patients shed active virus as they suffered from watery diarrhea which may be another contributing factor for rapid spread under poor hygienic conditions (Holmes, 2003). SARS appears to cause more severe respiratory distress in humans than HCoV-HKU and HCoV-NL63 and can potentially infect cats, mice, ferrets and monkeys (Kuiken et al., 2003a; Kuiken et al., 2003b; Martina et al., 2003; Subbarao and Roberts, 2006).

### 2.2.2 *Virus entry and pathogenesis*

Upper respiratory tract and lungs appear to be gateways and also targets of SARS-CoV entering the human body. A specific ligand-receptor interaction determines virion entry into the host cells. The viral tropism in coronavirus is determined by S protein selectively binding to a specific receptor present only on the target cells. The angiotensin-converting enzyme 2 (ACE2) on the epithelial cells of respiratory and gastrointestinal tract has been demonstrated to be the cellular receptor for S protein present on virions (Li

et al., 2003). Interaction of S protein with ACE2 leads to a membrane fusion event releasing the genomic RNA into the host cell cytoplasm (Ng et al., 2003). In a mouse model, the initial virus entry is shown to knock out a protective function of ACE2 that is necessary for recovering from acute lung injury and hence has been implicated in SARS pathogenesis (Imai et al., 2005; Kuba et al., 2005). As the virus multiplies, it destroys alveolar and bronchial epithelial cells resulting in extensive lung injury and triggers more systemic damage by inflammation mediated by cytokine storms. Clinically, severe SARS cases are characterized by lymphopenia, neutrophilia and hemophagocytosis (Wong et al., 2003). The virus is also thought to contribute to pathogenesis by multiplying in macrophages and lymphocytes and is also detected in high concentrations in intestine, kidney and brains of deceased patients. After 10-15 days of onset, the viral titers decrease in nasal secretion but clinically conditions often worsen due to persistent inflammation (Chan et al., 2004; Farcas et al., 2005; Gu et al., 2005; Mazzulli et al., 2004; Peiris et al., 2003).

### *2.2.3 Genome organization and expression of functional gene products*

SARS-CoV genomic RNA is 30334 nucleotides long with 14 predicted ORFs (Figure 2.3). The 5' end is capped with Cap1 structure and the 3'end has a long poly (A) tail. It has 265 and 342 nucleotide UTRs at 5' and 3'end respectively excluding the poly (A) tail. The virus entry in host cells is followed by uncoating of nucleocapsids to release viral genomic RNA into the cytoplasm which undergoes translation to yield polyprotein 1a (PP1a) of 4382 amino acids. A conserved “slippery sequence” UUUAAAC and a stem

loop present before end of PP1a ORF causes a ribosomal frameshift to the -1 position into ORF1b yielding a longer polyprotein (PP1ab) of 7073 amino acid residues (Thiel et al., 2003). Polyproteins PP1a and PP1ab are proteolytically processed into functionally mature proteins that interact with host factors generating a membrane-anchored multi-subunit viral replicase complex. Replicase is necessary for transcription of genomic RNA and eight nested mono/bicistronic sub-genomic RNAs from which structural genes are translated. All the subgenomic RNAs (sgRNAs) so produced have 72 nucleotide leader sequences at the 5'end which aid sgRNAs in translation. The leader sequence is added to the 5'end of these RNA by a unique mechanism that involves discontinuous synthesis (Thiel et al., 2003).

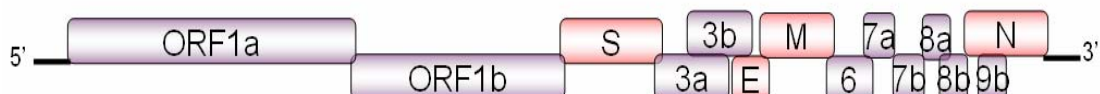


**Figure 2.3 Genome organization of SARS-CoV** (Modified from (Perlman and Dandekar, 2005). Genome is roughly 30 kb in length and contains several large and small ORFs. ORF1a and ORF1b account for about two-thirds of the genome, both encode large polyproteins. ORF1a gives rise to PP1a and ORF1b is expressed by a -1 ribosomal frameshift of ORF1a to produce PP1ab. The SARS-CoV genome encodes four structural proteins: spike (S), envelope (E), Matrix (M) and nucleocapsid (N).

#### 2.2.4 Polyprotein processing

SARS-CoV encodes 2 proteases namely PLpro (papain-like protease) and 3CLpro (picorna virus 3 Chymotrypsin-like protease) that are nested within ORFs of PP1a and PP1ab. These proteases excise themselves from the polyprotein as well as extensively process PP1a and PP1ab to generate 11 and 16 mature non-structural proteins (nsps) respectively. 3CLpro is one of the best studied coronavirus proteins to date with respect

its structure and function. It recognizes the following amino acid sequence P4-X-P2-Q↓-P1' (where P4=A/V/T/P, X=any amino acid, P2=L/I/F/V/M P1'=S/A/G/N) and cleaves after glutamine in polyproteins and is similar to other characterized coronavirus 3CLpros. All the 3CLpro cleavage sites are located in the central and C-terminal ends of PP1a and PP1ab polyproteins.

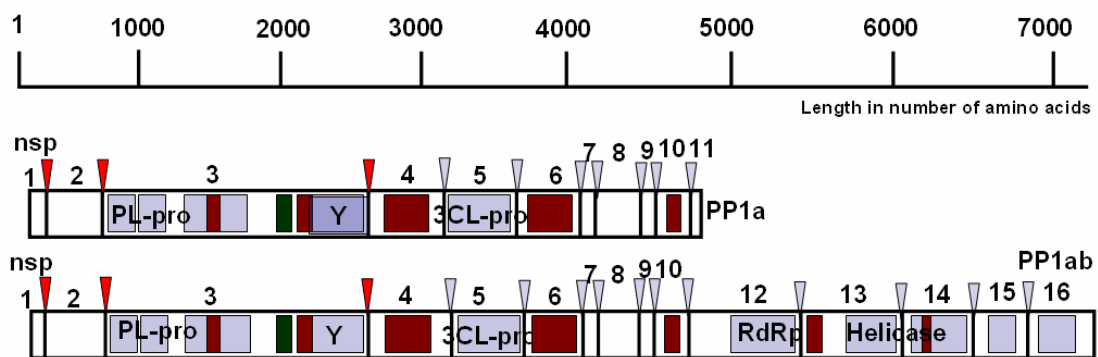


**Figure 2.4 Schematic representation of SARS-CoV PP1a and PP1ab polyprotein processing.** PLpro cleavages are indicated in red wedges and 3CLpro in grey wedges (Modified from (Ziebuhr, 2004)). PP1a is processed into nsp1-11 by the viral protease PLpro and 3CLpro. Similarly nsp1-16 is produced from PP1ab.

3CLpro is responsible for 70-80% of proteolytic cleavages made and hence, 3CLpro is the main protease involved in generating the replicative functions of the SARS-CoV (Fan et al., 2004; Hegyi et al., 2002; Thiel et al., 2003).

### 2.2.5 Papain like protease (PLpro)

SARS-CoV encodes a single papain like protease (PLpro) domain within the PP1a polyprotein while other corona viruses encode two proteases PLpro1 and PLpro2. The PLpro domain of SARS-CoV is present within nsp3, a 213-kDa membrane

associated replicase subunit. SARS-CoV PLpro is orthologous to PLpro2 of coronaviruses with two proteases and is predicted to contain a putative zinc finger motif between alpha-beta domains of the papain like fold. PLpro recognizes and cleaves after the motif LXGG and mediates proteolytic cleavages at the N-terminal regions of PP1a and PP1b generating non-structural proteins 1, 2, and 3 (Nsp1, Nsp2 and Nsp3).

Trans-cleavage assays involving expression of PLpro and PLpro substrates in mammalian cells demonstrate that Nsp1 is rapidly processed while the Nsp2/Nsp3 cleavage site is less efficiently processed and processing at the Nsp3/Nsp4 site requires expression of PLpro with an extended downstream region containing a hydrophobic stretch (Harcourt et al., 2004).

Homology model structure of SARS PLpro based on the structural relationship with the catalytic core domain of herpesvirus associated ubiquitin specific protease (HAUSP) predicts the presence of deubiquitinase activity associated with PLpro arising through residues K1632-E1847 involving a zinc finger motif (Sulea et al., 2005) but the functional significance this remains unexplained. Homology modeling suggests D1826 as an active site residue along with C1651 and H1812 that together form a catalytic triad. Mutation of cysteine residues involved zinc coordination is shown to abolish enzyme activity of PLpro from HCoV229E.

Deubiquitinase activity has been experimentally demonstrated using *E.coli* expressed SARS-CoV PLpro protein (residues 1507- 1858) and synthetic substrates like Ub-AMC, Z-LRGG-AMC (Lindner et al., 2005). From a branched polyubiquitin substrate, the purified enzyme is shown to disassemble 2-7 (Ub2-7) or Ub4 units by iso-

peptide bond cleavage. Enzyme activity was lost upon mutation of C1651A and D1826A of the catalytic triad (Barreto et al., 2005; Barreto et al., 2006; Lindner et al., 2005).

#### *2.2.6 Pathogenesis of SARS-CoV*

Although SARS-CoV pathogenesis is attributed to direct destruction of alveolar and bronchial epithelial cells resulting in extensive lung injury, to a larger extent it is also mediated by host immune dysregulation referred to as immunopathogenesis (Perlman and Dandekar, 2005). In mammalian hosts, virus infection immediately activates innate immune response characterized by transient synthesis of cytokines and chemokines just enough to stop the virus spread. This response is normal and arises from well regulated anti-viral signaling pathways triggered by viral signatures (PAMPs). However, this normal response can be derailed to produce massive uncontrolled inflammation leading to fatal destruction of host tissues and organs. Uncontrolled inflammation may be due to interference in feedback mechanisms or disruption of the normal sequence of innate immune signaling that regulate inflammation process, both actively mediated by virus to their advantage by employing one or more viral proteins. It has been shown that the replication of SARS-CoV in Vero cells can be suppressed by exogenously added interferon (IFN- $\beta$ ), a cytokine which is normally synthesized by cells in response to virus infection. However, no endogenous IFN-transcripts or IFN- $\beta$  promoter activity was detected in SARS-CoV infected cells (Spiegel et al., 2005; Spiegel et al., 2004) suggesting that SARS-CoV either evades host detection or actively interferes in interferon synthesis early during infection. Consistent with active inference, SARS-CoV

is suggested to cause blockade at the IRF3 activation step of anti-viral signaling. It may interfere with one or more of the well characterized events during IRF3 activation that include hyperphosphorylation, homodimerization, nuclear translocation and association with CBP/p300 to generate transcriptional activity necessary for the expression of interferon stimulatory genes and ultimately interferon  $\beta$ . Such disruption of the IFN response is also observed in influenza virus infections and is mediated by NS1 protein. An alternate hypothesis has been proposed in which the coronaviruses MHV and SARS-CoV do not block IRF3 activation but instead avoid inducing interferon by remaining undetected by host defenses during the course of infection.

## **CHAPTER 3: SARS-COV EVADES INNATE IMMUNE DEFENSES BY PLPRO MEDIATED DISRUPTION OF IRF3 ACTIVATION STEP OF ANTIVIRAL SIGNALING**

### **3.1 INTRODUCTION**

Upon virus infection, the immediate defense mechanism launched by an infected host is the innate immune response characterized by production of type I interferons. Interferons put a check on the virus infection by inducing expression of genes that prevent viral replication and spread to neighboring cells. Viruses such as SARS coronavirus, hepatitis C, influenza and many others have evolved to survive host defenses with several evasive mechanisms that include suppression of interferon production. Several viral encoded proteins have been shown to inhibit the activation of interferon response by inactivating signaling pathways. The viral encoded proteins do so by interacting directly or indirectly with the component proteins of the signaling cascade.

As discussed in chapter 2, SARS-CoV is a novel coronavirus that causes a highly contagious respiratory disease with a significant mortality rate of 10-15% (Peiris, 2003; Peiris et al., 2004). The first three quarters of the 29.7 kb genome of SARS-CoV is translated to produce two large replicase polyproteins (Yount et al., 2005; Ziebuhr, 2005; Ziebuhr, 2006) called as pp1a and pp1ab (Marra et al., 2003; Rota et al., 2003). The papain like protease (PLpro) and 3C-like protease (3CLpro) present within these polyproteins further process the polyprotein to generate 16 functional non-structural

proteins (nsp1-16). Unlike other coronaviruses which encode two papain-like proteases, whereas SARS-CoV encodes only one. SARS-CoV PLpro residing within the nsp3 product is found to co localize with synthesized viral RNA near the perinuclear sites consistent with its predicted role in viral RNA synthesis. The PLpro domain (SARS-CoV PLpro) present within the 213-kDa membrane associated replicase product of nsp3 has been cloned, expressed and assayed for protease activity by trans-cleavage assay and shown necessary to generate a functional replication complex by proteolytic processing (Barretto et al., 2005; Barretto et al., 2006; Harcourt et al., 2004). In addition to its protease function SARS-CoV PLpro has significant homology with herpesvirus associated ubiquitin-specific protease (HAUSP) suggesting associated deubiquitinating activity (Sulea et al., 2005; Sulea et al., 2006). PLpro has also been shown to recognize the consensus motif LXGG which is also recognized by cellular deubiquitinating enzymes (Barretto et al., 2005; Lindner et al., 2005). Zinc binding domains and a putative catalytic triad Cys1651-His1812-Asp1826 along with four Cys residues have been shown to be essential for its proteolytic activity and presumably deubiquitinating activity. Branched polyubiquitin chains Ub2-7 or Ub4 units have been shown to be disassembled by purified SARS-CoV PLpro involving an isopeptide bond cleavage (Barretto et al., 2005; Lindner et al., 2005).

It has been shown that the replication of SARS-CoV in Vero cells can be suppressed by exogenously added interferon (IFN- $\beta$ ), a cytokine which is normally synthesized by cells in response to virus infection. However, no endogenous IFN-transcripts or IFN- $\beta$  promoter activity was detected in SARS-CoV infected HEK 293

cells (Spiegel et al., 2005; Spiegel et al., 2004) suggesting that SARS-CoV either evades host detection or actively antagonizes in interferon synthesis early during infection. Consistent with active interference, several SARS-CoV proteins like ORF3b, ORF6, and nucleocapsid (N) and nsp1 have been shown to be IFN antagonists, based on their ability to inhibit the IRF3 activation step of anti-viral signaling. These proteins may interfere with one or more of the well characterized events of IRF3 activation that include hyperphosphorylation, homodimerization, nuclear translocation and association with CBP/p300 to generate transcriptional activity necessary for the expression of interferon stimulatory genes and ultimately interferon  $\beta$ . Studies with other coronaviruses have suggested alternative mechanism for evasion of host defenses. No interferon response was observed with Mouse Hepatitis Virus (MHV) infection leading to the hypothesis that viral mediated active suppression of interferon was not present in coronaviruses, but somehow, by an unknown mechanism, these virus were “able to avoid” host detection (Garlinghouse et al., 1984; Pewe et al., 2005; Zhou and Perlman, 2007). Even though SARS-CoV belongs to the coronavirus family maybe it may have adapted a different mechanism for its inhibition of interferon response unlike MHV.

Surprisingly, multiple activities such as protease, deubiquitinase and De-ISgylation associated with PLpro raise additional questions about their functional significance that suggest a possible role in interferon antagonism. In this chapter, the experimental work and results presented demonstrate PLpro is an interferon antagonist inhibiting IRF3 activation.

### **3.1 EXPERIMENTAL MATERIALS AND METHODS**

#### *3.2.1 Plasmids*

The cDNA expression plasmids were kind gifts from the respectively indicated contributors: pCDNA3-A20-myc (from Nancy Raab-Traub) ; p55C1Bluc, pEFBos N-RIG and pEFBos N-MDA5 (from Takashi Fujita) ; pcDNA3-Flag TBK1 and pcDNA3-Flag IKK $\epsilon$  (from Kate Fitzgerald) ; pIFN- $\beta$ -luc, IRF3-5D, GFP-IRF3 and GFP-IRF3 5D (from Rongtuan Lin) ; PRDII-Luc (from Michael Gale) ; (PRDIII-I)4-Luc (from Christina Ehrhardt); pEFTak-IPS-1 (from Michael Gale) ; pCDNA3-HA-TRIF (from Christopher Basler) bovine viral diarrhea virus (BVDV) Npro have been described (Chen et al., 2007b).

#### *3.2.1a Construction of WT and mutant PLpro-sol and PLpro-TM*

The soluble wild type PLpro (PLpro-sol) in mammalian cells was expressed from pCDNA3.1-V5/HISB (*Invitrogen*) containing human codon optimized SARS PLpro without any viral control sequences in the codon region such as potential splice sites and polyadenylation signal sequences. The resulting protein has the identical amino acid sequence as SARS CoV urbani strain (gene bank Accession AY278741) though the encoding nucleotide sequence is altered. The synthetic fragment was cloned at the *Bam* HI/*Eco* RI sites of pcDNA3.1 v5, so that the protein is made in frame with the V5 tag at the C-terminus. The same construct was used to generate single site specific mutant constructs (Stratagene quick change) pcDNA3.1-SARS-PLpro (PLproSol C1651A), pcDNA3.1-SARS-plpro (PLproSol C1810A) and pcDNA3.1-SARS-plpro (PLproSol D1826A) that encode soluble PLpro proteins having C1651A, C1810A and D1826A

respectively. These mutations were confirmed by DNA sequencing. These proteins were also expressed containing 546 amino acids at the C-terminus necessary for transmembrane anchorage. The nucleotide sequence encoding the transmembrane region from PLpro was PCR amplified of cDNA clone pPLpro-HD (Harcourt et al., 2004) and inserted between the *Eco* RI/*Xho* I sites and cloned downstream of the PLpro-sol of the above constructs resulting in pCDNA3.1-SARS- PLpro(TM WT), pcDNA3.1-SARS-PLproTM C1651A, pcDNA3.1-SARS- PLproTM C1810A and pcDNA3.1-SARS-PLproTM D1826A. The entire protein from 1541-2425 is translated in frame with a C-terminal V5 tag. The sequence coding for amino acids 1856-2425 was not altered from the original nucleotide sequence. The fusion of two amino acid fragments (1541-1855 and 1856-2425) resulted in the creation of an *Eco* RI site in the centre and also, an insertion of additional three amino acids W, N and S. However, this did not affect the catalytic function as tested in our assays for proteolysis and deubiquitination (Barretto et al., 2005; Harcourt et al., 2004).

### 3.2.1b Construction of WT and mutant of pTREBla-PLpro-TM

Inducible expression of PLpro tagged with transmembrane domain (PLproTM) was achieved by using the Tet off system. To introduce a selectable marker in the tetracycline responsive mammalian expression vector pTRE2 (*Clontech*), the blasticidin resistance gene from expression vector pcDNA6 V5HisB (*Invitrogen*) was PCR amplified with primers BlaSVPXhoIF: CTTCACTCGAGTGTGTCAGTTAGGGTGTGGAAAG and BlaSVpAXhoIR:

GTAAACTCGAGGCAGTGAAAAAAATGCT. The PCR product was digested with *Xho* I and cloned at *Xho* I site of pTRE2 (*Clontech*). The resulting plasmid is named pTRE2Bla (Chen et al., 2007a). To express PLproTM under a tetracycline (tet) responsive promoter, a 2.7 kb nucleotide fragment encoding PLpro TM from pCDNA3.1-SARS- PLpro(TM WT) was released by double digestion with *Hind* III/*Pme* I. This 2.7 kb fragment was cloned at *Hind* III/*Eco* RV site of pTRE2Bla to generate pTRE2Bla-PLproTM which expressed SARS-CoV PLproTM under the tet-regulated promoter.

### 3.2.2 Cell lines

Human embryonic kidney (HEK) 293, 293T, and HEK293 TLR3 (a gift from Kate Fitzgerald) cell lines were grown and maintained in Dulbecco's minimal essential medium with 10% FBS and the medium for 293FT contained 200 µg/ml Geniticide (*Invitrogen*). HeLa tet off cell lines (*Clontech*) was cultured according to manufacturer's instructions.

#### 3.2.2a Generation of stable HeLa cell line with conditional expression of SARS-CoV PLpro TM

HeLa tet off cells (*Clontech*) transfected with pTRE2Bla-PLproTM using FuGene 6 (*Roche*) were double selected in a media containing 100 µg/ml G418, 2 µg/ml tetracycline and 1 µg/ml blasticidin. Isolated individual cell colonies were observed after three weeks, which were picked and expanded individually. These colonies were tested for SARS-CoV PLpro-TM expression upon tetracycline removal by indirect immunofluorescence using mouse monoclonal antiserum against the V5 epitope

(Invitrogen) diluted 1:500. A clone of cells designated as Hela PLpro-TM 4 and PLpro-TM 10 exhibited tight regulation of SARS-CoV PLproTM expression under tetracycline control and was selected for further characterization. A similar process to generate SARS-CoV PLproTM mutant clones remained unsuccessful even after several repeated attempts, which may be attributable to the toxicity of the mutant construct to the cells.

### 3.2.3 Sendai virus infection

Cells were infected with Sendai virus SeV: Cantell strain (*Charles River laboratory*) for 1 hr at 37 °C using an inoculum of 100 hemagglutinin units/ml (HAU/ml) in a minimum volume of DMEM without antibiotics to ensure virus adherence to the cells. After infection, medium containing antibiotics was added; cells were incubated for 16 hours and then harvested for reporter assays and immunoblot analysis. For each experiment, control cultures were maintained similarly in the absence of virus. Blots were probed with sendai virus-specific antiserum to rule out the possibility of PLproTM interfering with Sendai virus infection or replication.

### 3.2.4 PolyI:C treatment

PolyI:C (*Sigma*) was added directly to the medium at 50 µg/ml (m-pIC) or complexed with lipofectin for transfection (t-pIC). Cells were assayed for polyI:C induced responses at 6hr after treatment.

### *3.2.5 Transfection and Reporter gene assays*

24-well plates containing  $5 \times 10^4$  cells in 1ml of DMEM were transfected in triplicate with 400 ng of plasmid DNA using Fugene 6 transfection reagent (*Roche*) as per the manufacturer's instructions. 100 ng of pCMV- $\beta$ gal plasmid DNA (*Clontech*) per well was used to normalize for transfection efficiency. At 24hrs post-transfection, cells were either treated with 50  $\mu$ g /ml of polyI:C or 100 HAU/ml of SeV for 6 or 16 hrs respectively and then assayed for firefly luciferase and  $\beta$ -galactosidase activities. The luciferase activity was normalized to  $\beta$ -galactosidase activity. Data was expressed as mean relative luciferase activity with standard deviation from a representative experiment carried out in triplicate. A minimum of three separate experiments were performed to confirm the trend in each observation. The fold induction of promoter activity was calculated by dividing the relative luciferase activity of stimulated cells with that of mock treated cells.

### *3.2.6 Indirect Immunoflourescence staining (immunostaining)*

Chamber slides containing  $5 \times 10^4$  cells were either transfected or infected with SeV as described above. After incubation (16 hr for SeV infection or 24-48 hr for transfection), slides were washed with PBS and fixed with 4% Para formaldehyde for 30 min at room temperature. Cells were permeabilized with a solution of 1xPBS containing 0.2% Triton-X100 for 15 min followed by blocking for 30 min in 3% BSA in 1xPBS. After rinsing in 1xPBS, the slides were incubated with rabbit polyclonal antiserum against human IRF3 (kindly provided by Dr. Michael David) diluted 1:500 in 3% BSA

for 1hr or with mouse monoclonal V5 antibody diluted 1:500 in 3%BSA (*Invitrogen*). The slides were washed thrice with 1xPBS and incubated for 1hr with FITC conjugates of goat anti rabbit or anti mouse IgG antibodies (*Southern Biotech*) diluted 1:200 in 3%BSA. Slides were washed thrice with 1xPBS and allowed to dry. Slides were mounted with a thin layer of vectashield solution (*Vector labs*) and sealed with a coverslip. Cells were examined under a Zeiss 510 META laser scanning confocal microscope in the UTMB Optimal Imaging Core.

### 3.2.7 Assay for IRF3 nuclear translocation

A clone of the Hela tet off cell line transgenic for PLpro-TM was induced to express the protein by tetracycline withdrawal for 3 days.  $5 \times 10^4$  cells expressing PLpro TM were plated in 4-well chamber slide and infected with SeV (100 HAU/ml). After 16 hr the cells were washed with 1xPBS, fixed with 4% paraformaldehyde and blocked with 3% BSA, 1xPBS. The cells were immunostained with rabbit anti-IRF3 and mouse anti-V5 antibodies in separate slides and were observed by immunofluorescence microscopy. Cells showing nuclear translocation of IRF3 were counted using 20x and 40x magnification. At 20x magnification, four fields were counted and 40x magnification, ten fields were counted. The data is collectively taken as average and plotted.

### 3.2.8 Reverse transcription PCR (RT-PCR)

Total cellular RNA was isolated from Hela PLpro-TM stable cell lines using TRIzol reagent (*Invitrogen*). Similarly, total RNA was also extracted from the cells superinfected with SeV. The RNA samples were treated with DNaseI to remove genomic

DNA contamination and further purified using Rneasy Mini Kit (*Qiagen*). The RNA was annealed with oligo (dT) primers and first strand cDNA synthesis was carried out using reverse transcriptase (*Clontech*). The resulting cDNA was subjected to semi-quantitative PCR to quantitate the expression of several genes using the primers listed in the table below (Table 3.1).

<b>Transcript</b>	<b>5' to 3' primer sequence</b>	<b>product length</b>
ISG56	ISG56 +: TAGCCAACATGTCCTCACAGAC ISG56 -: TCTTCTACCCTGGTTTCATGC	394bp
IFN- $\beta$	IFN $\beta$ 107+: TCCTGtTGTGcTTCTCCAC IFN $\beta$ 383-: GTCTCATtCCAgCCAGTGCT	276bp
GAPDH	GAPDH 86 +: TGAAGGTCGGAGTCAACGGATTGGT GAPDH 1068-: CATGTGGGCCATGAGGTCCACCAC	980bp
ISG54	ISG54+ : AGAAATCAAGGGAGAAAGAA ISG54- : CTAAAGGTGACTAAGCAAATG	509bp
SARS	SARS 15250+ : CTAACATGCTTAGGATAATGG SARS 15270+ : GCCTCTCTTGTCTTGCTCGC SARS 15617- : CAGGTAAGCGTAAACTCATC	347bp
SeV	SeV P890+ : aataggggacccgctctgtct SeV P1226- : ttccacgctctttggatct	336bp

**Table 3.1 List of primers used for Semi-quantitative RT-PCR**

The quantity of the cDNA template included in these reactions and the number of amplification cycles were optimized to ensure that reactions were stopped during the linear phase of product amplification, permitting semi-quantitative comparisons of mRNA abundance between different RNA preparations. To exclude the possibility of contamination DNA control reactions were performed in parallel in the absence of reverse transcriptase. PCR products were visualized by agarose gel electrophoresis. The Table 3.1 shows the sequence of primers pairs used for RT-PCR.

### 3.2.9 Immunoblot Analysis

For the detection of SeV virus proteins or SARS-PLpro TM protein, interferon stimulatory gene 56 (ISG56) and actin, cells were harvested and the total cellular extracts were prepared and subjected to immunoprecipitation and immunoblot analysis as described previously (Chen et al., 2007a; Foy et al., 2003). For experiments that involved analysis of IRF3 to estimate the amount of hyperphosphorylated (activated) isoform of IRF3, cells were harvested and lysates were prepared according to the procedure of Hiscott and colleagues (Lin et al., 1998). Gels containing 7.5% polyacrylamide were used to resolve IRF3 isoforms. After electrophoresis, proteins were transferred to hybond-NC nitrocellulose membrane (*Amersham*) and the blots were processed for immunodetection of proteins as described (Foy et al., 2003). The blots were probed using monoclonal (mAb) or polyclonal (pAb) as listed below rabbit anti-IRF3-396P pAb 1/10000 dilution (a gift from John Hiscott), mouse anti-Actin mAbs 1/10000 dilution (*Sigma*); mouse anti-V5 mAb 1/5000 dilution (*Invitrogen*); rabbit anti-IRF3 pAb 1/5000 dilution (a gift from Michael David, university of California San Diego); rabbit anti-CBP pAb 1/500 dilution and mouse anti-IRF3 mAb 1/200 dilution (*Santa Cruz*); rabbit anti ISG56 pAb 1/500 dilution (a gift from Ganes Sen, Cleveland Clinic); rabbit anti-SeV pAb 1/5000 dilution (a gift from Ilkka Julkunen, National Public Health Institute, Helsinki); mouse anti-GFP mAb (*Roche*), mouse anti-flag M2 mAb and pAb (*Sigma*) and horseradish peroxidase-conjugated goat anti-rabbit 1/5000 dilution and goat anti-mouse pAbs 1/2000 dilution (*Southern Biotech*). Protein bands were visualized using ECL Plus Western Blotting

Detection reagents (*GE HealthCare*) or SuperSignal West Pico Chemiluminescent Substrate (*Pierce*), followed by exposure to X-ray film.

### *3.2.10. Native Polyacrylamide Gel Electrophoresis (PAGE)*

Native PAGE was performed using gels containing 7.5% acrylamide without SDS or reducing agent. The gel was pre run with 25 mM Tris and 192 mM glycine with pH 8.4 with and without 1% deoxycholate (DOC) in the cathode and anode chamber, respectively for 30 min at 40mA. Samples in the native PAGE sample buffer (10 $\mu$ g protein, 62.5mM Tris-Cl pH 6.8, 15% glycerol and 1% DOC) were applied to the gel and electrophoresed for 80 min at 25 mA (Iwamura et al., 2001). Immunoblotting was performed as described previously. For the detection of human IRF3, rabbit anti-IRF3 pAb diluted 1/5000 (a gift from Michael David, university of California, San Diego) was used.

### *3.2.11 Immunoprecipitation*

Hela cells with and without the expression of SARS-PLpro-TM were infected in the presence and absence of SeV and incubated for 16 hr. The cells were lysed for 10 min at 4°C in RIPA buffer (25 mM Tris-Cl pH 7.5, 150mM NaCl, 1% Triton X-100) containing protease inhibitors (*Sigma*). After lysis, the samples were centrifuged at 6000 g to pellet down the cell debris. The amount of protein in the lysate supernatant was estimated and a volume of supernatant corresponding to 400 $\mu$ g of protein was used for each immunoprecipitation experiment. Prior to immunoprecipitation, the lysate was precleared with protein A-sepharose beads. Precleared lysate was incubated with a specific antibody

(mouse anti-V5 or rabbit anti-IRF3, rabbit anti-CBP) overnight at 4°C. Subsequently, protein A-sepharose beads were added to the above mixture and incubation was continued for 2 more hours. After incubation, beads were pelleted and washed 3 times with RIPA buffer. The beads were resuspended in SDS loading buffer (8% SDS, 0.2 M Tris pH 8.8, 4 mM EDTA, 0.1% bromophenol blue, 40% glycerol and 0.5 M DTT) and boiled for 10 min prior to electrophoresis of immunoprecipitated protein. Immunoprecipitated proteins were separated on 7.5% SDS-PAGE gels (*BioRad*). Proteins were transferred to membranes by electro blotting and probed with primary antibodies: rabbit-anti IRF3 diluted 1/2000, rabbit-anti CBP diluted 1/500, mouse-anti GFP diluted 1/2000 and mouse-anti V5 diluted 1/5000 followed by horseradish peroxidase-conjugated goat anti-rabbit and goat anti-mouse secondary Ab diluted 1/5000 (*Southern Biotech*). Protein bands were visualized using ECL Plus Western Blotting Detection reagents (*GE HealthCare*) or SuperSignal West Pico Chemiluminescent Substrate (*Pierce*), followed by exposure to X-ray film.

### 3.2.12 Okadaic acid treatment (*Phosphatase inhibitor*)

For *in vivo* experiments, HeLa PLpro-4 cells were grown in the presence or absence of tet and were therefore either repressed or induced for PLpro expression. Cells were then either mock-infected or infected with SeV for 12 hr, followed by 4 hr incubation with or without 0.05 µg/ml of okadaic acid (OA, *Calbiochem*) prior to cell lysis and immunoblot analysis. For *in vitro* experiments, 40 µg of whole cell lysate of HeLa cells infected with SeV were mock-treated, or incubated with 5 units of calf

intestine alkaline phosphatase (CIP, *New England Biolabs*) in CIP buffer, or incubated with 0.05 µg/ml of OA, or treated with CIP in the presence of OA, respectively, at 30°C for 2 hr.

### 3.3 RESULTS

#### 3.3.1 SARS-CoV PLpro inhibits TLR3 and RIG-I induced activation of IFN- $\beta$

SARS-CoV PLpro was recently shown to have deubiquitination activity. As ubiquitination plays a pivotal role in many cellular processes, including innate immune signaling, role of PLpro in regulation of viral induced IFN response evaluated by a series of reporter assays stimulating TLR3 pathway by addition of a synthetic dsRNA analog, polyI:C, to culture medium of HEK293 cells that stably express TLR3 (293-TLR3).

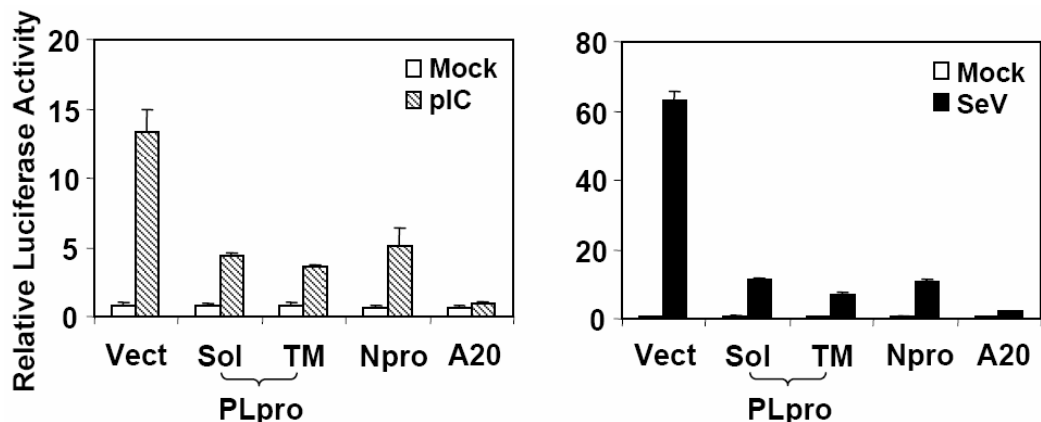


**Figure 3.1 SARS-CoV PLpro domain inhibits activation of IFN- $\beta$  promoter stimulated by TLR3 or RIG-I pathways.** HEK293-TLR3 cells were cotransfected with pIFN- $\beta$ Luc and pCMV- $\beta$ gal plasmids, and a vector encoding SARS PLpro-Sol or SARS PLpro-TM, BVDV Npro, or A20, or an empty vector. Twenty-four hours later, cells were either mock-treated (empty bars), or incubated with 50 µg/ml polyI:C in culture medium for 6 hr (hatched bars, left panel), or infected with SeV at 100 HAU/ml for 16 hr (solid bars, right panel) prior to cell lysis for both luciferase and  $\beta$ -galactosidase assays. Bars show relative luciferase activity normalized to  $\beta$ -galactosidase activity, i.e. IFN- $\beta$  promoter activity.

A 16-fold induction from IFN- $\beta$  promoter was observed, but was reduced by 70% in cells ectopically expressing the catalytic core domain of SARS-CoV PLpro (Sol), or PLpro-TM that encodes PLpro-Sol in conjunction with its downstream hydrophobic transmembrane domains (Figure 3.1 left panel). A similar phenomenon was noticed with IFN- $\beta$  promoter activity in the presence of PLpro-Sol and PLpro-TM when IFN response was stimulated by SeV, which activates the RIG-I pathway (Figure 3.1, right panel). As positive controls, ectopic expression of known viral or mammalian inhibitors of the IFN response, i.e., the papain-like protease of bovine viral diarrhea virus, Npro, or a human deubiquitination enzyme, A20, respectively, also strongly suppressed activation of the IFN- $\beta$  promoter by polyI:C or SeV (Figure. 3.1, left and right panels). Thus, the data suggest that expression of the catalytic core domain of SARS-CoV PLpro is sufficient for inhibiting activation of the IFN- $\beta$  promoter via both TLR3 and RIG-I pathways.

### *3.3.2 Inhibition of PRR stimulated IFN- $\beta$ promoter activity is independent of PLpro's protease activity*

Next, to test the role of protease activity of PLpro in inhibition of cellular IFN response, mutations in the active site triad (C1651-H1812-D1826) known to abolish the PLpro catalytic activity, were generated. Co-expression analysis of the C1651A or D1826A PLpro mutants with SARS-CoV nsp1-3 polyprotein substrate confirmed these mutants were indeed deficient in protease activity, as neither of them could mediate the processing of the nsp1-3 polyprotein, when compared to WT PLpro (Devaraj et al., 2007). Corroborating earlier observations from (Figure 3.1), wild-type (WT) PLpro-Sol

inhibited the activation of IFN- $\beta$  promoter by SeV in a dose-dependent manner. However, there was no appreciable effect upon overexpression of catalytically inactive C1651A mutant suggesting that the protease activity of PLpro may not be essential for inhibiting IFN responses (Figure 3.2A and B).

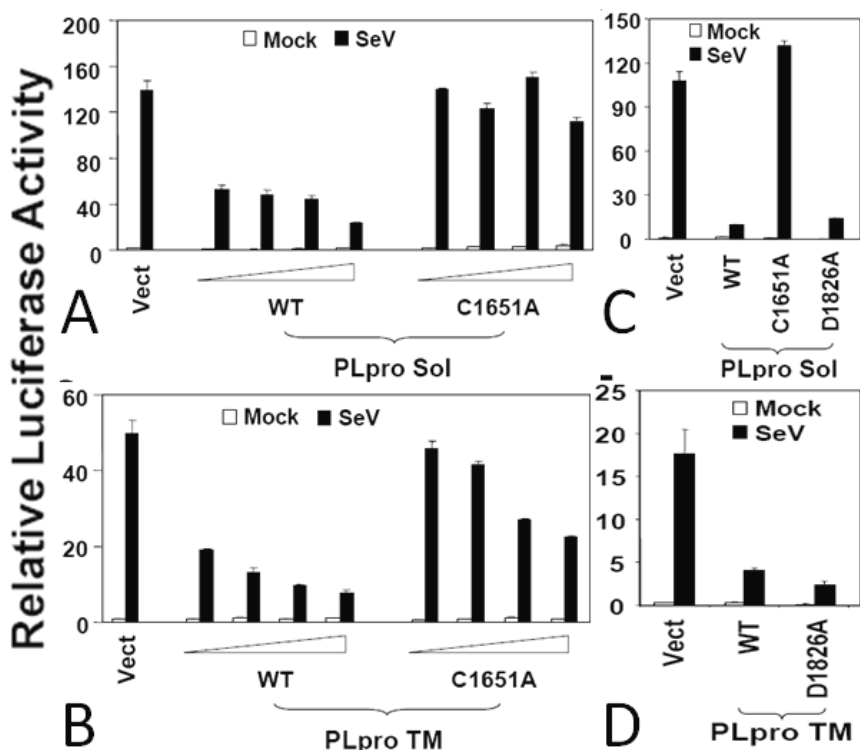


**Figure 3.2 Inhibition of PRR stimulated IFN- $\beta$  promoter is independent of PLpro protease activity.** **A** and **B**. IFN- $\beta$  promoter activity in HEK 293 cells transfected with increasing amounts of WT or C1651A mutant PLpro-Sol-expressing plasmid (**A**) or increasing amounts of WT or C1651A mutant PLpro-TM (**B**), and supplemented with a control vector to keep the total amount of DNA transfected constant, then mock-infected or infected with SeV for 16 hr. **C** and **D**. SeV induced activation of IFN- $\beta$  promoter in HEK293 cells with and without expression of WT or various mutant forms of PLpro-Sol (**C**), or of WT or D1826A mutant form of PLpro-TM (**D**).

However, when PLpro was expressed in conjunction with its downstream hydrophobic transmembrane domains (PLpro-TM), the C1651A mutant was still able to inhibit activation of the IFN- $\beta$  promoter by SeV (Figure. 3.2A and B ) albeit less potently. To resolve whether PLpro need its protease activity for inhibiting IFN responses, I tested another catalytically inactive mutant, D1826A. The D1826A mutant PLpro suppressed activation of IFN- $\beta$  promoter as efficiently as the WT protein, regardless of whether it was expressed in the context of PLpro-Sol or -TM (Figure 3.2C and D). This data indicates that the protease activity of PLpro is not essential for inhibition of IFN response. It is likely that PLpro-sol C1651A mutant does not inhibit IFN induction due to mis-folding/solubility independent of its disruption of the protease active site. Consistent with this hypothesis, my collaborators have noticed a significant reduction in the yield of PLpro-Sol containing the C1651A mutation when purifying the protein from *E.Coli*. This set of data shows that the PLpro domain of SARS-CoV is capable of inhibiting the induction from IFN- $\beta$  promoter independent of the protease activity.

### *3.3.3 PLpro inhibits transcription from IFN- $\beta$ promoter by affecting the activation of transcription factor of IRF3.*

Transcriptional activation of IFN- $\beta$  promoter is dependent on the latent cellular transcription factor IRF3. To determine whether PLpro inhibition of the IFN- $\beta$  promoter is mediated through suppression of IRF3, luciferase reporter assays were carried out utilizing a well characterized IRF3-responsive synthetic promoter, 55C1B , stimulated by polyI:C treatment or SeV challenge.

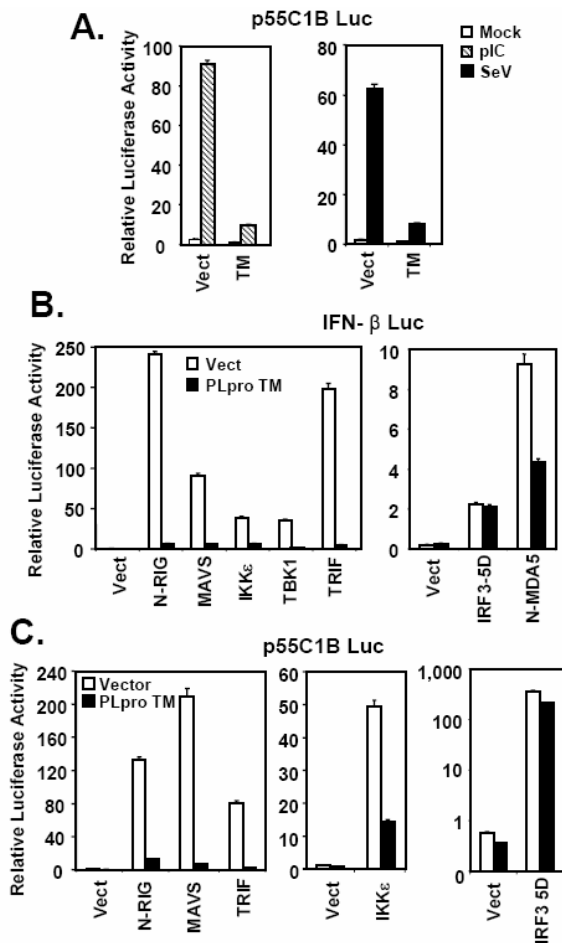


**Figure 3.3 PLpro inhibits transcription from IFN- $\beta$  promoter by affecting transcription factor IRF3.** **A.** Activation of p55C1B, an IRF3-dependent synthetic promoter, by medium polyI:C (hatched bars) or SeV infection (solid bars) in HEK293-TLR3 cells with expression of SARS-CoV PLpro-TM (TM) or a control vector (Vec). **B** and **C.** Activation of IFN- $\beta$  (**B**) and p55C1B (**C**) promoters by ectopic expression of various signaling molecules within TLR3 and RIG-I/MDA5 pathways at or above the level of IRF3 in HEK293 cells with (solid bars) or without (empty bars) expression of SARS-CoV PLpro-TM. N-RIG and N-MDA5 denote the CARD domain of RIG-I and MDA5, respectively.

PolyI:C or SeV stimulated activation of 55C1B promoter was almost completely ablated by ectopic expression of PLpro-TM (Figure. 3.3A). IRF3 is activated by phosphorylation of its C-terminal domain by two noncanonical I $\kappa$ B kinases, TBK1 and IKK $\epsilon$ . The kinase

activities of TBK1 and IKK $\epsilon$  are stimulated by signaling from PRRs including RIG-I/MDA5 and TLR3 and by their adaptor proteins MAVS and TRIF respectively. To dissect the PLpro induced blockade of IRF3 activation, the PLpro blockade was studied using the above mentioned reporter assays (both IFN- $\beta$  and p55C1B promoter) in cells expressing PLpro-TM along with signaling proteins known to participate upstream of IRF3 activation, in RIG-I/MDA5 and TLR3 pathways. Consistent with earlier results, PLpro-TM strongly inhibited the activation of IFN- $\beta$  promoter in presence of constitutively active CARD domain of RIG-I (N-RIG) or MDA5 (N-MDA5) (Figure 3.3B). PLpro-TM blockade was not relieved by ectopic expression of MAVS, TRIF, TBK1, or IKK $\epsilon$  (Figure 3.3B). In contrast, the constitutively active, phospho-mimetic IRF3 mutant, IRF3-5D, was able to relieve PLpro-TM induced blockade from IFN- $\beta$  promoter to a level that was comparable to that in cells transfected with a control vector (Figure 3.3B). Similar results were obtained when p55C1B-Luc was used in place of IFN- $\beta$ -Luc to probe the signaling (Figure 3.3C). The results from these experiments support the conclusion that PLpro disrupts TLR3 and RIG-I/MDA5 signaling by acting at a level that is downstream of the IRF3 kinases and proximal to IRF3.

#### 3.3.4 Conditional expression of PLpro in HeLa-Tetoff cell modulate ISG56

To unravel the mechanisms underlying the SARS-PLpro mediated disruption of cellular IFN responses, I developed tetracycline regulated HeLa cells that conditionally express PLpro-TM under the control of the Tet-Off promoter.

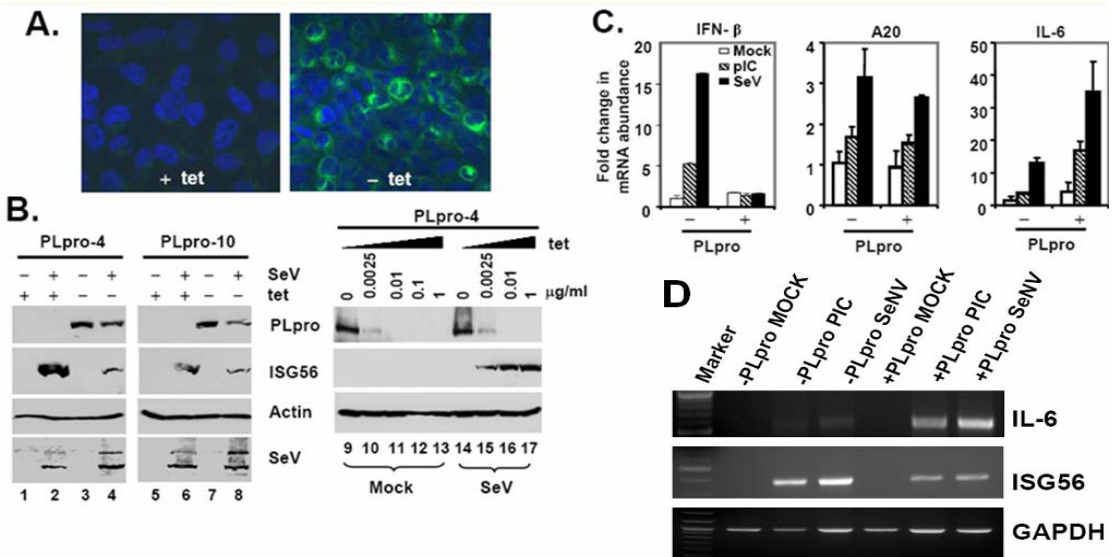


**Figure 3.4 Conditional expression of PLpro in HeLa-Tetoff cells modulate ISG56.** **A.** Immunofluorescence staining of PLpro-TM in HeLa PLpro-4 cells cultured in the presence or absence of 2  $\mu\text{g}/\text{ml}$  tetracycline for 3 days followed by confocal microscopy. PLpro-TM showed green fluorescence staining (detected with a V5 tag antibody), while nuclei were counterstained blue with DAPI. **B.** The left panels show HeLa PLpro-4 and PLpro-10 cells that were cultured with and without tetracycline for 3 days and subsequently mock-infected or challenged with SeV for 16 hr prior to cell lysis and immunoblot blot analysis of PLpro (using a V5 tag antibody), ISG56, actin and SeV. The right panels show HeLa PLpro-4 cells that were cultured in the indicated concentrations of tetracycline for 3 days prior to mock infection (lanes 9 through 13) or infection of SeV (lanes 14 through 17) for 16 hr. Expression of PLpro-TM, ISG56, and actin were determined by immunoblot analysis. **C.** Real-time RT-PCR analysis of IFN- $\beta$  (left), A20 (middle), and IL-6 (right) mRNA transcripts in HeLa PLpro-4 cells repressed or induced for PLpro-TM expression, and mock treated (empty bars), treated with 50  $\mu\text{g}/\text{ml}$  polyI:C in culture medium (hatched bars), or infected with SeV (solid bars) for 16 h. mRNA abundance was normalized to cellular 18S ribosomal RNA. Fold changes were calculated by dividing the normalized mRNA abundance under various treatment conditions by that of the mock-treated cells without PLpro expression. **D.** Semi-quantitative RT-PCR analysis

Two clonal cell lines, PLpro-4 and PLpro-10 showed PLpro expression that was tightly coupled to the concentration of tetracycline in the culture medium (Figure. 3.4B). Confocal microscopy revealed PLpro-TM was present in the cytoplasm distributed closely around the nucleus similar to SARS-CoV nsp3 in infected cells (Figure. 3.4A,

right panel). Consistent with my previous results, expression of PLpro under tetracycline modulation significantly reduced the SeV stimulated endogenous ISG56 expression in dose dependent manner (Figure. 3.4B, Right and Left panels). However, PLpro did not interfere with SeV replication, as similar levels of SeV proteins were detected, regardless of PLpro-TM induction status (Figure. 3.4B, SeV panel). A similar inhibition of polyI:C induced ISG56 expression by PLpro-TM was also observed in these cells (Figure. 3.5A, ISG56 panel, compare lane 6 vs 2) regardless of signaling pathway activated (TLR3 or MDA5) determined by delivery route of polyI:C either added direct to culture medium or introduced into cells by transfection, respectively (Alexopoulou et al., 2001; Kato et al., 2006). Real-time RT-PCR analysis showed that PLpro-TM expression abolished the up regulation of IFN- $\beta$  mRNA upon polyI:C or SeV stimulation, while the levels of NF- $\kappa$ B-dependent A20 mRNA transcripts were not affected (Figure. 3.4C, left and central panels). However, PLpro-TM increased the induction of IL-6 mRNA by polyI:C or SeV (Figure. 3.4C, right panel) in these cell lines. The above results suggest that SARS-CoV PLpro specifically targets the IRF3 arm of IFN responses for inhibition.

### *3.3.5 SARS-CoV PLpro inhibits IRF3 activation by interfering with its phosphorylation, dimerization and nuclear translocation*

PRR dependent IRF3 activation involves hyperphosphorylation, homodimerization, nuclear translocation and association with CBP/p300 to generate transcriptional activity necessary for the expression of interferon stimulatory genes. In order to understand the mechanism of PLpro induced IRF3 inhibition, IRF3 activation

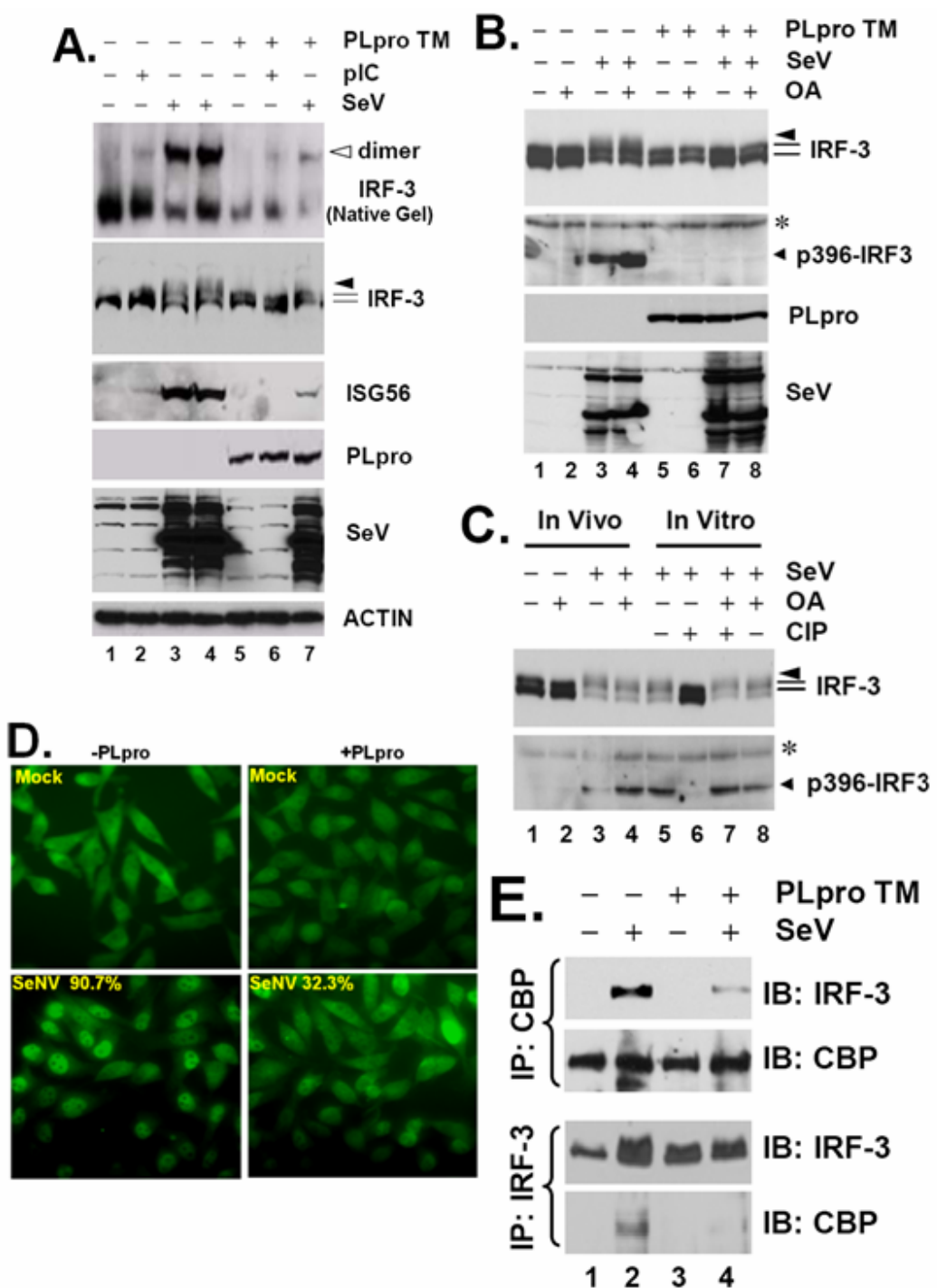


**Figure 3.5. SARS-CoV PLpro inhibits IRF3 activation by interfering phosphorylation, dimerization and nuclear translocation.**

**A.** Expression of PLpro-TM in HeLa PLpro-4 cells was controlled by growing them with in presence and absence tetracycline 3 days prior to 50 µg/ml polyI:C treatment for 6 hr, or SeV challenge for 16 hr. Cell lysates were separated on native PAGE followed by immunoblot

analysis to detect IRF3 monomer and dimer forms (top panel, empty arrow indicates IRF3 dimer), or subjected to SDS-PAGE and immunoblot analysis of IRF3, ISG56, PLpro, SeV and Actin (lower panels). **B.** HeLa PLpro-4 cells expressing PLpro-TM were mock-infected or infected with SeV for 16 hr followed by 0.05 µg/ml of okadaic acid (OA) in the culture medium during last 4 hr of SeV infection. Cells were then harvested for immunoblot analysis of IRF3, p396-IRF3, PLpro (anti-V5), and SeV. \* denotes a nonspecific band. **C.** Lanes 1 through 4, HeLa cells were mock-infected or infected with SeV for 16h. Where indicated, OA was included in the last 4hr duration of infection/mock infection. Lanes 5 through 8, Cell lysates of HeLa cells infected with SeV were mock-treated, treated with CIP, or OA, or CIP in the presence of OA, as indicated in the Experimental Procedures. IRF3 and p396-IRF3 were detected by immunoblot analysis. \* denotes a nonspecific band. **D.** Immunofluorescence staining of IRF3 subcellular localization in HeLa PLpro-4 cells repressed (upper panels) or induced (lower panels) for PLpro-TM expression, and mock-infected (left) or infected (right) with SeV for 16hr. Numbers in SeV-infected cells were the averages of the percentage of cells that had IRF3 nuclear translocation and were counted from ten random fields (40 X magnification). **E.** HeLa PLpro-4 cells under induction/repression of PLpro-TM were mock-infected or infected with SeV for 16hr. Cell lysates were subjected to immunoprecipitation with a rabbit anti-CBP antibody (upper panels) or with a rabbit anti-IRF3 antiserum (lower panels). The immunoprecipitates were separated on SDS-PAGE, followed by immunoblot analysis of IRF3 (using mAb anti-IRF3) or CBP (using a rabbit anti-CBP antibody).

status was assessed by its phosphorylation, oligomerization and its intracellular localization in PLpro-inducible HeLa-Tetoff cells following polyI:C or SeV stimulation. The expression of PLpro-TM significantly reduced IRF3 phosphorylation (IRF3 panel) and dimerization (native gel panel, Figure. 3.5A). Expression of PLpro-TM also inhibited SeV-induced phosphorylation of IRF3 on Ser396 (Figure. 3.5B, compare lane 7 vs 3), a critical phospho-acceptor site required for in vivo activation of IRF3 in response to virus and dsRNA . The decreased phosphorylation of IRF3 observed may not be due to a cellular phosphatase, as treatment of PLpro-expressing cells with a potent PP2A phosphatase inhibitor, OA (Stertz et al., 2007) , failed to restore SeV-induced IRF3 phosphorylation (Figure. 3.5B, compare lane 8 vs. 7 and 4). As positive controls, treatment of SeV-infected HeLa cell lysates with CIP effectively de-phosphorylated IRF3

(Figure. 3.5C, compare lane 5 vs. 6). The CIP activity, however, was completely blocked by OA (Figure. 3.5C, compare lane 7 vs. 6). Consistent with the inhibition on IRF3 phosphorylation and dimerization, SeV- induced IRF3 nuclear translocation (Figure. 3.5D), and its association with the transcriptional co-activator CBP (Figure. 3.5E, compare lane 4 vs 2) was greatly reduced in PLpro-expressing cells.

### 3.3.6 SARS-CoV PLpro physically interacts with IRF3

To explain PLpro mediated phosphorylation/dimerization/nuclear translocation of IRF3, co-immunoprecipitation (co-IP) experiments were performed to see whether PLpro physically interacts with IRF3. As evident from Figure. 3.6A (right panel), PLpro-TM interacts with IRF3. The association of PLpro with IRF3 appears to be specific, as it was detected only by IRF3 antiserum, but not by control serum (Figure. 3.6A, right panels, compare lanes 3 and 4 vs. 7 and 8). Furthermore, consistent with their ability to inhibit IRF3 activation, both the protease-deficient mutant forms C1651A and D1826A of PLpro-TM all interacted with IRF3 (Figure. 3.6B). In the case of PLpro-Sol, while D1826A substitution had no effect on its association with IRF3, the C1651A Sol mutant lost its ability to interact with IRF3 (Figure. 3.6C). This is in agreement with the fact that D1826A PLpro Sol is similar to WT protein in inhibiting IFN induction (Figure. 3.2B), while C1651A PLpro Sol is no longer able to do so (Figure. 3.2D and 3.2D). Addition of the downstream TM domains to PLpro may somehow protect PLpro C1651A substitution associated misfolding, thereby allowing C1651A PLpro-TM to retain its ability to interact with IRF3. Next, it was of interest to determine whether PLpro interacts with IRF3 5D, a

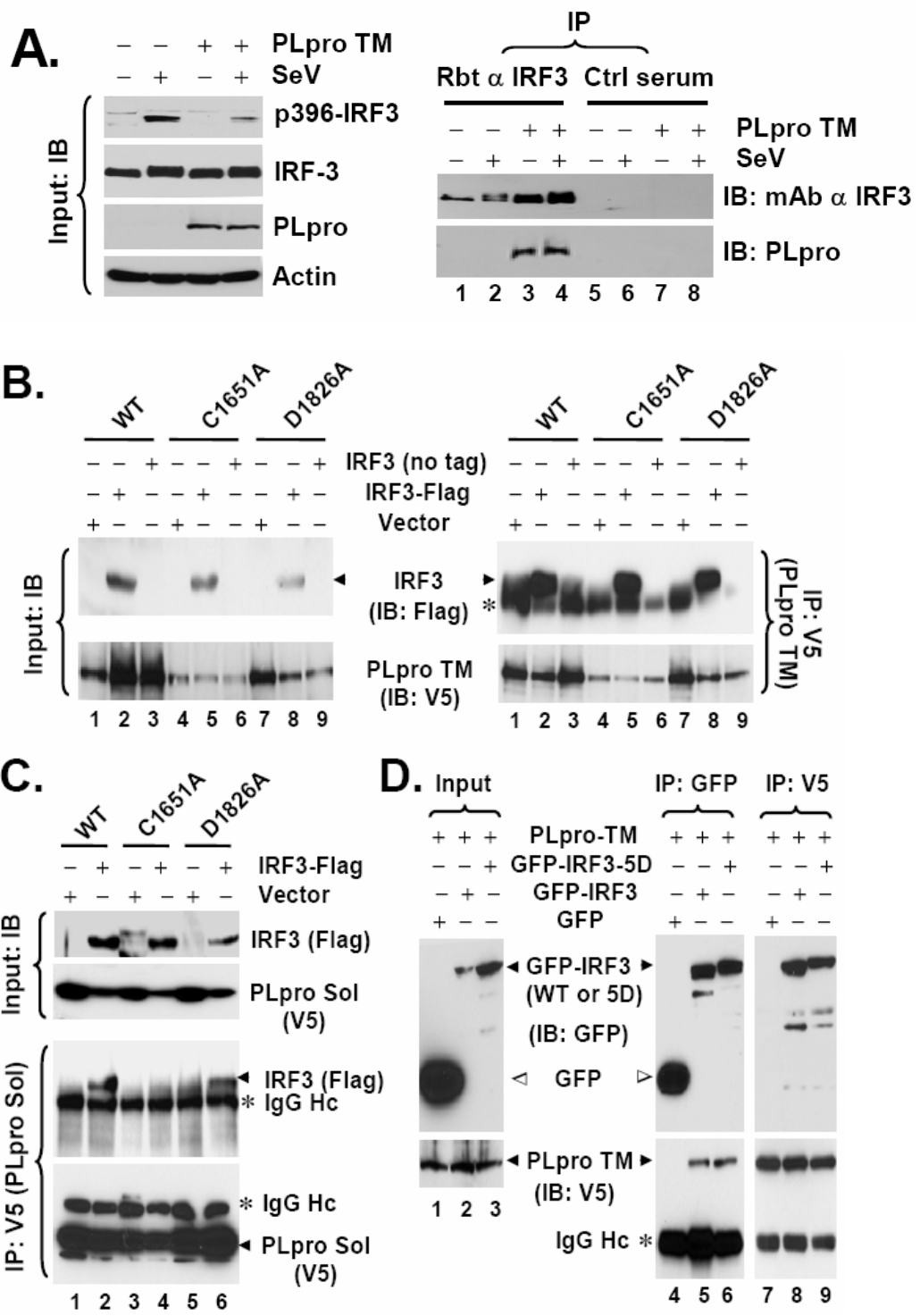


**Figure 3.6 SARS-CoV PLpro interacts with IRF3 A.** HeLa PLpro-4 cells were cultured

to repress or induce PLpro-TM expression and subsequently mock-infected or infected with SeV for 16 hr. In left panels, expression of p396-IRF3, total IRF3, PLpro and actin proteins in cell lysates were determined by immunoblot analysis. In right panels, cell lysates were subjected to immunoprecipitation with a rabbit anti-IRF3 antibody (lanes 1 through 4) or a control rabbit serum (lanes 5 through 8). The immunoprecipitates were separated on SDS-PAGE, followed by immunoblot analysis of IRF3 (using mAb anti-IRF3) and PLpro (using mAb anti-V5 tag). **B.** HEK293 cells were transfected with WT (lanes 1 through 3), C1651A (lanes 4 through 6), or D1826A (lanes 7 through 9) PLpro-TM, respectively, and where indicated, along with an empty vector (lanes 1, 4, and 7), or a vector expressing Flag-IRF3 (lanes 2, 5, and 8) or untagged IRF3 (lanes 3, 6, and 9). Cell lysates were immunoprecipitated with anti-V5 (PLpro-TM), followed by immunodetection of Flag-IRF3 (anti-Flag) or PLpro-TM (anti-V5) (right panels). \* denotes IgG heavy chain. Immunoblot analysis of input for Flag-IRF3 and PLpro-TM is shown in left panels. All 3 forms of PLpro-TM interacted with IRF3. **C.** HEK293 cells were transfected with WT (lanes 1 and 2), C1651A (lanes 3 and 4), or D1826A (lanes 5 and 6) PLpro-Sol, respectively, and where indicated, along with an empty vector (lanes 1, 3, and 5) or a vector expressing Flag-IRF3 (lanes 2, 4, and 6). Cell lysates were immunoprecipitated with anti-V5 (PLpro-Sol), followed by immunodetection of Flag-IRF3 (anti-Flag) or PLpro-Sol (anti-V5) (lower panels). Immunoblot analysis of input for Flag-IRF3 and PLpro-Sol is shown in upper panels. Note that WT and D1826A PLpro-Sol interacted with IRF3, while C1651A PLpro-Sol did not. **D.** HeLa PLpro-4 cells induced for PLpro-TM expression were transfected with GFP, GFP-IRF3, or GFP-IRF3-5D, respectively. Cell lysates were subjected to Co-IP experiments using either GFP antibody or V5 antibody for immunoprecipitation, followed by immunoblot analysis of the immunoprecipitates using anti-GFP or anti-V5 antibodies. Note that both GFP-IRF3 and GFP-IRF3-5D were associated with PLpro-TM (detected by anti-V5), while free GFP was not.

constitutively active mutant that mimics the C-terminal phosphorylated IRF3. This is important because IRF3 5D was alone able to relieve PLpro mediated repression from IFN- $\beta$  promoter in the reporter assays (Figure. 3.3B and C). Both WT and 5D versions of GFP-tagged IRF3 interacted with PLpro-TM, while the GFP control did not (Figure. 3.6D). This data suggests the PLpro interaction with IRF3 may not be phospho-specific, i.e., PLpro does not appear to discriminate between phosphorylated or non-phosphorylated form of IRF3.

### **3.4 DISCUSSION**

Interferon production in response to coronavirus infection has been a controversial topic IFN-transcripts or IFN- $\beta$  promoter activity were not detected in response to MHV and SARS-CoV infection leading to the belief that viral mediated active suppression of interferon was not present in coronaviruses or interferon response is suppressed very early during infection, or the viruses were “invisible” to host detection by some unknown mechanisms (Garlinghouse et al., 1984; Pewe et al., 2005; Zhou and Perlman, 2007). In agreement with the hypotheses of active interference in the IFN response, several SARS-CoV proteins like ORF3b, ORF6, and nucleocapsid (N) and nsp1 have been shown to act as IFN antagonists, based on their ability to inhibit IRF3 activation step of anti-viral signaling.

Since viral proteases such as NS3/4A of HCV and N-Pro of BVDV have interferon antagonism activities (Chen et al., 2007b; Foy et al., 2005; Li et al., 2005a; Li et al., 2005c), I searched for similar protein/s encoded by SARS-CoV that could suppress host interferon response. Surprisingly, SARS-CoV PLpro has deubiquitinase and De-ISgylation activities in addition to protease activity, raising questions about their functional significance which prompted me to test for a possible role in interferon antagonism by simple cell-based reporter assays. By a series of experiments, I was able to demonstrate that PLpro suppresses IFN induction by acting at the level of the IRF3 kinases, TBK1 and IKK $\epsilon$ , and inhibits the induction of IRF3-dependent genes via both TLR3 and RIG-I/MDA5 pathways (Figures. 3.1 through 3.4). Using transient expression of PLpro and PLpro protease mutants, it was clear that that PLpro inhibitory effect was

dose-dependent (Figure 3.2A and 3.2B) and does not rely on its protease activity to disrupt IFN responses (Figure 3.2C and 3.2D) unlike NS3/4A of HCV and GBV-B or 3ABC of HAV where protease activity is important for the interferon antagonistic function. To better understand the role of PLpro in IFN inhibition, I was able to generate HeLa tetoff cell lines where PLpro expression is tunable by tetracycline. Using these cell lines, I determined that PLpro decreased SeV and Poly(I-C) induced phosphorylation and PLpro interacts with IRF3 (Figure 3.6) subsequently affecting its dimerization and nuclear translocation of IRF3 (Figure 3.5), all prerequisites for its role as a transcription factor to turn on the type I IFN response. The involvement of PLpro-IRF3 interaction in PLpro's IFN antagonist function is supported by the fact that the ability to interact with IRF3 by various PLpro mutants (Figure 3.6B and 3.6C) seems to correlate with their capability of inhibiting IFN response (Figure 3.2C and 3.2D). Specifically, the C1651A PLpro-Sol mutant that loses its inhibitory effect on IFN response (Figure 3.2 A and B) is also unable to interact with IRF3 (Figure 3.6C). However, the precise mechanism by which this interaction contributes to inhibition of IFN response is not known. Given limited levels of IRF3 in the cells, it is possible this interaction may help PLpro to sequester IRF3 away from the kinases preventing its phosphorylation or interaction with other cellular partners essential for IRF3 nuclear translocation. Based on the restoration of IFN response by IRF3-5D transfection (Figure 3.3B and 3.3C), PLpro acts at a step before the phosphorylation of IRF3, and it does not seem to inhibit the downstream IFN induction once IRF3 is phosphorylated and activated. A potential caveat in this

experiment is that expression of transfected phospho-mimetic IRF3-5D may be so high that it might overcome PLpro mediated sequestration.

At present, we do not know whether the DUB/De-ISgylation activity contributes to PLpro's function in disrupting IRF3 activation. DUB/De-ISgylation enzymes inhibit innate immune signaling independent of their DUB/De-ISGylation function. For instance, the ubiquitin editing enzyme A20 acts through its C-terminal zinc finger domain of the ubiquitin ligase to inhibit IRF3-dependent gene expression, as deletion of the N-terminal DUB domain has no significant effect on the inhibitory effect of A20. Similarly, the ubiquitin-specific protease Ubp43 negatively regulates IFN signaling through its interaction with the IFNAR2 subunit and independent of its isopeptidase activity towards ISG15. Although we have shown that its protease activity is dispensable, thus far we have not been able to identify specific mutation(s) in PLpro that allow us to dissect the protease activity of PLpro from its DUB activity. The D1826A protease-inactive mutant PLpro loses ~99% of the DUB activity *in vitro*, yet still acts as efficiently as the WT protein to inhibit the IFN response (Figure 3.2B and 3.2D).

Although the biological relevance of this newly discovered function for these SARS-CoV proteins remains to be carefully determined in the context of SARS-CoV infection, it suggests that limiting IRF3-dependent innate immunity is important for establishment of SARS-CoV infection. However, it will be necessary to determine whether PLpro can inhibit IRF3 activation when expressed in the context of the entire nsp3 protein. However, thus far we have not been able to clone the full-length nsp3 cDNA in a mammalian expression vector. The reasons for this remain unclear, but could

be due to a toxic effect of nsp3 in *E. coli*. One may also speculate that PLpro, as an essential viral protease involved in viral replication, is sequestered within the replication complex in SARS-CoV-infected cells, preventing its binding to IRF3. Future reverse genetics approaches engineering viable SARS-CoV mutants, which carry substitutions in PLpro that disrupt its interaction with IRF3 while retaining the protease activity, would help us to fully understand the contribution of PLpro-IRF3 interaction in regulation of host innate immunity in SARS-CoV infected cells.

## CHAPTER 4: HEPATITIS C VIRUS

### 4.1 FLAVIVIRIDAE

#### 4.1.1 Classification

The Flaviviridae group of viruses derived their name from the color yellow (flavus) as they cause yellow fever characterized by jaundice like symptoms (yellowing of palms and eyes due to dysfunctional bile secretion). Yellow fever virus (YFV) was first discovered by Walter Reed member of this group when it was shown to transmit through filtered patient sera and by mosquitoes. The family Flaviviridae includes three genera namely flavivirus, pestivirus and hepacivirus (Figure. 4.1). Though, the virus members in these three genera share similar structural and genomic organization, they

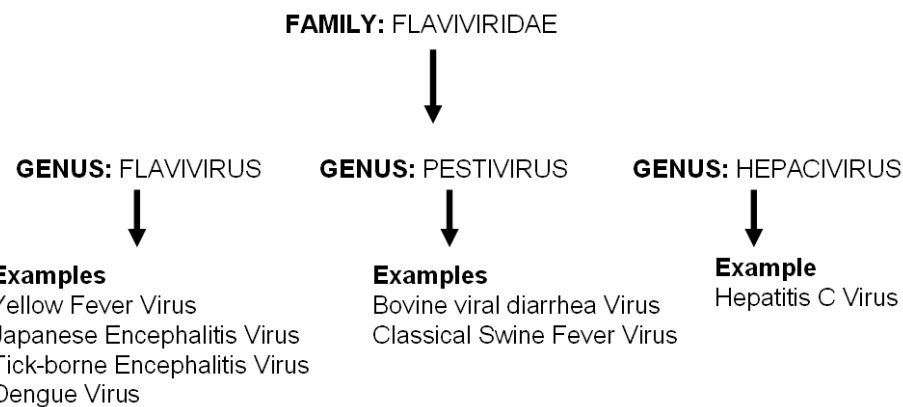


**Figure 4.1 Classification of Flaviviridae.**  
differ in their biological characteristics of pathogenesis and show no serological cross reactivity (Lindenbach et al., 2006).

## **4.2 HEPATITIS C VIRUS**

Hepatitis C virus (HCV) infection is a major problem worldwide that affects 170 million people causing persistent infection associated with cirrhosis of liver leading to hepatocellular carcinoma. The detailed mechanism of HCV pathogenesis leading to chronic liver disease and development of liver cancer is still not understood. In United States, HCV infection is responsible for 10,000-20,000 deaths annually (Alter and Houghton, 2000; Alter and Seeff, 2000). The development of novel and effective therapies for HCV infection has been partly impeded due to the lack of a good disease model. Presently, the chimpanzee (*Pan troglodytes*) is the best model to study HCV viral clearance, analysis of immune response to infection and the development of vaccines (Lanford et al., 2001). Current HCV therapies include interferon treatment which is inefficient in many patients and is associated with side effects. Small molecule inhibitors to proteases become obsolete as the virus develops drug resistance quickly (De Francesco and Migliaccio, 2005). Combination treatment with ribavirin along with IFN- $\alpha$  and development of pegylated interferon where recombinant IFN- $\alpha$  is attached to poly ethylene glycol (PEG) resulted in better response to virus in some patients (Feld and Hoofnagle, 2005; McHutchison et al., 2002a; McHutchison et al., 2002b).

### *4.2.1 Genome organization, expression strategies and virus life cycle*

HCV is a hepacivirus member of Flaviridae family that has a positive sense RNA of ~9.3 kb as genome; it was identified as the blood borne causative agent of non-A, non-B viral hepatitis in 1989. Inflammation of the liver is observed after 2 months of infection

(Choo et al., 1989; Feinstone et al., 1975; Hoofnagle, 2002; Neumann et al., 1998).

Hepatocytes appear to be the major target of HCV replication *in vivo* though the virus can replicate in other cell types (Deforges et al., 2004; Forton et al., 2004a; Forton et al., 2004b).

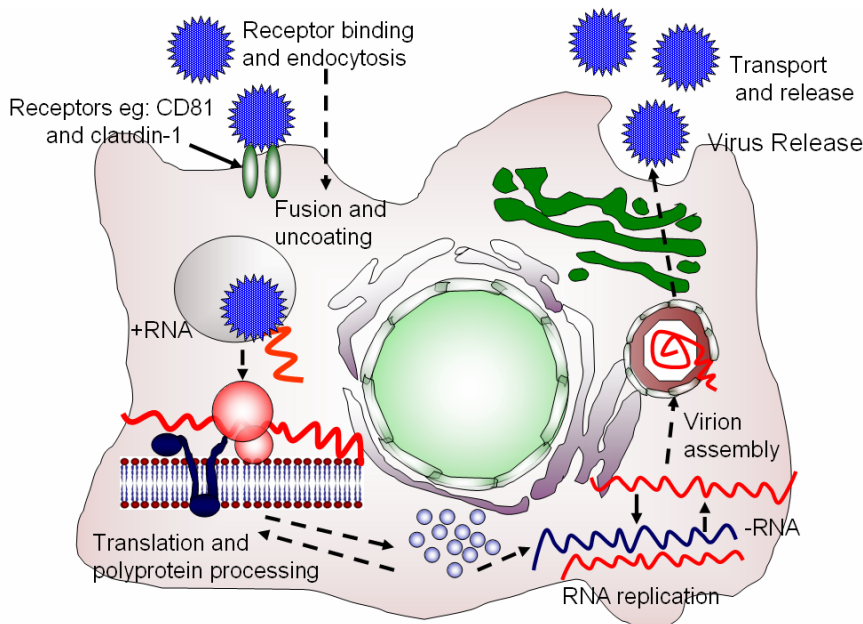


**Figure 4.2 Schematic representation of HCV life cycle.** The virus enters by endocytosis involving CD81 and claudin-1 like receptors. Once internalized the virus membrane fuses with endosomal membrane releasing the genomic RNA, which undergoes translation to produce virus polyprotein. The polyprotein is processed as explained in earlier slide and resulting functional protein products that serve in replication of the genomic and structural protein leading to the generation of mature virus particles. The mature virus particles bud out from the cell membrane. Virus life cycle takes place in cytoplasm.

The cellular entry of the virus involves receptor mediated endocytosis and cell surface receptors CD81, LDL, SR-BI, claudin-1 (CLDN1) and occludin (Calvo et al., 1997; Calvo and Enrich, 2000; Enjoji et al., 2000; Evans et al., 2007; Pileri et al., 1998; Ploss et al., 2009) are thought to help the virus in docking and internalization. Once

internalized, the viral membrane undergoes fusion with endosomal membrane triggered by the acidic environment to release the genomic RNA into cytoplasm (Figure. 4.2). The HCV genome encodes a single long polyprotein flanked by short 5' and 3' non-coding regions (NCR). An internal ribosome entry site (IRES) present in the 5' NCR aids in the translation initiation during polyprotein expression in the absence of a 5' cap.

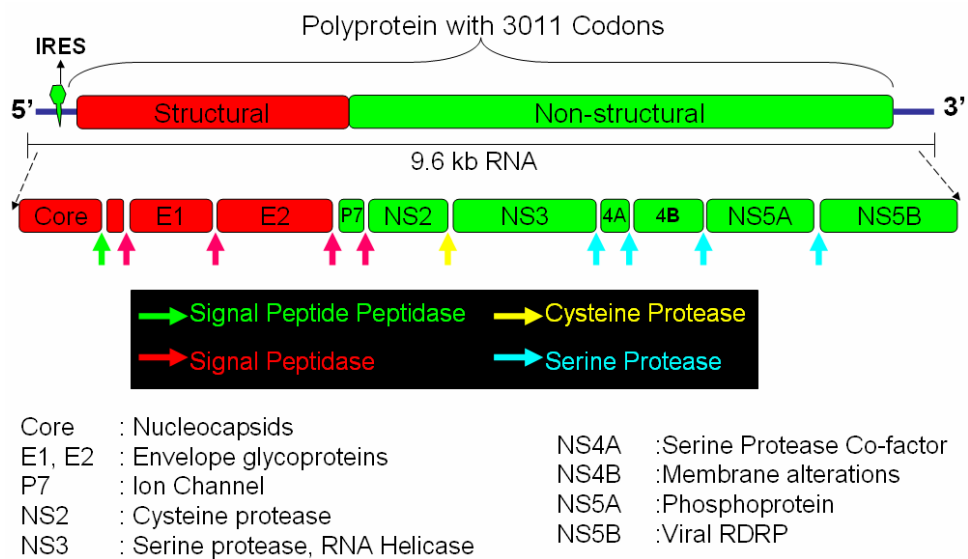


**Figure 4.3 Schematic representation of HCV genome organization.** HCV encodes a single polyprotein from its ~10 kb genomic RNA. The structural proteins are present at N-terminus of the polyprotein and processed by host signal peptidase and signal peptide peptidase. The non-structural proteins constitute rest of 2/3 of the polyproteins and processed by viral cysteine and serine proteases.

The polyprotein is proteolytically processed to functional products including polymerase and other proteins. The structural proteins, E1, E2 and core, are present at the N-terminus of the polyprotein are proteolytically processed into functional products by host signal peptidase and signal peptide peptidases (Figure. 4.3). The remaining part of the polyprotein carries the non-structural proteins (NS) and is processed into functional

units by NS2, a cysteine protease and NS3, a serine protease. The NS3 also has DExH/D RNA helicase domain at the C-terminus. NS4A act as serine protease cofactor. NS3/4A is responsible for cis- and trans-cleavage of other non structural proteins. NS4B helps in the membrane alterations. NS3/4A can cleave proteolytically host anti-viral signaling adaptor protein molecules (TRIF and MAVS) and thus can help the virus evade the innate immune system of the host. NS5A interacts with many cellular proteins including PKR (Gale et al., 1998). NS5B is the replication machinery encoding the RNA dependent RNA polymerase (RdRp) (Figure 4.3). The +ve sense, genomic RNA serves as template for –ve strand RNA synthesis, and from the –ve strand RNA, progeny genomic RNAs made which are encapsidated into mature viral particles that bud out from the cell membrane to infect neighboring cells. The entire life cycle of HCV takes place in cytoplasm (Lindenbach and Rice, 2005).

#### *4.2.2 HCV and Innate Immune response*

The mechanism by which HCV evades host innate immunity leading to persistent infection and disease progression is not well understood. DNA micro array analysis have indicated a dramatic increase in various interferon response genes related to all three classical interferon antiviral pathway in the liver of chimpanzees infected with HCV indicating a biphasic mechanism of viral clearance reflecting the action of both innate and adaptive immune response. These studies provided an insight into the response of the liver to a hepatotropic viral infection (Bigger et al., 2001). In order to survive in the host, HCV has evolved to resist antiviral defenses with several evasive mechanisms that

include suppression of interferon production. Several viral encoded proteins are shown to inhibit interferon response by inactivating key proteins in anti-viral signaling pathways by direct or indirect interaction.

NS5A has been shown to interact with PKR. Interferon sensitivity-determining region (ISDR) present in NS5A was shown to mediate IFN resistance by directly interacting with one or more cellular proteins associated with the IFN-mediated antiviral response. It is shown that NS5A abolished PKR activity through a direct interaction with protein kinase catalytic domain by the help of ISDR (Gale et al., 1998). The NS3/4A protease was shown to block RIG-I dependent antiviral signaling. Disruption of NS3/4A protease function by mutation or using a ketoamide peptido-mimetic inhibitor relieved the blockade and restored the IRF3 phosphorylation after cellular challenge with Sendai virus (Foy et al., 2003). HCV RNA replication was enhanced or suppressed when dominant negative or constitutively active IRF3 mutants were ectopically expressed in hepatoma cell lines (Sumpter et al., 2005). Later studies have shown that NS3/4A cleaves mitochondrial antiviral signaling molecule (MAVS) and a toll-interleukin-1 receptor domain-binding molecule (TRIF or TICAM-1), the adapter proteins for RIG-I and TLR3 respectively (Foy et al., 2005; Li et al., 2005b; Loo et al., 2006). This specific mechanism by which NS3/4A protease disarms both TLR3 and RIG-I mediated anti-viral signaling may have profound implications in causing persistent and chronic HCV infection (Figure.4.2). A dynamic model has been proposed, where the induction of antiviral genes are maximum due to activation of IRF3 at an early stage of infection to stop replicating virus (Loo et al., 2006). However, if the virus is not cleared during an early response,

then it is possible that NS3/4A accumulates to a critical threshold that completely shuts down interferon response by proteolysis of MAVS.

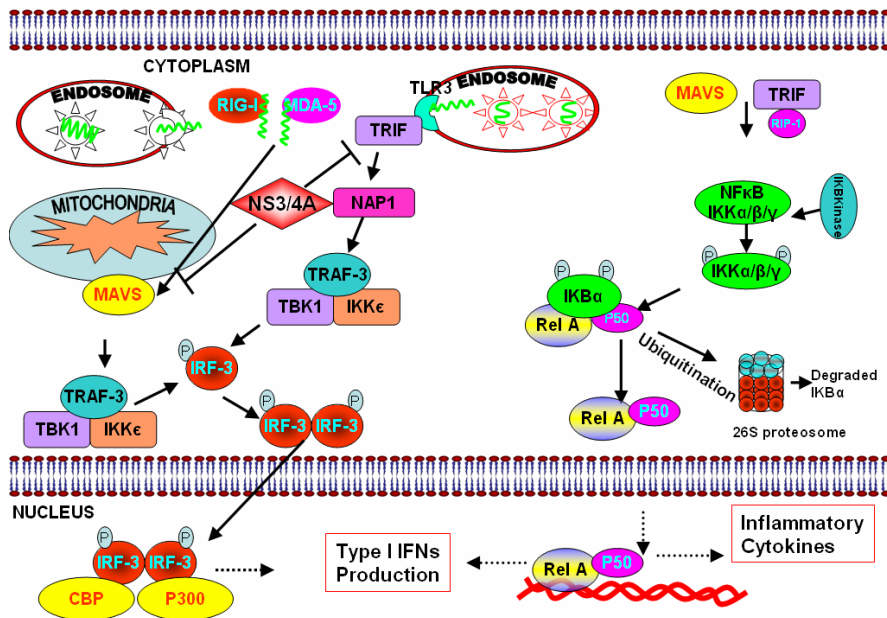


**Figure 4.2 HCV NS3/4A protease inhibits host innate immune response.** HCV NS3/4A protease cleaves the adapter molecules MAVS and TRIF of RIG-I and TLR3 antiviral signaling pathways.

More than one viral protein may be responsible for evasion of immune response in HCV, although protease inhibitors restored function of MAVS but over expression of RIG-I did not restore the interferon response completely suggesting the involvement of some other proteins other than NS3 (Cheng et al., 2006).

#### 4.2.3 *HCV and its Cellular permissiveness*

The genotype strain 2a (JFH1), a virus clone from an individual suffering with fulminant hepatitis was recently shown to replicate efficiently and supports secretion of

viral particles after transfection into human hepatoma cell line (Huh7). These secreted viral particles are proven to be infectious upon re-infection in naïve Huh 7 or Huh 7.5 cells as well as chimpanzees (Wakita et al., 2005). This full length genomic clone was shown to be devoid of any adaptive mutations. Also, many other groups have shown that genotype 2a can produce infectious viral particles (Kato et al., 2003; Zhong et al., 2005). The chimeric full length genomes between different strains such as H77-genotype 1a, J6-genotype 2a, GT3a/JFH1, GT2a/2a (Lindenbach et al., 2005) have shown to secrete viral particles in high titer than parental isolates (Pietschmann et al., 2006). It has been shown that the genotype 1a H77S strain, the most common in US and the most refractory to interferon therapy can secrete viral particles (Yi et al., 2007; Yi et al., 2006). This cell culture system of producing HCV virus in human hepatoma cells provides an excellent tool to study the host-virus interactions which further helps in developing antiviral drugs and vaccines for this medically important pathogen.

Huh7, a human hepatoma cell line established from a hepatocellular carcinoma can be propagated indefinitely in a chemically defined selenium containing medium. Under these conditions, Huh7 was shown to produce a number of plasma proteins and liver specific enzymes. Besides plasma proteins albumin, pre-albumin, fibrinogen, fibronectin etc, two liver specific enzymes G6Pase and FDPase were present in Huh7 when analyzed for carbohydrate metabolizing enzymes (Nakabayashi et al., 1982). Currently, the only cell lines known to support robust HCV replication are Huh7 based cell lines indicating that favorable conditions exist within these cells. Self replicating subgenomic RNAs were shown to replicate in Huh7 cells upon transfection. Such

subgenomic replicon containing cells were subjected to prolonged alpha interferon treatment resulting in cell lines that were completely cured of the subgenomic replicon. Some of the replicon cured cell lines called Huh 7.5 are highly permissive for HCV replication compared to the parent Huh7 and could support both sub-genomic and full length HCV RNA replication (Blight et al., 2002). The increased permissiveness of Huh7.5 hepatoma cell line may be due to their poor ability to produce type 1 interferon (Keskinen et al., 1999). Though normal, healthy hepatocytes are targets of HCV infection, they are not permissive for HCV replication in culture, an example of one such cell line is PH5CH, a non neoplastic human hepatocyte cell line immortalized with simian virus 40 large T Antigen. HCV RNA was detected after 25 days of post infection in a derivative clone of PH5CH (PH5CH8) when infected with serum collected from the HCV infected patient. These cells were further show to respond to interferon treatment (Ikeda et al., 1998; Kato et al., 1996). Huh7 cells do not show an interferon response upon stimulus with PolyI:C due to defective TLR3 pathway whereas Huh7.5 do not respond either to polyI:C or SeV due to a defective RIG-I and TLR3 pathways. However, PolyI:C as well as SeV can stimulate interferon response in PH5CH8 cells indicating the presence of both intact TLR3 and RIG-I antiviral signaling pathways, (Li et al., 2005a). The lack of HCV replication in PH5CH8 and other cultured cells may be at least in part, due to the presence of functional antiviral signaling pathways.

## **CHAPTER 5: ANTIVIRAL SIGNALING BY TLR3 RECEPTOR IS COMPARTMENTALIZED TO MEMBRANE ASSOCIATED HCV REPLICATION COMPLEX**

### **5.1 INTRODUCTION**

Chronic hepatitis C virus (HCV) infection is one of the leading causes of liver disease and cancer affecting 170 million people worldwide (Alter and Houghton, 2000; Alter and Seeff, 2000). Hepatocytes appear to be a major target of HCV RNA replication *in vivo* though HCV has been shown to replicate in other cell types (Deforges et al., 2004; Forton et al., 2004a; Forton et al., 2004b). The double stranded RNA (dsRNA) intermediate produced during the replication of an RNA virus acts as molecular pattern recognized by the host defense system to initiate antiviral innate immune response characterized by the production of type I interferons. Several pattern recognition receptors (PRRs) such as toll like receptor-3 (TLR3), cytoplasmic RNA helicase retinoic acid-inducible gene (RIG-I) and melanoma differentiation-associated gene5 (MDA5) have been implicated in viral dsRNA recognition and interferon induction to curtail virus infections (Kang et al., 2002; Kawai and Akira, 2006a; Kawai and Akira, 2006b; Yoneyama and Fujita, 2004a; Yoneyama and Fujita, 2004b).

Structurally, TLR3 is transmembrane protein, with a single membrane spanning region, an extracellular ectodomain domain (ECD) having ligand binding functionality and a cytoplasmic Toll/IL-1 receptor homology domain (TIR) that harbors signaling potential. Signaling from TLR3 is initiated when two TIR domains come in close

association due to TLR3 dimerization upon dsRNA binding to ECD. Double stranded RNA binds directly to the TLR3 ECD under acidic conditions involving residues H539E and N541A on the glycan free lateral face (Bell et al., 2006a; Bell et al., 2006b; Bell et al., 2005). Apart from these, conserved amino acid residues such as H39, H60 and H108 on the glycan-free surface at the N-terminus interact with consecutive phosphate groups and are also thought to contribute to dsRNA binding (Liu et al., 2008). Normal, hepatocytes in culture are not permissive for HCV replication; an example of one such cell line is PH5CH8, a non neoplastic human hepatocyte cell line immortalized with simian virus 40 large T Antigen. However, cultures of human hepatoma cells such as Huh7 and its derivative Huh7.5 have shown to be permissive to HCV replication atleast in part because of their poor ability to produce type 1 interferons due to defective PRRs (Keskinen et al., 1999). Huh7 cells do not produce interferon upon treatment with PolyI:C, a TLR3 agonist, due to defective TLR3 pathway while Huh7.5 cells do not respond to either polyI:C or SeV due to defects in both RIG-I and TLR3 pathways. In contrast, PolyI:C as well as SeV can stimulate interferon response in PH5CH8 cells indicating the presence of both intact TLR3 and RIG-I antiviral signaling pathways (Li et al., 2005a; Li et al., 2005b). To further investigate the action of PRRS in host defense against HCV infection I investigated the mechanistic role of TLR3 and RIG-I in modulating HCV replication and virus secretion in Huh7 cells.

## **5.2 MATERIALS AND METHODS**

### *5.2.1 Cell lines*

Human hepatoma cell lines Huh7 and its derivative Huh7.5 (Sumpter et al., 2005) were grown and maintained in Dulbecco's minimal essential medium with 10% FBS. The medium for cells expressing TLR3 and its mutant H539E, N541A and P554S contained 2 µg/ml of Blasticidin (*Invitrogen*). The BOSC23 cells (Pear et al., 1993) were cultured in Dulbecco's Eagle's medium containing 10% FBS in 10 cm diameter collagen coated dishes (*Biocoat Collagen I Cellware; Becton Dickinson Labware*).

### *5.2.2 HCV virus*

HCV was produced by DMRIE-C (*Invitrogen*) mediated transfection of *in vitro* transcribed RNA from pJFH-1 containing JFH-1 HCV genotype 2a infectious genome (a gift from T. Wakita, Tokyo Metropolitan Institute for Neuroscience, Tokyo; (Zhong et al., 2005). The virus was concentrated by PEG precipitation as described in (Tscherne et al., 2006). HCV RNA replication studies were carried out using FL-J6/JFH1-5'C19Rluc 2AUbi (Tscherne et al., 2006) capable of supporting efficient genome replication in Huh7 cells. FL-J6/JFH1-5'C19Rluc 2AUbi GND that contains a mutation in the active site of the HCV polymerase was used as a non-replicating control throughout the replication studies.

### *5.2.3 HCV virus infection*

Huh7 and its derivatives with various TLR3 backgrounds were infected by incubating

with HCV for 8 hr at 37 °C using at a known MOI in a minimum volume of DMEM with antibiotics and 10% FBS necessary to cover the cells. After infection, the cells were trypsinized and cultured in fresh plates to various harvest points of 24, 48, 72, 96, 120hr. The supernatant from each time point were stored at 4°C for virus titer assays and the cell lysates were harvested for immunoblot analysis. For each experiment, control cultures were maintained similarly in the absence of virus.

#### *5.2.4 Determination of HCV titer by counting immunofoci*

Huh7.5 cells were used to determine the titers of the virus released into cell supernatants from various cell lines. Briefly, the Huh7 cells were plated in 8 well chamber slides (*Nunc*) at  $5 \times 10^4$  cells/well and infected with 100 µl of 10 fold serial dilutions of cell supernatants. At 24 hr post infection cells were fed with 200 µl of fresh medium. After 72 hr, the cells were washed twice with PBS and fixed with 1:1 methanol-acetone for 15 minutes. Cells were washed with PBS and then incubated with 3% BSA in 1Xpbs for 30 minutes. Cells were incubated with HCV core antibody (*Abcam*) diluted 1:300 in 3% BSA 1xPBS at 37°C for 1 hr. Cells were washed extensively to remove excess core antibody and then incubated with FITC conjugated goat anti mouse secondary antibody (*Southern Biotech*) diluted 1:200 in 3% BSA in 1x PBS at 37 °C for 1hr. After extensive washing to remove excess secondary antibody, the chamber slide was mounted with mounting media containing DAPI (*Vectashield*) and observed by immunofluorescence microscopy (*Zeiss*). Fluorescent foci were counted for each dilution in duplicate.

### *5.2.5 Plasmid constructs*

Retroviral construct pCX4Bsr2xflagTLR3 capable of expressing functional full length TLR3 protein in mammalian cells was constructed by inserting TLR3 cDNA in pCXBsr (Akagi et al., 2002) at *Eco* RI site. Similarly, a construct pCX4Bsr2xflagTLR3ΔTIR encoding a TIR domain deleted version of TLR3 was generated by cloning a 2.3 kb TLR3 PCR fragment amplified using primers ΔTIRf 5'ccggaattcgtagtgaaccgtcag3' and ΔTIRr 5'ccgga attcttattcaaactgttctgtctgtc3'. Constructs containing a single site-specific mutation of either H539E or N541A or P554S were generated in pCX4Bsr2XflagTLR3 backbone using Quikchange kit (*Stratagene*). Mutations were confirmed by DNA sequencing. HCV non-replicating control construct FL-J6/JFH1-5'C19Rluc 2AUbi GND was generated by cloning 2.2 kb *Xba* I/*Rsr* II insert containing GND mutation from pSGR-JFH1-GND (a gift from T.Wakita, (Kato et al., 2003) into similarly digested pFL-J6JFH1-5'c19rluc2ubi (a gift from C. Rice (Tscherne et al., 2006).

### *5.2.6 Retrovirus mediated TLR3 expression*

Recombinant Retroviral constructs encoding vector alone (pCX4-BsrVec), GFP (pCX4-BsrGFP (Chen et al., 2004), wildtype (pCX4-BsrTLR3) and mutant version of TLR3s (pCX4-BsrTLR3ΔTIR, pCX4-BsrTLR3H539E, pCX4-BsrTLR3N541A or pCX4-Bsr TLR3P554S) were co-transfected into Bosc23 cells (at 50-60% confluency) with pCL-Ampho (Naviaux et al., 1996) using Fugene 6 transfection reagent (*Roche*) or TransIT-LT1 (*Mirus*). The medium was replaced with fresh medium at 18 hr after

transfection, and the supernatant containing pseudotype viruses were collected after 48 hr. The supernatant were filtered through 0.45  $\mu$ m filters and used as pseudotype inoculum with 8  $\mu$ g/ml polybrene to infect Huh7 and its derivatives. The inoculum was then replaced with fresh growth medium and the infected cells were allowed to grow at 37°C for 96 hr. populations of cells expressing TLR3 or its mutants were selected in medium containing 2  $\mu$ g/ml of Blasticidin (*Invitrogen*).

#### 5.2.7 *Poly(I:C) and Sendai virus treatments*

To functionally evaluate TLR3 in Huh7 cells and derivative TLR3 expressing cell lines, were treated with PolyI:C (*Sigma*) in medium at 50  $\mu$ g/ml for 24 hr before assaying for polyI:C induced responses. To initiate innate immune signaling through RIG-I, SeV (*Charles Laboratories*) was used to infect cells at 100 HAU/ml.

#### 5.2.8 *Renilla luciferase assay to monitor HCV RNA replication*

Huh7 cells and its derivative TLR3 expressing cell lines were plated in 6 well plates and transfected with *In Vitro* transcribed (*Ambion*) HCV RNA from FL-J6/JFH-5'C19Rluc 2AUbi (Tscherne et al., 2006) and FL-J6/JFH1-5'C19Rluc 2AUbi GND using DMRIE-C reagent (*Invitrogen*) according to manufacturer's instructions. After 6 hr of transfection, the cells were washed, trypsinized and plated in twelve well plates at 1x10<sup>4</sup> cells in 1ml of DMEM and incubated to various time points. The cells were harvested at 6, 24, 48, 72, 96 and 120 hr and were lysed in 1x passive lysis buffer (*Promega*) and stored at -80 °C until assayed for renilla luciferase activity (*Promega*) according to manufacturer's protocol. HCV RNA replication was determined by relative luciferase activity

normalized to 6 hr time point. Data was expressed as mean relative luciferase activity with Standard Deviation from a representative experiment carried out in duplicates. A minimum of three separate experiments were performed to confirm the trend in each observation.

#### 5.2.9 *Confocal Immunofluorescence microscopy*

Four well chamber slides containing  $4 \times 10^3$  cells were mock treated or infected with HCV as described above. After incubation for 72 hr, slides were washed with PBS and fixed with 4% paraformaldehyde for 30min at room temperature. Cells were permeabilized with a solution of PBS containing 0.2% triton-X100 for 15min followed by 30min incubation in 3% BSA in 1x PBS. After a PBS rinse, the slides were incubated with one of the following primary antibodies: mouse anti-dsRNA (a gift from N.Lukacs (Bonin et al., 2000), rabbit anti-NS5B (*Virogen*), goat polyclonal anti-NS3 (*Abcam*), mouse anti-TLR3 (*Imgenex*), rabbit anti-TLR3 (*Anaspec*), rabbit anti-FLAG, mouse anti-FLAG (*Sigma*). The slides were washed thrice with PBS and incubated with one the following Alexa-flour (*Invitrogen*) or FITC conjugated secondary antibodies such as donkey anti-mouse or Goat anti-rabbit (*Southern Biotech*) for 1 hr. Co-localization experiments involving two antibodies staining were performed sequentially with each primary antibody followed by its secondary antibody. After incubation with the final antibody, slides were washed thrice with PBS, allowed to dry, overlayed with a thin layer of Vectashield solution containing DAPI (*Vector Labs*) and then mounted and sealed with

coverslip. The slides were examined under a Zeiss 510 META laser-scanning confocal microscope in the UTMB Optical Imaging Core.

#### *5.2.10 Sub-cellular fractionation of HCV replication complex by sucrose density gradient ultracentrifugation*

Huh7 cells stably expressing TLR3 were infected with JFH1 HCV at 0.5 MOI. After 5 days of infection, cells were washed twice with PBS, homogenized with 5 strokes of dounce homogenizer in 10mM HEPES, 10mM NaCl, 5mM MgCl<sub>2</sub> 5mM DTT pH 7.5 in presence protease inhibitor cocktail (*Roche*). Cell lysate (0.8 ml) was mixed with 60% sucrose (5 ml) in 50mM Hepes, 150 mM NaCl, 5 mM MgCl<sub>2</sub> pH 7.5 with protease inhibitors (TC buffer) and was place at the bottom of Beckmann 12 ml clear Ultra centrifuge tubes. On top this 3 ml of 45% and 3.5 ml 20% sucrose in TC buffer were layered successively. The tubes were spun at 34000 rpm in Beckmann SW 41 rotor for 16 hr. After 16 hr, the contents of the centrifuge tubes were fractionated as 1 ml fractions from the top the tube and analyzed by Western blot analysis (Protocol from Dr. Ilya Frolov).

#### *5.2.11 Immunoblot analysis*

To detect FLAG-tagged RIG-I, TLR3, ISG56, Calnexin, Rab1b, Lamp1, HCV core, NS5B, NS3 and actin, the protein in the cell lysates were resolved on 7.5% SDS-PAGE gels (10% SDS-PAGE for HCV core). After electrophoresis, proteins were transferred to hybond-NC nitrocellulose membrane (*Amersham*) and the blots were processed for immunodetection of proteins using the following antibodies mouse anti-

FLAG (*Sigma*), mouse anti-TLR3 (*Imgenex*), rabbit anti-ISG56 (a gift from Ganes Sen, Cleveland Clinic), rabbit anti-calnexin (*Sigma*), rabbit anti-Rab1b (*Santa Cruz*), mouse anti-Lamp1 (*Abcam*), mouse α HCV core (*ABR*), rabbit anti-NS5B (*Virogen*), goat anti-NS3 (*Abcam*) and mouse anti-actin (*Sigma*). Peroxidase-conjugated secondary anti-rabbit, anti-goat and anti-mouse pAbs were purchased from (*Southern Biotech*). Protein bands were visualized using ECL Plus Western Blotting Detection reagents (*GE HealthCare*) and SuperSignal West Pico Chemiluminescent Substrate (*Pierce*), followed by exposure to X-ray film.

#### 5.2.12 Immunoprecipitation

To detect the interaction between TLR3 and NS3, equal volumes of sucrose gradient fractions were treated with 2x RIPA buffer (50 mM Tris-Cl pH 7.5, 300 mM NaCl, 2% Triton X-100) containing protease inhibitor cocktail (*Roche*) in the presence and absence of RNase A. Such treated fractions were precleared with protein A-sepharose beads and incubated with the specific antibodies mouse anti-TLR3 or goat anti-NS3 overnight at 4 °C. Protein A-sepharose beads were added to the above mixture and incubation was continued for 2 more hours. After incubation, beads were pelleted and washed with RIPA buffer, the beads were boiled with minimal volume of the buffer along with SDS loading buffer (8% SDS, 0.2 M Tris pH 8.8, 4 mM EDTA, 0.1% bromophenol blue, 40% glycerol and 0.5 M DTT) for 10 min prior to electrophoresis of the supernatant. Samples were analyzed by immunoblot analysis to detect NS3.

## 5.3 RESULTS

### 5.3.1 Functional reconstitution of RIG-I and TLR3 in human hepatoma cell lines

Despite several reports implicating RIG-I in antiviral defenses against HCV to trigger interferon response and reduce replicating RNA, its role is unclear in the context of cell culture infectious HCV. To characterize the role of RIG-I in modulating HCV replication using the recently developed cell culture infectious JFH1 strain of HCV, I reconstituted the RIG-I defective Huh7.5 cells line with functional RIG-I. RIG-I expression was tightly regulated from the stably integrated transgene and could be turned on by tetracycline removal from the culture media (Figure 5.1A). We confirmed the RIG-I mediated interferon response in these cells by detecting ISG56 expression upon SeV stimulation (Figure 5.1B). Huh7 and Huh7.5 cells do not produce interferon upon treatment with PolyI:C, a TLR3 agonist, due to defective TLR3 gene. To examine the role of TLR3 in cellular permissiveness to HCV replication, I reconstituted functional TLR3 in Huh7 and Huh7.5 cells by stable expression and found these cells can produce ISG56 upon stimulation with polyI:C (Figure 5.1C). As experimental controls, cells were also reconstituted with TLR3 lacking functionally important C-terminal TIR domain. To probe the mechanistic role of TLR3 in modulating HCV infection, Huh7 and Huh7.5 cells were also reconstituted with functionally inactive TLR3 mutants such as H539E and N541A that were shown to be defective in dsRNA ligand binding and initiation of signaling (Bell et al., 2006a; Bell et al., 2006b). We also reconstituted recently reported P554S TLR3 mutation that was discovered in human patients and shown to confer

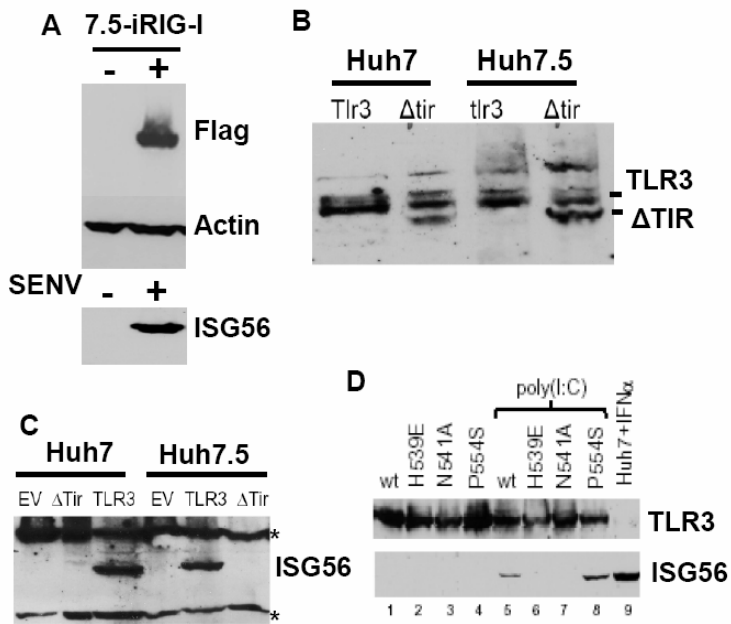


**Figure 5.1 Interferon responses in Huh7 and Huh7.5 human hepatoma cells.** (A). Huh7.5 cells expressing FLAG-tagged RIG-I under tet off system upon tet removal from the culture media for 5 days. After 5 days, cells were treated with 100 HAU/ml SeV for 24 hours. Cell lysates were prepared and analyzed by immunoblotting with anti-FLAG, anti-ISG56 and anti-actin antibodies. Lane + indicates induction of RIG-I upon removal of tetracycline (B). Immunoblot analysis using anti-TLR3 antibody to detect the expression of TLR3 and TLR3 $\Delta$ TIR in transgenic Huh7 and Huh7.5 cells generated by retrovirus transduction. (C) Huh7 and Huh7.5 cells expressing TLR3 or TLR $\Delta$ TIR were stimulated with 50 $\mu$ g/ml of polyI:C for 24hrs. The cell lysates were subjected to immunoblot analysis using anti-ISG56 antibodies. EV denotes cells transduced with empty retroviral vector pcXBSR. \* represents non-specific band (D). Huh7 cells expressing functionally inactive TLR3 mutants by retrovirus mediated insertion treated with 50 $\mu$ g/ml of polyI:C for 24hrs and blotted with anti-TLR3 and anti-ISG56 antibodies. Lysate from Huh7 cells treated with 500units/ml IFN- $\alpha$  for 24 hrs is used as positive control for ISG56.

dominant negative phenotype (Zhang et al., 2007). Interestingly, in contrast to H539E and N541A, substitution of P554S with serine did not fail to activate the interferon response (Figure 5.1D, Lane 8).

### 5.3.2 RIG-I reconstitution limits HCV replication in Huh 7.5 cells

To characterize the role of RIG-I in modulating HCV replication, Huh7.5 cells functionally reconstituted with RIG-I were transfected with *in vitro* transcribed full length HCV RNA carrying the Renilla luciferase gene and capable of supporting efficient genome replication.

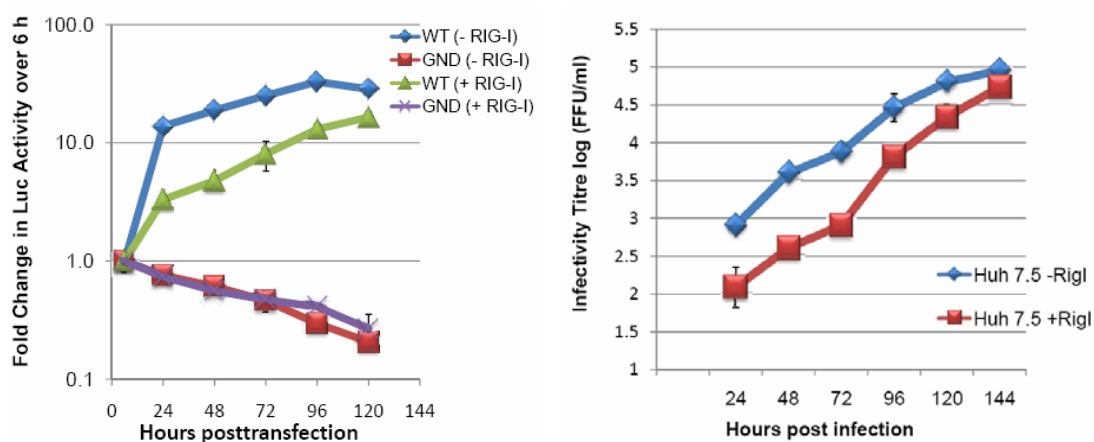


**Figure 5.2 RIG-I inhibit HCV propagation in Huh7.5 human hepatoma cells. (Left).** Renilla luciferase activity arising due to the replication of HCV genomic RNA was monitored in Huh7.5 cells in the presence and absence of RIG-I expression at 6, 24, 48, 72, 96 120 hr post transfection. Non-replicating HCV RNA encoding GDD to GND mutation in the RdRP active site was used a negative control. The data is normalized to 6 hour time point and plotted as means of duplicates with standard deviations. **(Right).** HCV titers in infectious supernatants collected at 24, 48, 72, 96 and 120 time points from the HCV infected Huh7.5 cells in the presence and absence of RIG-I expression. Huh7.5 cells with and without RIG-I expression were infected with HCV at 0.5 moi. After 8hrs of infection, the cells were trypsinized, replated and allowed to grow. The supernatants collected at indicated times were used to infect naïve Huh7.5 cells at 10-fold serial dilution in chamber slides. The cells were fixed and probed with rabbit anti HCV-core primary and goat anti-rabbit FITC secondary antibodies. The fluorescent foci were counted using immunofluorescence microscopy to determine HCV titer in foci forming units/ml.

The HCV replication was quantified by assaying Renilla luciferase activity for 5 days after transfection. A five fold decrease in genome replication was observed in the Huh7.5

cells expressing RIG-I compared to those that do not express RIG-I (Figure 5.2 left). We see a slight decrease in the genome replication compared to native Huh7.5 cells (compare to Figure 5.1) due to possible leaky expression even in presence of tet in the culture media. I also examined replication of virus by titration of secreted virus in the culture supernatant by focus forming assay over a five day period. Expression of RIG-I in Huh7.5 cells was able to reduce the HCV titer by 8-10 folds (Figure 5.2 right) over the initial 60 hours following infection. However, as time progressed, HCV replication in RIG+I cells was able to catch up to the similar levels as in RIG-I cells (Figure 5.2 right) and a similar trend can be observed at later time points in genome replication assay (Figure 5.2 right).

### 5.3.3 TLR3 limits HCV replication in Huh7 and Huh7.5 cells

To test, whether TLR3 has any role in limiting HCV replication, I transected replication competent HCV RNA into Huh7 and Huh7.5 cells reconstituted with functional and defective versions of TLR3. I monitored HCV replication by assaying Renilla luciferase activity. A greater than 20 fold reduction in replication of HCV RNA was seen after 48 hours in Huh7 cells in the presence of functional TLR3 (Figure 5.3A, compare the data of TLR3 with that of ΔTIR and EV). In contrast, Huh7.5 cells showed only a 2-8 fold reduction in HCV RNA replication after 48 hours (Figure 5.3B). Results from experiments to measure the secreted virus corroborates well with genome replication data in presence of functional TLR3 showing two fold lower virus titer in

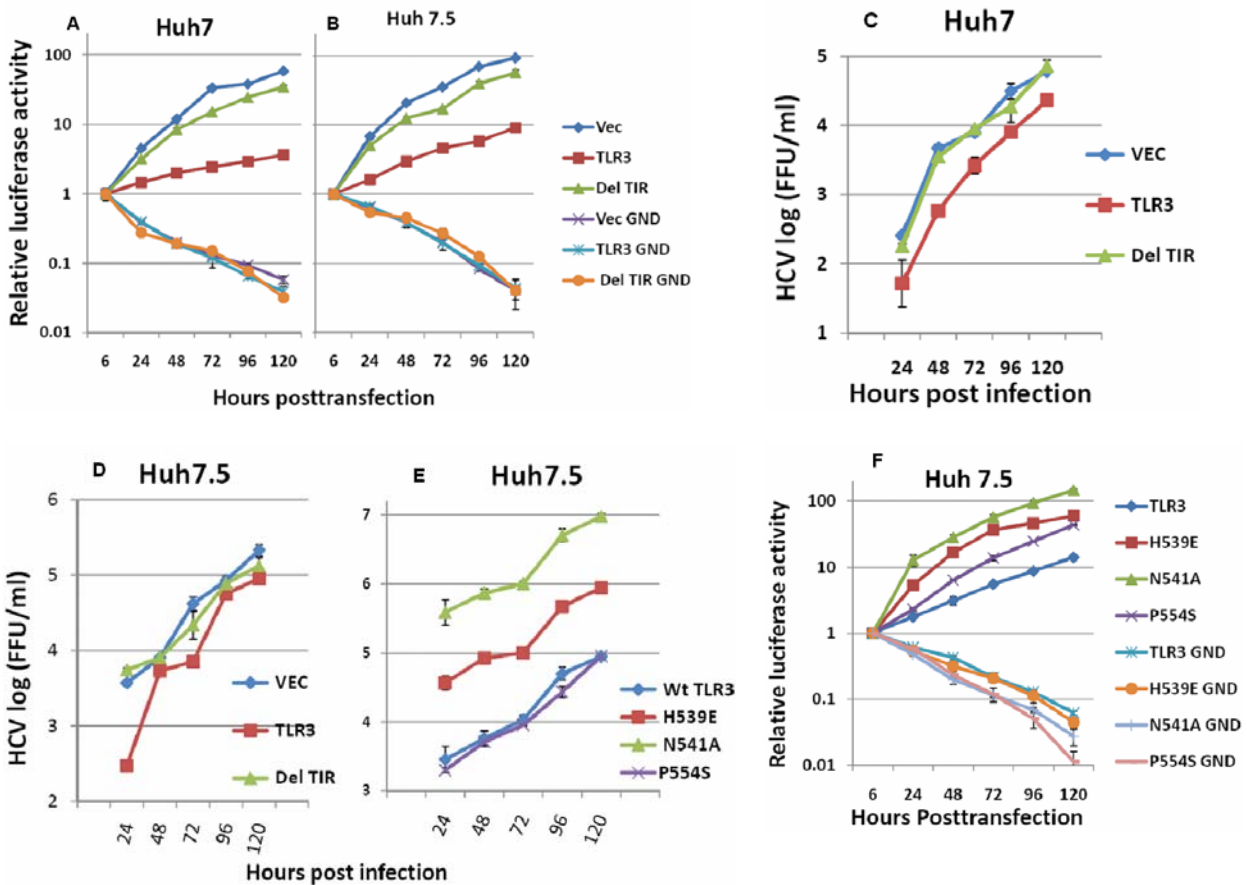


**Figure 5.3 TLR3 inhibits HCV replication.** TLR3 inhibits HCV replication. (A) and (B). Renilla luciferase activity arising due to the replication of HCV genomic RNA was monitored in Huh7 and Huh7.5 cells expressing TLR3 and TLR3 $\Delta$ TIR along with vector controls over 6, 24, 48, 72, 96, 120 hrs time points. Non-replicating HCV RNA encoding GDD to GND mutation in the RdRP active site was used a negative control. The data is normalized to 6 hour time point and plotted as means of duplicates with standard deviations. (C) and (D) HCV titers in cell culture supernatants collected at 24, 48, 72, 96 and 120 time points from the HCV infected Huh7 and Huh7.5 cells expressing TLR3 and TLR3 $\Delta$ TIR along with vector controls. (E) HCV titers in infectious supernatants collected at 24, 48, 72, 96 and 120 time points from the HCV infected Huh7 and Huh7.5 cells expressing TLR3 and its mutants H539E, N541A and P554S. (F) Renilla luciferase activity arising due to the replication of HCV genomic RNA monitored in Huh7.5 cells expressing TLR3 and its mutants H539E, N541A and P554S over 24, 48, 72, 96 120 hrs time points.

Huh7 cells in contrast to Huh7.5 at 24 hours time point (Figure 5.3A and 5.3B). However

after 48 hours of infection, an 8-10 fold decrease in virus titer in both Huh7 cells and

Huh7.5 cells were observed in the presence of functional TLR3 (Figure 5.3C and 5.3D).

These data suggest either an additive or synergistic effect of TLR3 and RIG-I to inhibit

HCV multiplication in Huh7 cells. The additive or synergistic effect of TLR3 and RIG-I may be due to cumulative activation of IRF3, a convergence point in either signaling pathways or a yet unknown mechanism by which TLR3 or RIG-I may abrogate HCV replication/secretion. To delineate the mechanistic role of TLR3 in this process, HCV RNA replication and virus secretion was examined in Huh7.5 cells reconstituted with functionally inactive TLR3 mutants such as H539E, N541A and P554S. Renilla luciferase activity reporting on HCV genome accumulation was 10 fold higher in Huh7.5 cells with the N541A TLR3 mutant than in wt TLR3 cells, while in P554S and H539E cells, luciferase activity was 2 and 4 fold higher respectively throughout the course of replication (Figure 3F). I expected the secreted virus level to be 10 fold higher in case of cells expressing the N541A mutant compared to wt TLR3 based on Renilla luciferase activity data. However, a 100 fold higher virus secretion was observed with N541A and 10 fold in the case of H539E compared to wt TLR3 (Figure 3E). Virus secretion in the case of the P554S mutant expressing cells was slightly lower than in wt TLR3 expressing cells, correlating well with the slightly higher level of ISG56 expression in these cells compared to cells expressing wt TLR3 (Figure 5.1D and 5.3E). A similar phenomenon is observed in Huh7 cells reconstituted with TLR3 and its mutants (data not shown). However, a slight discrepancy was observed in with respect to genome accumulation and virus secretion in TLR3 mutants suggesting that genome accumulation and virus secretion may be distinctly regulated events and TLR3 may have a role in modulating these events in addition to its role in interferon synthesis.

### 5.3.4 TLR3 co localizes with HCV virus replication complex.

Though it is clear from our data that the TLR3 initiated interferon response is able to reduce HCV replication and virus secretion, the cellular context of TLR3 and its ligand HCV dsRNA, as well as the associated signaling events remain unclear.

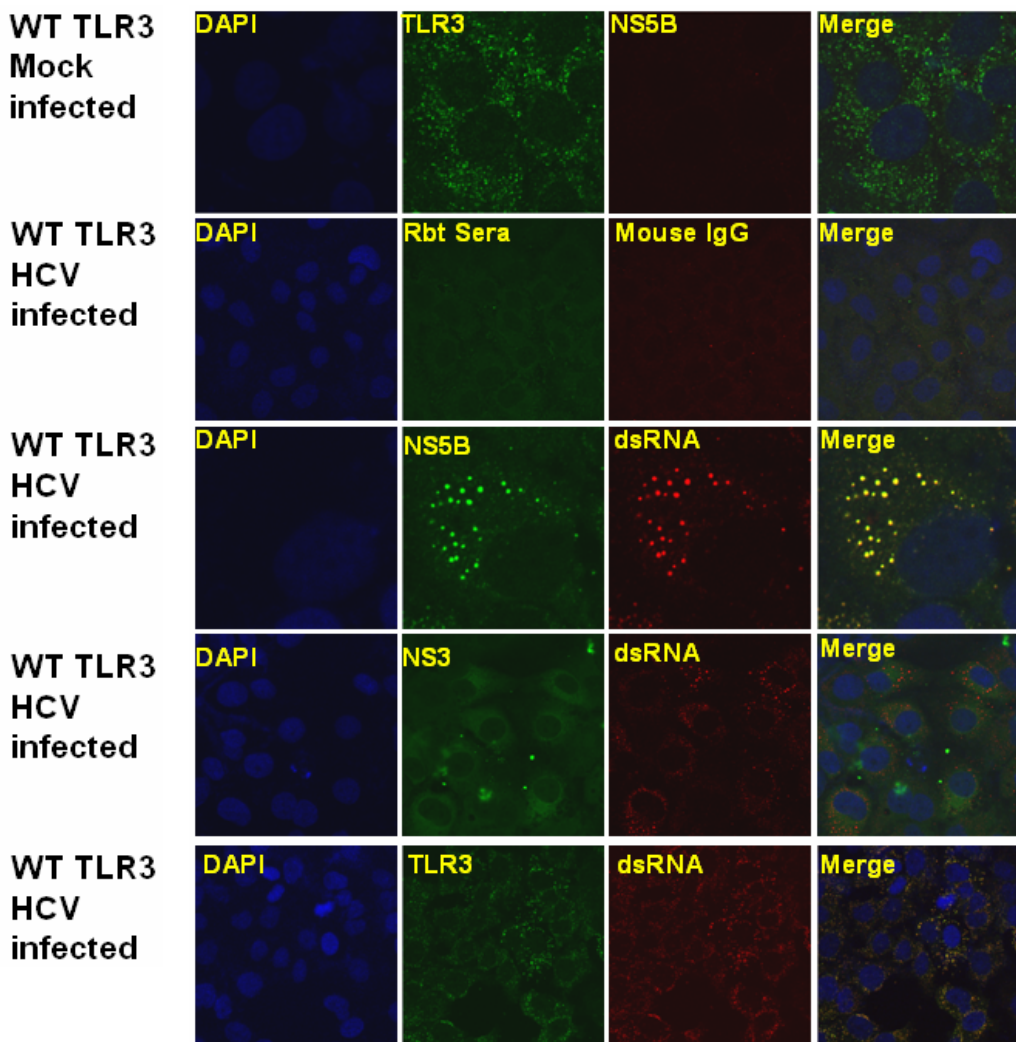


**Figure 5.4 TLR3 and its mutants H539E, N541A and P554S co localize with HCV dsRNA and NS5B.** Confocal images of Huh7 cells expressing TLR3 staining with antibodies targeting dsRNA, NS5B, NS3 and TLR3.

To test whether TLR3 interacts with HCV replication complex proteins to affect viral replication or virus secretion, I decided to examine the TLR3 localization in HCV infected cells expressing TLR3 or its mutants. To determine the cellular location and potential interactions between TLR3, HCV dsRNA and NS5B, Huh7 cells expressing TLR3 and its mutants were infected with HCV or mock infected for 72 hours and examined by confocal fluorescence microscopy following staining with specific antibodies. In uninfected cells, TLR3 can be localized to small foci spread through out the cytoplasm of the cells but not in nucleus or plasma membrane (Johnsen et al., 2006), while in the HCV infected cells the foci were slightly larger and were predominantly closer to the nucleus. Thus, a marked difference in distribution of TLR3 was observed in the infected over the non-infected cells (Figure 5.4). It has been suggested that TLR3 is localized to ER (Johnsen et al., 2006) and upon transfection of dsRNA, TLR3 is suggested to move from ER to early endosomes where it encircles dsRNA. Based on the pattern of distribution observed, I propose that TLR3 is recruited to sites of HCV replication by a similar mechanism. TLR3 mutants had similar cellular distribution profile as wild type suggesting that mutations do not affect the cellular localization (Figure 5.4, data not shown), however H539E and N541A were non-functional in inducing interferon response (Figure 5.1D), since these mutation affect RNA binding or receptor activation or both. By staining HCV infected Huh7 cells with both dsRNA specific and HCV NS5B antibodies, I was able to localize HCV dsRNA and NS5B to a set of large uniformly sized foci that appear to be the sites of HCV replication. TLR3 was localized to the sites of HCV replication as based upon the observation of co localizing

fluorescence signals when the TLR3 antibody was used in combination with either dsRNA or NS5B antibodies. This suggests that TLR3 interacts with HCV dsRNA or protein components in HCV replication complex. Both functionally active (P554S) and inactive TLR3 (H539E and N541A) mutants co localized to the sites of HCV replication complex proteins. These results may be possibly indicated that these mutations do not affect the interaction of TLR3 with HCV replication complex. The alternative possibility would be suggested that the mutation may affect the effector function TLR3 rather interaction with dsRNA ligand. This may be due to the presence of RNA binding sites on the N-terminal TLR3 ectodomain which is still active. The TLR3 mutations H539E, N541S and P554S are important for the interferon signaling activity. It is suggested that although interaction of TLR3 with HCV replication complex is necessary, it may not be sufficient to initiate interferon response. Although it has been suggested that NS3 protein is a component of the HCV replication complex, I could not detect co-localization of NS3 with TLR3, nor could I detect co localization of NS3 with HCV replication complex.

#### *5.3.5 TLR3 localizes to membrane fractions containing HCV replication protein*

To further examine the cellular localization of TLR3 and replication complex proteins of HCV, I analyzed cellular membrane fractions by sucrose density gradient centrifugation. Huh7 cells expressing TLR3 were mock or HCV infected for 96 hrs and dounce homogenized in the absence the detergents.

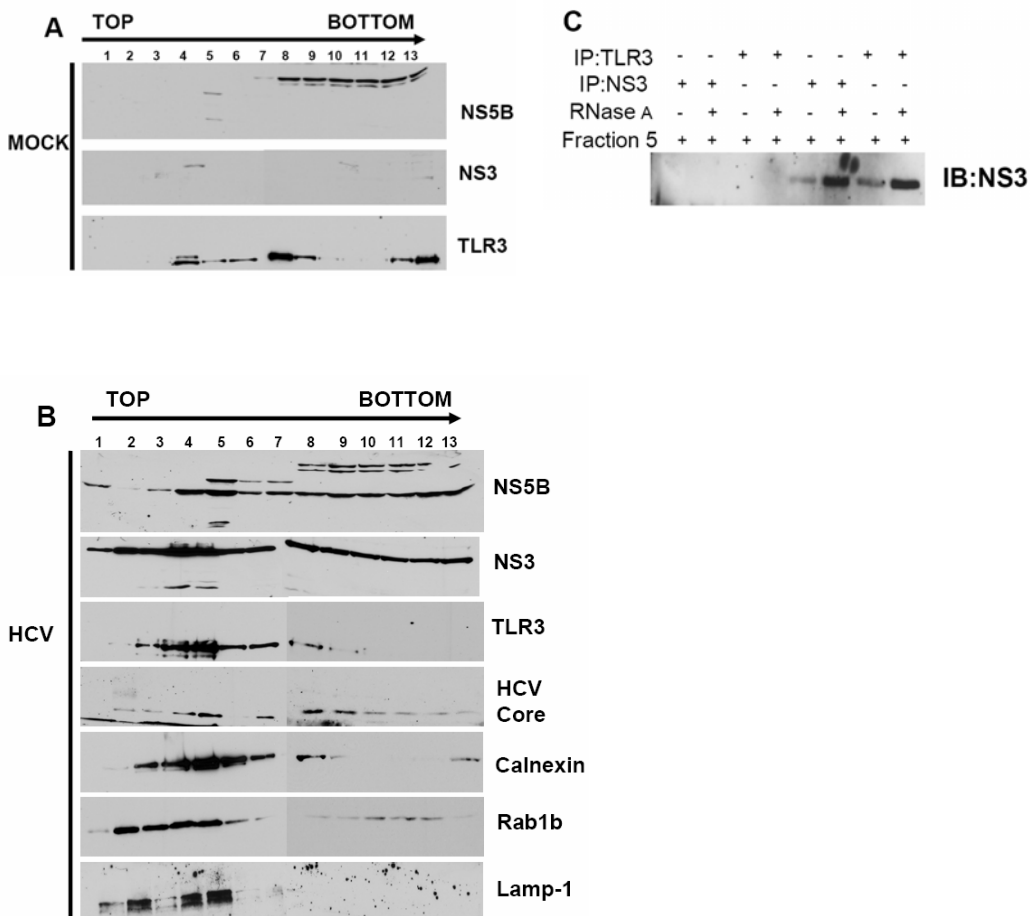


**Figure 5.5 TLR3 redistributes to membrane compartments containing HCV replication complex (A).** Immunoblot analysis of sucrose density centrifuge fractions to detect sub cellular fractionation TLR3 in mock infected Huh7 cells expressing TLR3. **(B)** Immunoblot analysis of sucrose density centrifuge fractions to determination sub cellular fractionation TLR3, NS5B, NS3 in comparison to various cellular markers such as calnexin, rab1b and Lamp1 in HCV infected Huh7 cells expressing TLR3. **(C)** Immunoprecipitation of HCV NS3 from sucrose gradient fraction 5 of mock and HCV infected samples using TLR3 and NS3 antibodies. Prior immunoprecipitation, equal volume fraction 5 was diluted 2X RIPA buffer and immunoprecipitation was carried out in presence and absence of RNase A.

The cell lysates were subjected to sucrose density gradient as described in the methods, and the fractions collected from top to bottom. The fractions were analyzed by

western blots using specific antibodies against TLR3, HCV proteins and cellular markers for ER and endosomes. In mock infected cells TLR3 was found in density gradient bottom fractions 4-8, a pattern similar to calnexin suggesting its ER localization (Figure 5.5A and 5.5B). In contrast, TLR3 peaked in density gradient top fractions 4 and 5 gradients of HCV lysates, a distribution similar to endosomal markers Rab1b and Lamp1 (Figure 5.5B), suggesting that TLR3 distribution is endosomal in agreement with the distribution observed by confocal microscopy. This data suggests that TLR3 may be recruited to endosomes upon HCV infection. HCV replication is thought to occur in close association with membranes possibly in endosomes. In HCV infected cells, TLR3 localization may correspond to the late endosomes as the fluorescence signals observed during confocal microscopy were close to nucleus. A major fraction of HCV proteins NS5B and NS3 co localized to the same density fractions as TLR3 in infected cells suggesting a possible interaction between the HCV proteins and TLR3. To examine, possible interaction between HCV proteins and TLR3, gradient fractions 4 and 5 from the infected lysates were detergent treated and used for immunoprecipitation with TLR3 and NS3 antibodies followed by immunoblotting with NS3 antibody. HCV NS3 protein could be immunoprecipitated with both TLR3 and NS3 antibodies in the gradient lysate. Increased levels of NS3 were observed upon immunoprecipitation upon treatment of the gradient fraction with RNase A suggesting that NS3 may be associated with complex containing RNA (Figure 5.5C). This data suggests TLR3 interaction with HCV NS3 may not be direct and can involve other cellular partners or dsRNA. RNase treatment may break large RNA-protein complexes into smaller units that could be better amenable for

immunoprecipitation. Alternatively, if TLR3 is directly interacting with NS3, RNase digestion may lead to the exposure of buried protein surface of NS3 necessary for interacting with the TLR3.

## 5.1 DISCUSSION

TLR3 and RIG-I are the major viral dsRNA sensors that trigger host antiviral innate immune response to limit viral infection caused by many RNA viruses including hepatitis C virus (HCV). TLR3 is located on intracellular membranes, although in some cells, it is also present on the plasma membrane. TLR3 is unique with respect to its localization to membrane compartments as opposed to MDA5 and RIG-I that are predominantly cytoplasmic and there appears to be some significance to membrane localization of TLR3 (Johnsen et al., 2006) since RNA replication is membrane associated in several virus families. With respect to signaling, TLR3 is unique in the way that it recruits adapter protein TRIF instead of MyD88 or MAVS used by other TLRs and RIG-I or MDA5 respectively. TRIF activity is necessary to engage other downstream signaling proteins like TRAF, TBK1 and IKK- $\epsilon$  that lead to activation of IRF3 to turn on transcription from IFN- $\beta$  promoters. Studies undertaken to examine TLR3 function in a cellular context have used synthetic dsRNA analogue polyI:C as a direct ligand for TLR3 to model virus infection and monitor the expression of interferon stimulatory genes (e.g.,ISG56) to infer functional phenotype (Alexopoulou et al., 2001; Doyle et al., 2002; Jiang et al., 2003; Matsumoto et al., 2002; Oshiumi et al., 2003a; Oshiumi et al., 2003b; Schmidt et al., 2004). Similarly, RIG-I function can be assessed by SeV infection. I was able to successfully reconstitute functional TLR3 in Huh7 and Huh7.5 that were originally defective in responding to politic. ISG56, a marker for IFN inducible gene was

detected in response to polyI:C and SeV stimulation in case TLR3 and RIG-I respectively. These cells were used study the HCV replication using infectious virus as well as replicons. Reconstitution of the functional TLR3 in human hepatoma cells drastically decreased HCV replication and infection. However, at later time points we observe that HCV infection reached similar level to that in cells without reconstitution of PRRs, suggesting possible viral evasion that may be mediated by the accumulation of the viral NS3/4A protease which can antagonize IFN signaling. TLR3 inactive mutants did not affect HCV replication indicating that TLR3 function plays a major role in the outcome of HCV infection. Taken together, these results suggest that the early interferon response mediated by TLR3 appears to be an important component in limiting HCV infection during the acute phase. Further investigation revealed TLR3 is localized to HCV dsRNA and NS5B indicating that anti-viral signaling mediated by TLR3 is initiated in close association to membrane compartment containing HCV replication complexes. Specific protein-protein interactions between TLR3 and viral proteins of replication complex may mediate the localization of TLR3 to membrane compartments containing HCV replication complex.

## **CHAPTER 6: INFLUENZA VIRUS EVADES INNATE IMMUNE DEFENSES BY NS1 MEDIATED ANTAGONISM INVOLVING RIG-I INHIBITION**

### **6.1 ORTHOMYXOVIRIDAE**

The current outbreak of H1N1 swineflu in Mexico and United States has spread world-wide across 74 countries and WHO has declared “Swine Flu” as “Pandemic” on June 11 2009. In US alone, swine flu outbreak has caused more than 13000 cases and 27 deaths so far in June 2009. Under current economic conditions, pandemic outbreaks could have severe socio-economic consequences globally. Several laboratories around the world are on high alert to understand viral pathogenesis and develop vaccine/therapeutic strategies to combat emerging threats from influenza outbreaks. At present, tamiflu is the best drug available to treat infected people and the drug appears to be in short supply due to pandemic fear stockpiling. In this context, this chapter aims to summarize influenza virus biology, role of non-structural protein 1 (NS1) in host immune evasion and some initial results suggesting that NS1 blockade of interferon response by antagonizing RIG-I. In addition, studies were undertaken to clone, sequence and rescue swine flu isolates by reverse genetics in order to study its interaction with host immune system.

#### *6.1.1 Classification*

Ortho- and Paramyxoviridae are so named because of their ability to bind to mucous (Myxa). They both are negative strand RNA viruses, paramyxovirus members have non-segmented genome, while orthomyxovirus have segmented genome. According

to initial ICTV classification orthomyxoviridae is divided into four genera namely Influenza A, Influenza B, and Influenza C and Thogoto virus. However, recent classification includes a new genera called and ISAV virus (Infectious salmon anemia virus) based on serological, biochemical and genetic relationships (Kawaoka Y Virus Taxonomy VIIth report ICTV). Orthomyxoviruses infect many vertebrate animals including humans, birds, swine, horses, dogs, cats, whales and seals. Influenza A, B, C of orthomyxoviruses differ from each other in their antigenic properties with respect to the nucleoprotein (NP) and matrix protein (M1) (Horimoto and Kawaoka, 2005). Influenza A is further classified based on the major surface antigens on the virus particles, which are hemagglutinin (HA or H for subtype) and Neuraminidase (NA or N for subtype). There are currently 16 naturally occurring variants of haemagglutinin (H1-H16) and 9 variants of neuraminidase (N1-N9). Birds belong to the orders Anseriformes (eg. Duck, geese and swan) and Charadriiformes (Gulls, surf birds and sand pipers) serve as natural reservoirs for influenza A and provide background for the emergence of novel H and N combination by antigenic drift and antigenic shift. HA subtypes like H3 and H6 are predominantly isolated from ducks, whereas H4, H9, H11, H13 are isolated from shore birds and gulls. NA subtypes like N2, N6 and N8 are isolated from ducks and N6, N9 in shore birds and seagulls (Webster et al., 1992). In humans, influenza virus causes chills with fever, sore throat, muscle pain, severe head ache, cough, weakness, discomfort and in severe cases pneumonia in all ages of people, although elderly population, young children and infants are more susceptible (Barker and Mullooly, 1982; Mullooly and Barker, 1982). Historically, influenza viruses have caused devastating effects on human

race, where an estimated 20-50 million people died due to 1918 Spanish Influenza Pandemic. Every year, seasonal influenza infects 50 million people in United States.

#### 6.1.2 Virus architecture, entry, genome organization, virus replication and pathogenesis

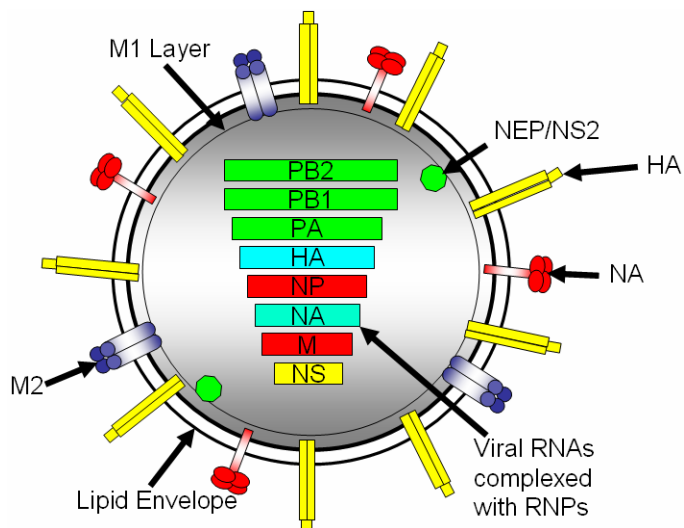


**Figure 6.1 Schematic representation of influenza virion.**  
Viral particle has outer lipid bilayer studded with HA and NA and other structural proteins like matrix. Interior to the envelope the segmented RNA genome is present as helical nucleocapsids (RNPs).

Influenza viral genome of ~14 kb is divided among eight single-stranded negative sense RNA segments in Influenza A and B and seven segments in Influenza C (Palese, P. & Shaw, M. L. (2007) *Othomyxoviridae: the viruses and their replication* *Fields Virology*, 5th edn, pp. 1647–1689). These segments are named based on the protein they encode i.e., PB2 (polymerase basic 2), PB1 (polymerase basic 1), PA (Polymerase acidic), HA (Hemagglutinin), NP (Nucleoprotein), NA (Neuraminidase), M (Matrix) and NS (Non-

structural). Influenza virus particles are highly heterogeneous and pleomorphic in structure ranging from spherical to filamentous forms revealed by electron microscopy.

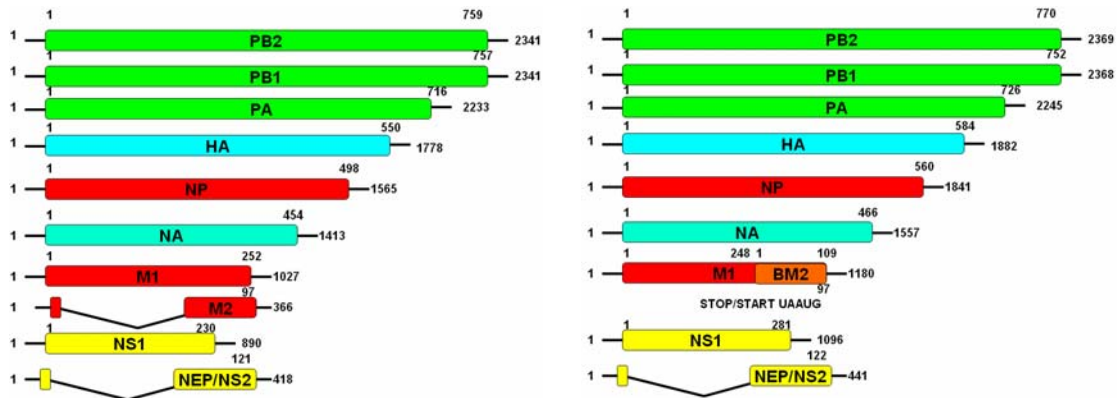


**Figure 6.2 Schematic representation of genomic segments of influenza A (top) and influenza B (bottom).** Genome organization of Influenza A and B viruses, they both have eight segments, a total of ~14 kb. Viral proteins PB1, PB2, PA, and structure proteins HA, NP, NA are expressed from one segment each in both viruses. However, there is slight difference in the organization and expression of M1, M2, NS1 and NS2 proteins.

Spherical forms are 50-180 nm in diameter and filamentous forms are 200-300 nm long and 20 nm in diameter. The virus particle is composed of outer lipid bilayer, from which two characteristic spikes radially project out. The rod shaped spikes made of HA outnumber mushroom shaped spikes composed of NA by 4 to 5 times (Edwards et al., 1994; Hashimoto et al., 1983). HA and NA are large glycoproteins and form major epitopes recognized by the host for adaptive immune response. In addition to HA and NA, the lipid envelope contain M protein called matrix protein. M1 underlying the lipid envelope is the most abundant viral protein that serves as structural and scaffolding role by interacting with “Ribonucleoprotein complexes” (RNP) present interior to matrix and the lipid envelope. M2 is an ion-channel that traverses lipid envelop and matrix. Eight

distinct helical RNPs structures (one each for PB2, PB1, PA, HA, NP, NA, M and NS) are present in virions that are composed of PB2, PB1, PA, NP protein and negative sense genomic RNA. In contrast to RNPs structure of paramyxoviruses, influenza RNPs are highly susceptible to RNase digestion suggesting a different structure where each NP protein appears to shield 20 nucleotides along with additional proteins such as PA, PB1, PB2 and NS2.

Influenza virus preferentially binds to sialic acid present on the surface of target cells to gain cellular entry. Human viruses use penultimate galactose sugar linked by a  $\alpha$ -2,6 linkage (SA  $\alpha$  2,6 Gal) while avian viruses mostly bind to sialic acid  $\alpha$ - 2,3 linkage (Connor et al., 1994; Couceiro et al., 1993; Matlin et al., 1981). The virus is internalized as endosomes by endocytosis mediated by Clathrin-coated pits (Matlin et al., 1981). The acidic pH conditions of endosomes are necessary for activating fusion of the viral membrane with that of the endosomal membrane. Matrix protein M2 is proposed to play a role in mediating the uncoating and release of free RNPs from matrix protein M1 and the whole process of virus penetration is shown to occur within 30 minutes time span (Martin and Helenius, 1991; Stegmann et al., 1987a; Stegmann et al., 1987b). The component proteins of RNPs, NP PB1 PB2 and PA contain NLS signal and aid in active transport of RNPs into the nucleus where they undergo transcription to generate messenger sense RNAs (Figure 6.3) (Whittaker and Helenius, 1998) that serves to translate the viral proteins essential for virus life cycle.

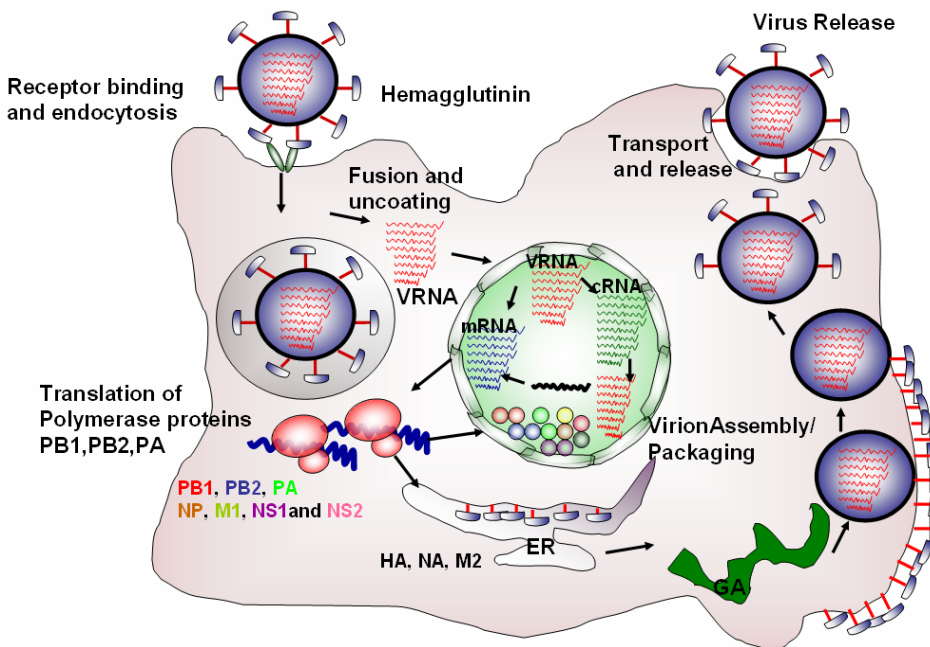


**Figure 6.3 Schematic representation of influenza virus life cycle.** The virus enters by endocytosis upon binding to sialic acid moiety on cell surface. Once internalized the virus membrane fuses with endosomal membrane releasing the RNPs, RNPs are translocate to nucleus where the viral RNA undergoes transcription to produce messenger RNA from which all the structural and non-structural proteins are produced.

In contrast to positive sense RNA virus, the replication of influenza RNA is known to occur in the nucleus and the polymerase function necessary for replicating 8 segments of RNA comes from the association of three distinct viral proteins namely PA, PB1 and PB2. The viral RNA polymerase complex, PA, PB1, PB2 and NP have shown to be involved in determining the virulence (Watanabe et al., 2009). The polymerase active site is present in PB1. However, this polymerase can not produce functional mRNAs unless a primer is provided (Krug et al., 1980a; Krug et al., 1980b; Plotch et al., 1981). Therefore, PB2 subunit uses a mechanism called “cap snatching” involving binding to 5'

caps of the host pre-RNAs (Pol II transcripts) followed by an endonuclease cleavage 10-13 downstream of the cap (Fechter et al., 2003; Guilligay et al., 2008; Li et al., 2001). Though, both PA and PB1 subunits contain endonuclease function, the origin of endonuclease activity responsible for cap snatching was not clear until recently where structural, mutational and cross linking experiments conclusively show to reside in N-terminus of PA (Dias et al., 2009; Yuan et al., 2009). The snatched pre-mRNA caps acts as primers whose elongation is initiated by adding a G residue by the viral polymerase. Elongation continues till a stretch of uridines are reached on the template strand. Then the transcription will terminate after the addition of poly (A) tails. These RNAs are further processed by nuclear machinery and exported for translation to the cytoplasm. Similar transcription without capped priming gives rise to cRNA. Synthesis of vRNA from the cRNA is accomplished by the viral polymerase again without primer. Newly synthesized vRNA interact with PB2, PB1, PA and NP to form RNP s that are exported from the nucleus to the assembly site at the apical plasma membrane where virus particles bud and are released.

#### *6.1.3 Non-structural protein (NS1) of influenza virus*

NS1 is a non-structural protein with variable length across different strains expressed at high levels in infected cells. NS1 is a multifunctional protein that serves in several regulatory functions in the virus life cycle that including RNA synthesis, viral mRNA translation and splicing of NEP mRNA (Figure 6.4).

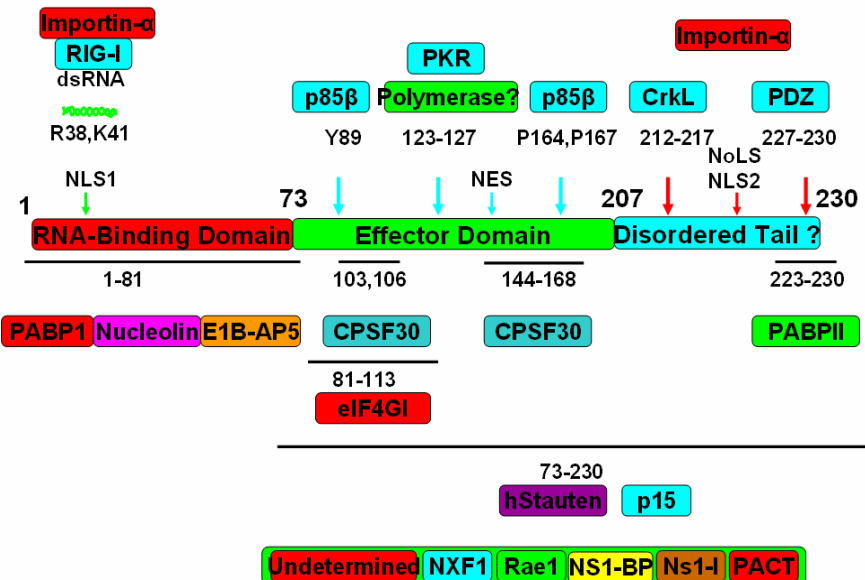


**Figure 6.4 Schematic representations of NS1 protein and its cellular interactors.** NS1 has N-terminal RNA domain and a C-terminal effectors through which it interacts with multiple host cell proteins (Hale et al., 2008b).

Although, differences in NS1 has been indicated to associate with severity of pathogenecity from strain to strain. The molecular basis for such differences contributing to virulence and pathogenecity is not clear given multiple roles attributed to NS1. Phylogenetic analyses have classified NS1 in two allelic categories Allele A shared by virus infecting avian, human, swine and equine and allele B exclusively observed in avian virus. However, it has been observed that highly pathogenic avian influenza viruses isolated from humans have Allele A. NS1 protein has two distinct functional domains; an N-terminal RNA-binding domain (residues 1-73) and a C-terminal effector domain (residues 74-230) that is thought to interact with host-cell proteins. A short linker connects the N and C-terminal domain of NS1 and this region comprises of varying

length of amino acids among different strains of flu (Hale et al., 2008a; Hale et al., 2008b). Structural analyses of NS1 implicate a tubular structure that can competitively sequester viral replicative intermediates without hindering the protein-protein interactions that are possible with cellular proteins as the binding sites are exposed on the outer surface (Bornholdt and Prasad, 2006; Bornholdt and Prasad, 2008). NS1 protein has been implicated in a multitude of functions that work to the advantage of the virus replication which includes RNA synthesis, viral mRNA translation, splicing of NEP mRNA and pathogenesis. NS1 delays viral-induced apoptosis by interfering PI3-Kinase pathway. It has been reported to inhibit the host cell antiviral responses by blocking 2'-5' oligoadenylate synthetase (2'-5'-OAS) and activation of RNase L. NS1 also limits RIG-I mediated IFN- $\beta$  response and also blocks PKR-mediated innate immune response. Most of the NS1 functions are mediated by protein-protein interaction with multiple host proteins arising from C-terminal domain, although the mechanisms remain unclear. Bioinformatic analyses of highly pathogenic avian influenza NS1 have revealed PDZ domain ligand (PL) motif at the C-terminal region (Obenauer et al., 2006). PDZ domains are protein-protein recognition modules that mediate formation of protein complexes at the membrane interface regulating a multitude of physiological functions such as epithelial fluid secretion. It has also been shown that NS1 protein C-terminus may interact with PDZ-binding proteins(s) and thus altering cellular physiology (Jackson et al., 2008; Obenauer et al., 2006). It has also been shown that when avian PL sequences were introduced into human influenza virus (WSN) virulence rate were enhanced

resulting in death, severe alveolitis and increased viral spread in the infected lungs of the mice (Jackson et al., 2008).

## 6.1 MATERIALS AND METHODS

### 6.2.1 *Plasmids*

The following plasmids are kind gifts from the respectively indicated contributors in parentheses: p55C1Bluc, pEFBos N-RIG and pEFBos N-MDA5 (from Takashi Fujita); pcDNA3-Flag TBK1, pCDNA3-Flag RIPI, pCDNA3-P65 and pcDNA3-Flag IKK $\epsilon$  (from Kate Fitzgerald); pCDNA3-TLR3 (from Ganes Sen) pIFN- $\beta$ -luc, IRF3-5D, GFP-IRF3 and GFP-IRF3 5D (from Rongtuan Lin); PRDII-Luc and pEFTak-IPS-1 (from Michael Gale); pCDNA3-HA-TRIF (from Christopher Basler); pHW2000, pHW198-NS (PR8 strain H1N1 A/Puerto Rico/8/34), pHM18-NS (H1N1 A/HongKong/218847/06, pHM38-NS (H3N2 A/HongKong/218449/06) and pSH128-NS (H5N1 A/Vietnam/1203/04, all NS1 plasmids were from Erich Hoffmann).

### 6.2.2 *Construction of mammalian expression plasmids expressing NS1*

The NS1 coding region was PCR amplified from plasmids pHW198-NS, pHM18-NS, pHM38-NS and pSH128-NS was ligated in *Bam* HI and *Eco* RI sites of pCDNA3.1 for expression in HEK293. The primers used for PCR amplification in each case is list in table 6.1. The NS1 coding region from pHW198-NS (PR8 strain) was amplified by primers containing sequences for *Eco* RI and *Xba*I (Table 6.1).

<b>PRIMER</b>	<b>5' TO 3' PRIMER SEQUENCE</b>
B-NS-TC1	5' TATAGGATCCATGGATTCCAACACTGTGTCAAG 3'
E-NS-TC18R	5' CGGAATTCTCAGCCACCGAACAGCCAGGACAACAGCCACCAACTTCTGACCTAATTG 3'
E-NS-TC38R	5' CGGAATTCTCAGCCACCGAACAGCCAGGACAACAGCCACCAACTTTGACCTAGCTG
E-NS-TC128R	5' CGGAATTCTCAGCCACCGAACAGCCAGGACAACAGCCACCCGTTCTGATTGGAGG 3' G
E-NS-TC1	5' TATAGAATTCATGGATTCCAACACTGTGTCAAG 3'
X-NS-TC198R	5' GCTCTAGATCAGCCACCGAACAGCCAGGACAACAGCCACCAACTTCTGACCTAATTGTTCCCGC 3'

**Table 6.1 Primers used for NS1 PCR amplification**

### 6.2.3 Cloning of A/Brisbane/59/2007/H1N1, A/California/04/2009/H1N1,

### A/Brisbane/10/2007/H3N2 and B/Florida/04/2006

RNA was isolated from the strains A/California/04/2009/H1N1 (a gift from Dr. Daniel Perez) A/Brisbane/59/2007/H1N1, A/Brisbane/10/2007/H3N2 and B/Florida/04/2006 (a gift from Dr. Joan Nichols) propagated in either embryonated eggs or MDCK cells using Qiagen RNeasy kit according to manufacturer's instruction. The RNA isolated was used as template in RT-PCR (Qiagen one step RTPCR kit according manufacturer's protocol) to amplify genomic segment of influenza strain employing primer sets described in (Table 6.2 (Hoffmann et al., 2001). The reverse transcription step involved incubation of the viral RNA with specific primer at 50 °C for 50 min followed by PCR amplification for 30 cycles involving 94 °C for 30 sec as denaturation, 56 °C for 30 sec as annealing and 72 °C for 1 kb/minute as extension. The PCR products were gel purified and cloned in *Bsm*BI or *Bsa*I digested pAH12 vector (EGFP cloned in pHW2000

vector). The PB1, PB2 and PA genes were PCR amplified using specific primers sets containing one of the *Bsm*BI or *Aar*I or *Bsa*I sites that results in two amplified fragments. The *Bsm*BI or *Aar*I or *Bsa*I sites present in the overlapping complementary primers corresponding to internal regions aid in exact fusion of the two amplified fragments in a three-piece ligation reaction with the *Bsm*BI digested vector pAH12.

PRIMER NAME	5' TO 3' PRIMER SEQUENCE
Aa-PB2-1 Aa-PB2-1240R Aa-PB2-1238 Aa-PB2-2341	5' TATTCACCTGCTACAGGGAGCGAAAGCAGGTC3' 5' TATACACCTGCTAACTGTTTATCATACAATCCTTGT3' 5' TATTCACCTGCTAAAAGCAGTTAGAGGTGACCTGAATTC3' 5' TATTCACCTGCTACATATTAGTAGAAACAAGGTGTTT3'
Bm-PB1-1 Bm-PB1-1245R Bm-PB1-1250 Bm-PB1-2341	5' TATTCGTCTCAGGGAGCGAAAGCAGGCA3' 5' ATATCGTCTCATCCAGGACTCAGTGATGCTGTGCCATC3' 5' TATTCGTCTCGATGATGATGGGCATGTTCAAYATG3' 5' ATATCGTCTCGTATTAGTAGAAACAAGGCATTT 3
Ba-PA-1 Ba-PA-1140R Ba-PA-1130 Ba-PA-2233R	5' TATTGGTCTCAGGGAGCGAAAGCAGGTAC3' 5' TATAGGTCTCTGCAGTTTCAAAGTCTACCTCTCTGG3' 5' TATTGGTCTCGAGAGACATAAGCGATTGAAAGCAATATG3' 5' ATATGGTCTCGTATTAGTAGAAACAAGGTACTT3'
Bm-HA-1 Bm-NS-890R	5' TATTCGTCTCAGGGAGCAAAGCAGGG3' 5' ATATCGTCTCGTATTAGTAGAAACAAGGGTGTTC3'
Bm-NP-1 Bm-NP-1565R	5' TATTCGTCTCAGGGAGCAAAGCAGGGTA3' 5' ATATCGTCTCGTATTAGTAGAAACAAGGGTATTTC3'
Bm-NA-1 Bm-NA-1413R	5' TATTGGTCTCAGGGAGCAAAGCAGGAGT 3' 5' ATATGGTCTCGTATTAGTAGAAACAAGGAGTTTC3'
Bm-M-1 Bm-M-1027R	5' TATTCGTCTCAGGGAGCAAAGCAGGTAG3' 5' ATATCGTCTCGTATTAGTAGAAACAAGGTAGTTTC3'
Bm-NS-1 Bm-890R	5' TATTCGTCTCAGGGAGCAAAGCAGGGTG3' 5' ATATCGTCTCGTATTAGTAGAAACAAGGGTGTTC3'
<b>Table 6.2 Primers used for RT-PCR amplification of influenza 8 segments</b>	

The plasmid encoding California H1N1-HA was found to contain three mutations distinct from the consensus sequences (Genbank Accession # FJ966082) based on direct sequencing of the RT-PCR product. These mutations were reverted to wild type

consensus sequence by site directed mutagenesis using Pfu Turbo DNA polymerase (*Stratagene Quickchange kit*). All the clones selected were subjected to DNA sequencing using segment specific primers and sequence analysis was carried out using Lasergene software.

#### 6.2.4 Cell lines

Human embryonic kidney (HEK) 293, 293T (a gift from Shinji Makino) and HEK293 TLR3 (a gift from Ganes Sen) cell lines were grown and maintained in Dulbecco's minimal essential medium with 10% FBS and the medium for 293FT contained 200ug/ml Geniticide (*Invitrogen*).

#### 6.2.5 Sendai virus infection

Cells were infected with Sendai virus (SeV) cantell strain (Charles River laboratory) for 1 hr at 37 °C using an inoculum of 100 HAU/ml in a minimum volume of DMEM without antibiotics to ensure virus adherence to the cells. After infection, medium containing antibiotics was added, incubated for 16 hr and then harvested for reporter assays and immunoblot analysis. For each experiment, control cultures were maintained similarly in the absence of virus.

#### 6.2.6 PolyI:C treatment

PolyI:C (*Sigma*) was added directly to the medium at 50 µg/ml (m-PIC). Cells were assayed for PolyI:C induced responses 6 hr after treatment.

#### *6.2.7 Transfection and Reporter gene assays*

Twenty four-well plates containing  $5 \times 10^4$  cells in 1ml of DMEM were transfected in triplicates with 400ng of plasmid DNA using Fugene 6 transfection reagent (*Roche*) as per the manufacturer's instructions. 100 ng of pCMV- $\beta$ gal (*Clontech*) per well was used to normalize the transfection efficiencies. Twenty four hours later, transfected cells were either treated with 50  $\mu$ g /ml of polyI:C or 100 HAU/ml of SeV for 6 or 16 hr respectively and then assayed for firefly luciferase and  $\beta$ -galactosidase activities. The luciferase activity was normalized to  $\beta$ -galactosidase activity. Data was expressed as mean relative luciferase activity with Standard Deviation from a representative experiment carried out in triplicates. A minimum of three separate experiments were performed to confirm the trend in each observation. The fold induction of promoter activity was calculated by dividing the relative luciferase activity of stimulated cells with that of mock treated cells.

#### *6.2.8 Rescue of PR8 strain of H1N1 A/Puerto Rico/8/34 by reverse genetics.*

To generate infectious influenza A based on A/PR/8/34 strain, 8-plasmids representing PB1, PB2, PA, HA, NP, NA, M and NS are transfected in 293T cells co-cultured with Madin-Darby canine kidney cells (MDCK) (Hoffmann et al., 2002; Hoffmann et al., 2000). Virus production was monitored by plaque assay (Figure 6.5).

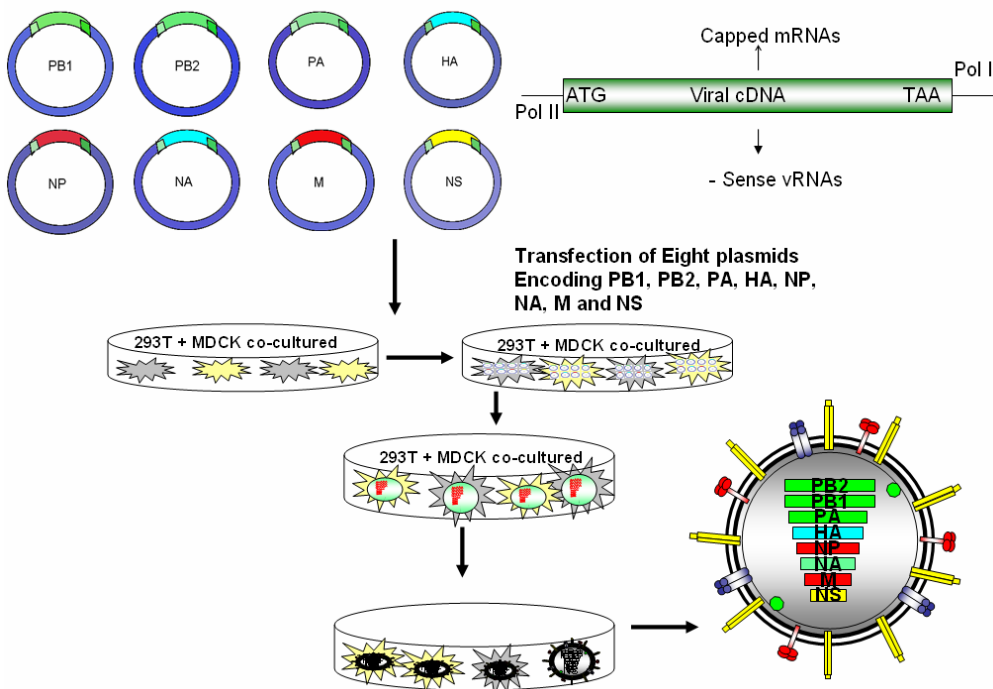


**Figure 6.5 Schematic representation of virus rescue using influenza reverse genetics system**

#### 6.2.9 Plaque assay to determine the virus titers

MDCK cells were cultured in Dulbecco's minimal essential medium (*Cellgro*) with 10% FBS in the presence of antibiotics. The supernatant containing infectious particles collected from the co-cultures of transfected 293T and MDCK cells was 10-fold serially diluted and used for infecting near confluent MDCK cells seeded at  $1 \times 10^6$  in 6 well plates. The virus supernatant were diluted in Dulbecco's minimal essential medium (*Cellgro*) in the presence of antibiotics and 1  $\mu$ g/ml concentration of TPCK-treated Trypsin (*Worthington Biochemicals*) without FBS. After 1 hour incubation with virus samples, the media was removed and cell monolayers were overlayed with 0.8% agarose (Difco Agar Noble, *BD Biosciences*) and incubated for 2 days. The agarose layer was

gently removed from each well and the cell monolayer was fixed with formaldehyde and stained using 0.2% crystal violet. The clear zones without crystal violet stain were considered as plaque where cell monolayer was lysed due to one virus particle/s. The plaques were counted in various dilutions and virus titer as plaque forming units/ml (PFU/ml) was determined by multiplying with appropriate dilution factor.

### 6.3 RESULTS

#### 6.3.1 *Influenza NS1 inhibits RIG-I but not TLR3 induced activation of IFN- $\beta$*

Although, NS1 protein is assigned with a multitude of functions, its involvement in host innate immune evasion appears to be most important for the virus lifecycle and pathogenecity. NS1 is suggested to overcome antiviral responses by blocking 2'-5' oligoadenylate synthetase (2'-5'-OAS) and activation of RNase L. NS1 also limits PKR-mediated innate immune response and suggested to block RIG-I mediated IFN- $\beta$  response. Unlike HCV NS3/4A and SARS-CoV PLpro, influenza NS1 does not contain conserved protease or deubiquitinase proposed function in immune evasion (Chen et al., 2007b; Devaraj et al., 2007; Foy et al., 2005; Li et al., 2005c). Hence, the mechanism of immune evasion mediated by NS1 appears to be distinct from that of SARS PLpro and HCV NS3/4A. Also, the molecular basis for strain specific differences in NS1 contributing to severity of pathogenecity is poorly understood. One such contributing factor may be the way in which, a given NS1 from a particular strain interacts with host proteins involved in activation of innate immune response. To understand the mechanisms of such strain specific differences of NS1 in mediating suppression of host

induced IFN response, reporter assays were conducted. NS1 expressing plasmids representing different influenza strains A/PR/8/34 (H1N1), A/HK/218847/06 (H1N1), A/HK/218449/06 (H3N2) and A/Vietnam/1203/04 (H5N1) were cotransfected along with either IFN- $\beta$  or pRDII (NF- $\kappa$ B) promoters. Figure 6.6 shows comparison of NS1 sequences from the above strains. PR8, H1N1 and H3N2 had variations at amino acid position 59 and 170 along with few conserved amino acid substitutions.

**Figure 6.6 Clustal W Alignment of NS1 proteins of Influenza A virus strains tested for NS1 antagonism in reporter assays.**

However H5N1 strain lacked the 5 amino acids close to N-terminus and 10 amino acids at C-terminus including conserved PDZ ligand motif (RSEV or ESEV or EPEV) that are normally found in avian H5N1 strains.

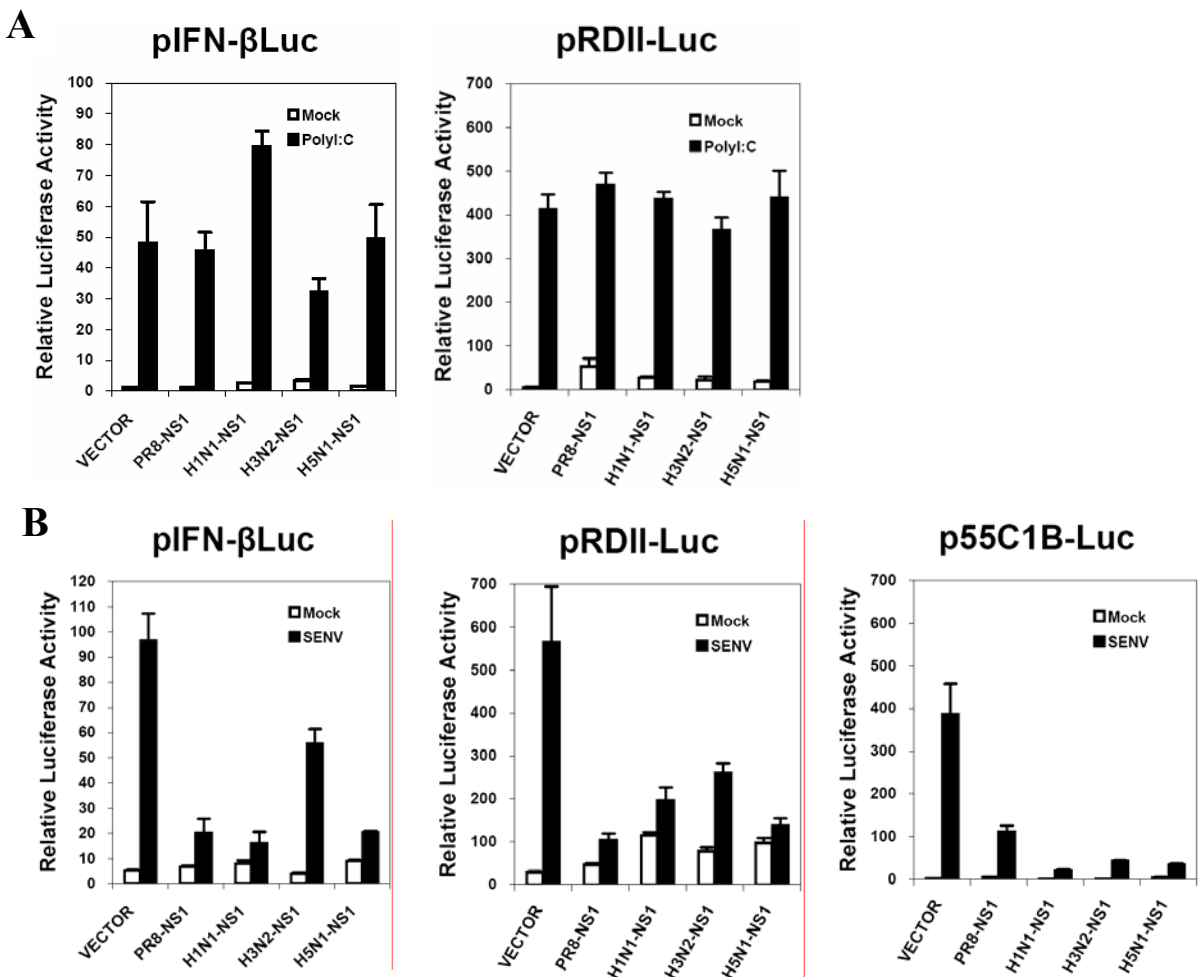


**Figure 6.7 NS1 protein of influenza inhibits activation of IFN- $\beta$  promoter stimulated by RIG-I pathway but not TLR3.** HEK293-TLR3 (A) and HEK293-T (B) cells were cotransfected with pIFN- $\beta$ -Luc and pCMV- $\beta$ gal plasmids, and a vector encoding various strains of influenza NS1 or an empty vector. Twenty-four hours later, cells were either mock-treated (empty bars), or incubated with 50  $\mu$ g/ml poly (I-C) in culture medium for 6 h (hatched bars, left panel), or infected with SeV at 100 HAU/ml for 16 h (solid bars, right panel) prior to cell lysis for both luciferase and  $\beta$ -galactosidase assays. Bars show relative luciferase activity normalized to  $\beta$ -galactosidase activity, i.e., IFN- $\beta$  promoter activity

The luciferase activity from IFN- $\beta$  and pRDII (NF- $\kappa$ B) promoters were monitored due to activation of TLR3 or RIG-I pathways upon stimulation with specific agonists. HEK293 cells that stably express TLR3 (293-TLR3) were stimulated by addition of synthetic

dsRNA analog, polyI:C, in culture medium. Luciferase activities were measured from above mentioned promoters in the presence and absence of NS1 expression from several influenza strains like A/PR/8/34, A/HK/218847/06, A/HK/218449/06 and A/Vietnam/1203/04 (Figure 6.7A). A 25 and 100 fold induction from IFN- $\beta$  and NF- $\kappa$ B promoters were observed upon polyI:C stimulation respectively (Figure 6.7A). Interestingly, none of NS1 protein from tested strains of influenza was able to abrogate the luciferase activity from these promoters (Figure 6.7A). Similar experiments were performed to determine the effect of NS1 on RIG-I induced activation of IFN- $\beta$ , p55C1B (IRF3) and pRDII (NF- $\kappa$ B) promoters upon Sendai virus (SeV) stimulation, which activates the RIG-I pathway (Figure 6.7B). A 20-40 fold induction (over the control) of luciferase activity was seen from the above promoters when stimulated with SeV. A 20-80% inhibition was observed from the stimulated promoters in the presence of NS1 from various strains (Figure 6.7B). Interestingly, slight strain dependent differences in inhibition of promoter activities were noticed that are further addressed by additional experiments in subsequent section. These results suggest that NS1 is able to inhibit activation of the IFN- $\beta$  promoter through RIG-I pathways but not TLR3 pathway.

#### *6.3.2 Influenza NS1 regulates RIG-I induced interferon blockade in strain specific manner*

In order to further evaluate the strain specific differences in NS1 contributing to RIG-I induced interferon blockade and to identify the molecules affected by NS1 in RIG-I signaling pathway, NS1 blockade was studied using above mentioned reporter assays.

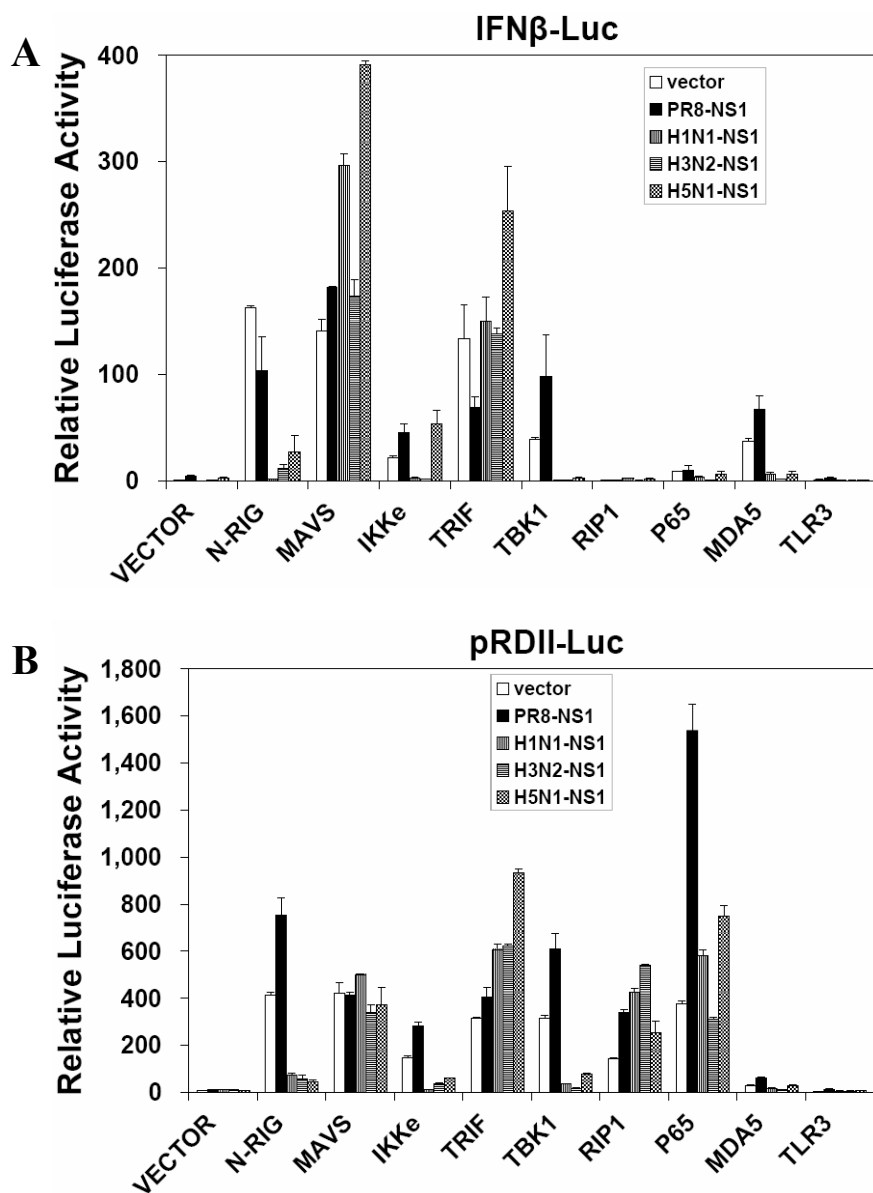


**Figure 6.8 NS1 protein of influenza regulates activation of IFN- $\beta$  and NF- $\kappa$ B promoter by RIG-I pathway.** HEK293T cells were cotransfected with pIFN- $\beta$ -Luc (A) or pRDII-Luc (B) and pCMV $\beta$ -gal plasmids along with a vector encoding various strains of influenza NS1 or an empty vector along with ectopic expression of various signaling molecules in RIG-I/TLR3/MDA5 pathways above the levels of IRF3. Bars show relative luciferase activity normalized to  $\beta$ -galactosidase activity, i.e. IFN- $\beta$  and NF- $\kappa$ B promoter activity.

Restoration of IFN- $\beta$  and PRDII promoter activity were monitored in 293T cells expressing NS1 along with ectopic expression of signaling proteins MAVS, IKK $\epsilon$ , TBK1, TRIF, IRF3-5D, MDA5, RIP1 and P65 that are known to participate upstream of IRF3 activation, in RIG-I pathway. MAVS and TRIF were able to relieve the NS1 (from all strains, Figure 6.8A and B) mediated inhibition from both promoters while RIP1 and P65 were able to relieve from PRDII promoter (Figure 6.8B). In contrast, constitutively active CARD domain of RIG-I (N-RIG) is able to relieve NS1 inhibition of interferon blockade caused by NS1 of PR8 strain alone but not other strains indicating strain specificity (Figure 6.8A and B). However, constitutively active CARD domain of MDA5 is also able to relieve NS1 inhibition of IFN responses in PR8 alone. The results from these experiments suggest that NS1 disrupts RIG-I/MDA5 mediated interferon response by blocking signaling from PRRs either by directly interacting with PRRs or by sequestering other partners that are important for PRR activation.

### *6.3.3 Cloning of A/Brisbane/59/2007/H1N1, A/California/04/2009/H1N1, A/Brisbane/10/2007/H3N2 and B/Florida/04/2006 and Rescue of PR8 strain*

Highly pathogenic avian influenza A (H5N1) virus that has a mortality rate of more than 60% and a recent global outbreak of H1N1 swine flu have raised fears regarding the emergence of potential human pandemic. The pathogenic virulence of Influenza virus depends on multi-gene trait involving variations in eight genes. The detailed mechanism of influenza pathogenesis still remains elusive; Mutations in NS1 are suggested to alter influenza virulence. Development of reverse genetics systems is

necessary to understand the functional basis of emerging viruses in regard to their virulence and pathogenicity. In this regard, all the eight RNA segments of influenza A virus strains A/Brasbne/59/2007/H1N1, A/California/04/2009/H1N1, A/Brasbne/10/2007/H3N2 and B virus strain B/Florida/04/2004 were reverse transcribed, PCR amplified and the PCR products were cloned in pAH12 vector (Figure 6.9).

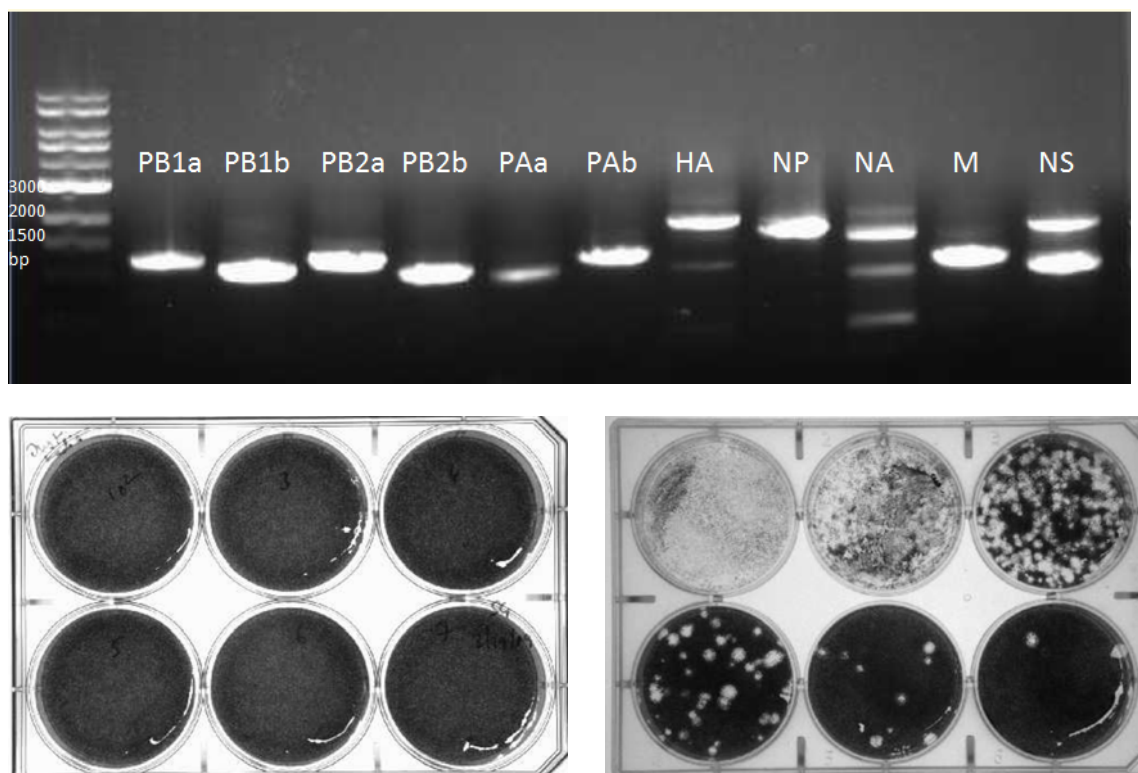


**Figure 6.9 Virus rescue and plaque formation of PR8 strain.** **Top.** Agarose gel analysis RT-PCR amplified genome segment products of A/California/04/2009 strain. The PB1, PB2 and PA genes were PCR amplified using specific primers sets containing one of the *Bsm*BI or *Aar*I or *Bsa*I sites that results in two amplified fragments. **Bottom.** Plaque assay stained with crystal violet. **Left.** MDCK cells infected with media without virus. **Right** MDCK cells infected with various dilution of PR8 strain of influenza rescued by co-culturing MDCK and HEK293 cells.

The viral cDNAs cloned into resultant plasmids were sequenced in their entirety and represent the consensus sequence of the eight segments of A/California/04/2009/H1N1. These plasmids were designated as pGH41-PB2, pGH42-PB1, pGH43-PA, pGH44-HA, pGH45-NP, pGH46-NA, pGH47-M and pGH48-NS. PR8 strain of influenza was rescued by co-culturing of MDCK and HEK293T transfected with 8 plasmids containing the complete genome of PR8 strains. The co-culture supernatant was titrated for the presence of infectious virus particles 3 days after infection by plaque assay and found to have  $3 \times 10^8$  Plaque forming unit/ml (PFU/ml) (Figure 6.9).

#### **6.4 DISCUSSION**

Recent WHO reports indicate several strains like H5N1, H1N1, H3N2 A/Brisbane/10/2007 have developed resistance to antivirals like amantadine, rimantadine and oseltamivir (Kiso et al., 2004; Treanor et al., 2000) by compensatory mutations in the target viral proteins. Immunomodulation is one more effective strategy to boost host innate immunity in addition to antivirals directed against the virus (Basu et al., 2009). NS1 is an important protein encoded by influenza viruses known to antagonize host interferon response.

NS1 is suggested to interact with multiple cellular proteins and is a potential target for anti-viral drug design for screening small molecules that disrupt NS1 interaction with cellular and viral factors involved in the mediating pathogenicity. Strain dependent sequence variation in NS1 may lead to altered binding affinities to host proteins that can result in dramatic effect on pathogenicity. Hence, detailed molecular

characterizations underlying protein-protein interactions of NS1 with host proteins are important in developing potent immunomodulators. Influenza virus replication is inhibited by the peptide mediated disruption of NS1-CPSF30 interaction in cell culture (Twu et al., 2006).

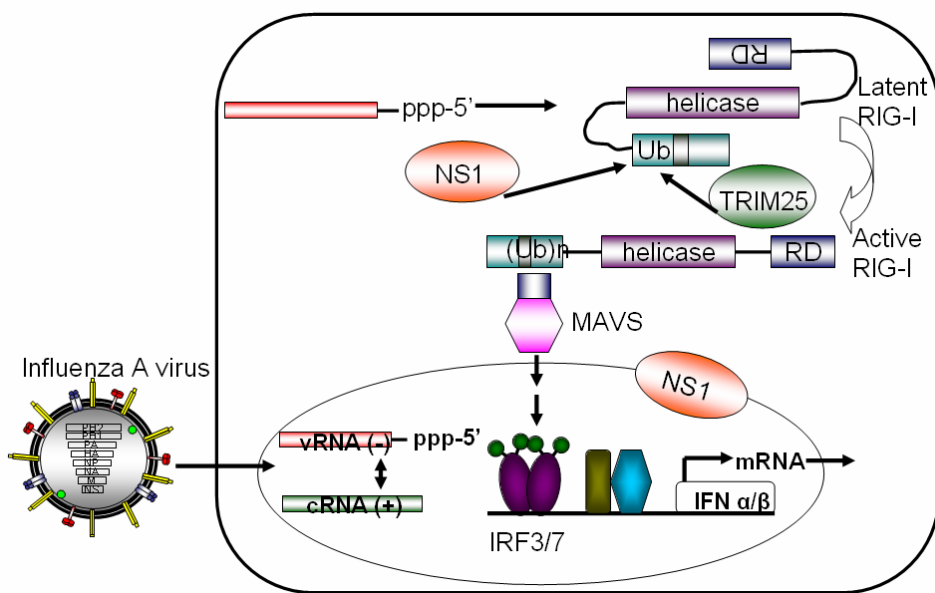


**Figure 6.10 Schematic representation of NS1 protein involvement with PRR RIG-I.** Influenza A virus inhibits the RIG-I signaling module by binding the viral NS1 protein to TRIM25. RIG-I binding to MAVS requires ubiquitination of RIG-I in the second CARD by the ubiquitin Ligase TRIM25. This interaction triggers subsequent signaling for the activation of the transcription Factors IRF3/7 that induce type I genes (Ludwig and Wolff, 2009)

The recently solved crystal structures of NS1 provide structural information necessary for rational designing of inhibitors that can disrupt protein-protein interactions of NS1 with cellular factors which helps indirectly to boost the immune response to combat flu

infection (Bornholdt and Prasad, 2006; Bornholdt and Prasad, 2008). During an early stage of infection, NS1 activates PI3 kinase by AKT phosphorylation that is thought to be anti-apoptotic leading to cell proliferation (Zhirnov and Klenk, 2007). NS1 proteins of avian origin, but not human are observed to hyper activate PI3 kinase by interacting with N-terminal SH3 domains of human signaling proteins Crk and CrkL by a conserved classII SH3 binding motif (Finkelstein et al., 2007; Heikkinen et al., 2008). Inhibition of PI3 Kinase using wortmannin (a fungal metabolite that specifically inhibits PI3 kinase, MAPK and myocin light-chain kinase MLCK) resulted in apoptosis of culture cells infected with the virus (Ehrhardt et al., 2007; Zhirnov and Klenk, 2007). NS1 has been shown to limit IFN- $\beta$  induction in a number studies. However, many studies reported that ablation of IFN- $\beta$  induction mediated by NS1 may be strain specific. In case of PR8 strain NS1 abrogates IFN- $\beta$  induction involving pre-transcriptional events (Guo et al., 2007; Mibayashi et al., 2007; Opitz et al., 2007; Pichlmair et al., 2006) while NS1 from other strains such as Tx/NS1 limitation of IFN- $\beta$  induction occurs by inhibition of post-transcriptional processing of IFN- $\beta$  pre-mRNAs (Kochs et al., 2007). It has also been shown that RIG-I can recognize influenza ssRNA not necessarily dsRNA which is replicative intermediate leading to the activation of IFN response (Pichlmair et al., 2006). It is also speculated that NS1 can sequester viral replicative intermediates (RNA) by RNA binding domain concealing it from cellular PRRs or NS1 can interfere with the function of one or more proteins in PRRs mediated interferon signaling. Several groups have shown that PR8 NS1 inhibits RIG-I/MAVS signaling pathway. Still the mechanism of PR8 NS1 interaction with RIG-I/MAVS is unclear. These studies corroborates with

my results showing NS1 from different strains can inhibit RIG-I/MAVS activated interferon response. Surprisingly, none of the NS1 protein from tested strains of influenza inhibits the host interferon activated by TLR3. In contrast, NS1 from all the strain are able inhibit RIG-I mediated interferon signaling. Strain specific difference in the ability of NS1 was observed in the nature of the interaction with the cellular signaling molecules that participate in RIG-I pathway.

Recent study show that NS1 inhibits TRIM25 mediated RIG-I CARD ubiquitination (Gack et al., 2009). TRIM25 has been shown to induce Lys-63 linked ubiquitination of the N-terminal CARD domain of RIG-I is critical for the activation of interferon response (Gack et al., 2009; Gack et al., 2008; Gack et al., 2007). NS1 mediates the RIG-I inhibition by blocking RIG-I/TRIM 25 interaction by sequestering TRIM25. The coiled coil domain of TRIM25 interacts with novel domain of NS1 consisting of E96/E97 residues. This interaction leads to blocking of multimerization of TRIM25 and ubiquitination of RIG-I CARD domain.

Influenza virus (FLU) affects millions of people as a worldwide pandemic and thousands in seasonal infection (Subbarao, 1999). Flu accounts for ~30,000 deaths each year in United States. Variation of the virus in host as it replicates due to genetic shift and genetic drift renders the development of a common flu vaccine a big challenge. However, in pursuit of an effective vaccine against potentially pandemic strains like H5N1 and H1N1, it is necessary to generate experimental evidence of protection against various influenza viruses by immunizing with live attenuated vaccine candidates derived from reverse genetic systems to understand the vaccine efficacy, disease pathogenesis and

virus evolution. This information is also valuable to rationalize the objective paths to continue the pursuit of such a vaccine to prevent the pandemic and seasonal flu. Development of influenza reverse genetics systems will have dual impact by hastening the process of vaccine development in a globally cost effective way and studying disease pathogenesis and interaction with host immune system. Towards these objectives and as part of this dissertation project, past few months were spent to characterize the role of NS1 in modulating innate immune response and to generate reverse genetics systems of various influenza A and B subtypes. All the eight RNA segments of influenza A virus strains                   A/Brisbane/59/2007/H1N1,                   A/California/04/2009/H1N1, A/Brisbane/10/2007/H3N2 and B virus strain B/Florida/04/2004 were reverse transcribed, PCR amplified and the PCR products were cloned in pAH12 vector (Figure 6.1). Currently, these clones are being sequenced for further characterization. The availability of reverse genetics system helps to study the NS1 and other viral proteins of their role in pathogenesis.

Most RNA viruses replicate in the cytoplasm unlike influenza virus that replicates in the nucleus and vRNA is exported into the cytoplasm as RNPs. This raises a question as to how RIG-I like helicases are able to detect the RNA complexed with RNPs. It may be possible all the RNAs exported out of the nucleus may not be packed as RNPs. A small fraction of the viral RNAs may be present protein free. Also defective RNAs can exist that potentially trigger RIG-I like helicases to induce IFN signaling. It is possible that NS1 shuttling between the nucleus and cytoplasm can compete with RIG-I and also interact with these RNAs and counter the host innate immune response. It would be

interesting to understand the mechanism of RIG-I mediated antiviral signaling in context of viral RNPs

## **CHAPTER 7: CONCLUSIONS AND FUTURE DIRECTIONS**

In order to achieve maximum protection against invading pathogens; a critical balance is necessary for activation of innate immune response between clearing the infection and resulting in severe inflammatory disease. Therefore, a detailed understanding of how this is achieved in humans will help tailor effective therapies based on molecular variability of pathogen and human disease susceptibility.

Pathogens are under constant biological pressure to evolve novel strategies to evade innate immune response and often this is achieved by small changes in their proteins to their advantage that changes their ability to interact with one or more host proteins involved in pathogen detection and clearance. However, innate immune response to invading pathogens appears to be more complex and redundant involving multiple actuators, effectors and signaling cascades. This is exemplified by numerous PRRs that detect a large number of PAMPs contributing to an efficient detection system where if one PRR fails or if a pathogen has developed an evading strategy to a particular PRR it will be eventually detected by other remaining PRRs in this complex system (Zak and Aderem, 2009). Evidence for the existence of such complex system comes from the gene knock-out studies, where PRR knockouts fail to show expected phenotype. In the absence of TLR3 dsRNA from the viral pathogens can be detected by other PRRs like RIG-I, MDA5 and TLR7 providing the necessary protection for the host against viral pathogens (Edelmann et al., 2004).

Complex systems are efficient because of “acquired properties” that cannot be predicted from oversimplified studies based on many assumptions. Understanding positive and negative feed back loops in controlling signaling and gene expression is necessary to appreciate “robustness” built in innate immune response. Robust antiviral state is achieved by production of type I IFN from activation of PRRs by the detection of viral sensors is an example of positive feed backloop that is accomplished by activated IFN regulatory factor-3 (IRF3) and IRF7 (transcription factors). The type I IFN then act on the cells in self-inducing fashion by activating IRF7 at higher levels necessary to prime the system for responding to smaller amounts of PAMPs (Honda et al., 2005b). In contrast, negative feed back loops are present to control inflammation that could arise due to background noise or over activation. In TLR pathway responding to dsRNA, the ubiquitin editing protein A20 induced by TLR activation acts as a negative regulator (Liew et al., 2005) by directly modulating the activation of key adaptors molecules like tumor necrosis factor receptor-associated factor 6 (TRAF6), TRIF and receptor-interacting protein 2 (RIP2) (Boone et al., 2004; Hitotsumatsu et al., 2008; Lin et al., 2006; Saitoh et al., 2005; Wang et al., 2004) necessary for TLR, RLR and NLR signaling.

To accomplish the detection of a diverse variety of microbial PAMPs, modular nature is inbuilt in both the signaling pathways and the PRRs. For example, the TLR family of PRRs comprise of 13 members that have highly variable N-terminal LRR domain and a highly conserved C-terminal TIR domain connected by a single

transmembrane domain. This variation in LRRs is necessary to detect diverse nature of ligand associated with pathogens (Roach et al., 2005).

In this dissertation, I have made an attempt to understand the complex antiviral signaling pathways at cellular level responding to infections/proteins of three distinct single strand RNA viruses namely, SARS-CoV, HCV and Influenza virus. Although, these viruses trigger similar PRR signaling pathways, significant difference are noticed with respect to PRRs they engage and the mechanistic nature in which they evade host detection.

Studies reported in chapter 3 of this dissertation provide insights about how SARS-CoV PLpro is advantageous to the virus in evading host interferon response. My studies constitute first report to present evidence that PLpro, a papain like protease help evades interferon response by blocking IRF3 phosphorylation, dimerization and nuclear translocation. My results indicate that protease activity is not required for mediating immune evasion unlike NS3/4A protease of HCV. Further studies are necessary to dissect the molecular basis of PLpro mediated immune evasion targeting its deubiquitination activity or its ability to interacts with other cellular signaling proteins.

In chapter 5, my studies probe the role of TLR3 and RIG-I contributing to cellular permissiveness of HCV infection in human liver cells. Reconstitution of the functional TLR3 and RIG-I in human hepatoma cells decreased HCV replication and infection. However, the replication was restored in TLR3 inactive mutants indicating that TLR3 plays a major role in the outcome of HCV infection. Hence, early sustained interferon response mediated by TLR3 appears to be an important component in limiting HCV

infection during acute phase. Further, my results demonstrate for the first time that TLR3 co-localizes to dsRNA abundant membrane compartments containing HCV replication complexes. Specific protein-protein interactions between TLR3 and viral proteins of replication complex may mediate the localization of TLR3 to membrane compartments containing HCV replication complex. However, further studies are necessary to demonstrate the molecular nature of these protein-protein and protein-nucleic acid interactions in generating an antiviral state.

Chapter 6 pertains about my studies on influenza NS1 protein and its interaction with host protein in innate immune signaling pathways. My studies demonstrate that NS1 is able to antagonize interferon response by blocking RIG-I/MDA5 activation. This chapter also describes generation of reverse genetics systems to various emerging influenza strains including strains from swine flu outbreak. The reverse genetics system is useful to probe the molecular basis of mutation in NS1 protein and the consequence associated in its interaction with host proteins of innate immune signaling and their subsequent contribution in pathogenesis by systems biology approach involving proteomics and quantitative mass spectrometry. Characterization of underlying protein-protein interaction of NS1 with host proteins is important in developing potent immunomodulators.

## REFERENCES

- Abbott, D. W., Wilkins, A., Asara, J. M., and Cantley, L. C. (2004). The Crohn's disease protein, NOD2, requires RIP2 in order to induce ubiquitinylation of a novel site on NEMO. *Curr Biol* 14, 2217-2227.
- Ahmad-Nejad, P., Hacker, H., Rutz, M., Bauer, S., Vabulas, R. M., and Wagner, H. (2002). Bacterial CpG-DNA and lipopolysaccharides activate Toll-like receptors at distinct cellular compartments. *Eur J Immunol* 32, 1958-1968.
- Akagi, T., Murata, K., Shishido, T., and Hanafusa, H. (2002). v-Crk activates the phosphoinositide 3-kinase/AKT pathway by utilizing focal adhesion kinase and H-Ras. *Mol Cell Biol* 22, 7015-7023.
- Akira, S., and Takeda, K. (2004). Toll-like receptor signalling. *Nat Rev Immunol* 4, 499-511.
- Alexopoulou, L., Holt, A. C., Medzhitov, R., and Flavell, R. A. (2001). Recognition of double-stranded RNA and activation of NF-kappaB by Toll-like receptor 3. *Nature* 413, 732-738.
- Aliprantis, A. O., Yang, R. B., Mark, M. R., Suggett, S., Devaux, B., Radolf, J. D., Klimpel, G. R., Godowski, P., and Zychlinsky, A. (1999). Cell activation and apoptosis by bacterial lipoproteins through toll-like receptor-2. *Science* 285, 736-739.
- Alter, H. J., and Houghton, M. (2000). Clinical Medical Research Award. Hepatitis C virus and eliminating post-transfusion hepatitis. *Nat Med* 6, 1082-1086.
- Alter, H. J., and Seeff, L. B. (2000). Recovery, persistence, and sequelae in hepatitis C virus infection: a perspective on long-term outcome. *Semin Liver Dis* 20, 17-35.
- Anderson, R., and Wong, F. (1993). Membrane and phospholipid binding by murine coronaviral nucleocapsid N protein. *Virology* 194, 224-232.
- Andrejeva, J., Childs, K. S., Young, D. F., Carlos, T. S., Stock, N., Goodbourn, S., and Randall, R. E. (2004). The V proteins of paramyxoviruses bind the IFN-inducible RNA helicase, mda-5, and inhibit its activation of the IFN-beta promoter. *Proc Natl Acad Sci U S A* 101, 17264-17269.
- Barker, W. H., and Mullooly, J. P. (1982). A study of excess mortality during influenza epidemics in the United States, 1968-1976. *Am J Epidemiol* 115, 479-480.
- Barretto, N., Jukneliene, D., Ratia, K., Chen, Z., Mesecar, A. D., and Baker, S. C. (2005). The papain-like protease of severe acute respiratory syndrome coronavirus has deubiquitinating activity. *J Virol* 79, 15189-15198.

- Barreto, N., Jukneliene, D., Ratia, K., Chen, Z., Mesecar, A. D., and Baker, S. C. (2006). Deubiquitinating activity of the SARS-CoV papain-like protease. *Adv Exp Med Biol* 581, 37-41.
- Barton, G. M., Kagan, J. C., and Medzhitov, R. (2006). Intracellular localization of Toll-like receptor 9 prevents recognition of self DNA but facilitates access to viral DNA. *Nat Immunol* 7, 49-56.
- Basu, D., Walkiewicz, M. P., Frieman, M., Baric, R. S., Auble, D. T., and Engel, D. A. (2009). Novel influenza virus NS1 antagonists block replication and restore innate immune function. *J Virol* 83, 1881-1891.
- Bell, J. K., Askins, J., Hall, P. R., Davies, D. R., and Segal, D. M. (2006a). The dsRNA binding site of human Toll-like receptor 3. *Proc Natl Acad Sci U S A* 103, 8792-8797.
- Bell, J. K., Botos, I., Hall, P. R., Askins, J., Shiloach, J., Davies, D. R., and Segal, D. M. (2006b). The molecular structure of the TLR3 extracellular domain. *J Endotoxin Res* 12, 375-378.
- Bell, J. K., Botos, I., Hall, P. R., Askins, J., Shiloach, J., Segal, D. M., and Davies, D. R. (2005). The molecular structure of the Toll-like receptor 3 ligand-binding domain. *Proc Natl Acad Sci U S A* 102, 10976-10980.
- Bigger, C. B., Brasky, K. M., and Lanford, R. E. (2001). DNA microarray analysis of chimpanzee liver during acute resolving hepatitis C virus infection. *J Virol* 75, 7059-7066.
- Blight, K. J., McKeating, J. A., and Rice, C. M. (2002). Highly permissive cell lines for subgenomic and genomic hepatitis C virus RNA replication. *J Virol* 76, 13001-13014.
- Bonin, M., Oberstrass, J., Lukacs, N., Ewert, K., Oesterschulze, E., Kassing, R., and Nellen, W. (2000). Determination of preferential binding sites for anti-dsRNA antibodies on double-stranded RNA by scanning force microscopy. *RNA* 6, 563-570.
- Boone, D. L., Turer, E. E., Lee, E. G., Ahmad, R. C., Wheeler, M. T., Tsui, C., Hurley, P., Chien, M., Chai, S., Hitotsumatsu, O., et al. (2004). The ubiquitin-modifying enzyme A20 is required for termination of Toll-like receptor responses. *Nat Immunol* 5, 1052-1060.
- Bornholdt, Z. A., and Prasad, B. V. (2006). X-ray structure of influenza virus NS1 effector domain. *Nat Struct Mol Biol* 13, 559-560.
- Bornholdt, Z. A., and Prasad, B. V. (2008). X-ray structure of NS1 from a highly pathogenic H5N1 influenza virus. *Nature* 456, 985-988.
- Bos, E. C., Heijnen, L., Luytjes, W., and Spaan, W. J. (1995). Mutational analysis of the murine coronavirus spike protein: effect on cell-to-cell fusion. *Virology* 214, 453-463.
- Bos, E. C., Luytjes, W., van der Meulen, H. V., Koerten, H. K., and Spaan, W. J. (1996). The production of recombinant infectious DI-particles of a murine coronavirus in the absence of helper virus. *Virology* 218, 52-60.

- Boursnell, M. E., Brown, T. D., Foulds, I. J., Green, P. F., Tomley, F. M., and Binns, M. M. (1987a). The complete nucleotide sequence of avian infectious bronchitis virus: analysis of the polymerase-coding region. *Adv Exp Med Biol* 218, 15-29.
- Boursnell, M. E., Brown, T. D., Foulds, I. J., Green, P. F., Tomley, F. M., and Binns, M. M. (1987b). Completion of the sequence of the genome of the coronavirus avian infectious bronchitis virus. *J Gen Virol* 68 (Pt 1), 57-77.
- Brayton, P. R., Ganges, R. G., and Stohlman, S. A. (1981). Host cell nuclear function and murine hepatitis virus replication. *J Gen Virol* 56, 457-460.
- Brinkmann, M. M., Spooner, E., Hoebe, K., Beutler, B., Ploegh, H. L., and Kim, Y. M. (2007). The interaction between the ER membrane protein UNC93B and TLR3, 7, and 9 is crucial for TLR signaling. *J Cell Biol* 177, 265-275.
- Calvo, D., Gomez-Coronado, D., Lasuncion, M. A., and Vega, M. A. (1997). CLA-1 is an 85-kD plasma membrane glycoprotein that acts as a high-affinity receptor for both native (HDL, LDL, and VLDL) and modified (OxLDL and AcLDL) lipoproteins. *Arterioscler Thromb Vasc Biol* 17, 2341-2349.
- Calvo, M., and Enrich, C. (2000). Biochemical analysis of a caveolae-enriched plasma membrane fraction from rat liver. *Electrophoresis* 21, 3386-3395.
- Cavanagh, D. (1997). Nidovirales: a new order comprising Coronaviridae and Arteriviridae. *Arch Virol* 142, 629-633.
- Cavanagh, D. (2008). SARS- and other coronaviruses. *Methods Mol Biol* 454, v-vi.
- Cavanagh, D., Brian, D. A., Brinton, M. A., Enjuanes, L., Holmes, K. V., Horzinek, M. C., Lai, M. M., Laude, H., Plagemann, P. G., Siddell, S. G., and et al. (1993). The Coronaviridae now comprises two genera, coronavirus and torovirus: report of the Coronaviridae Study Group. *Adv Exp Med Biol* 342, 255-257.
- Chan, K. H., Poon, L. L., Cheng, V. C., Guan, Y., Hung, I. F., Kong, J., Yam, L. Y., Seto, W. H., Yuen, K. Y., and Peiris, J. S. (2004). Detection of SARS coronavirus in patients with suspected SARS. *Emerg Infect Dis* 10, 294-299.
- Chen, C. J., Sugiyama, K., Kubo, H., Huang, C., and Makino, S. (2004). Murine coronavirus nonstructural protein p28 arrests cell cycle in G0/G1 phase. *J Virol* 78, 10410-10419.
- Chen, Z., Benureau, Y., Rijnbrand, R., Yi, J., Wang, T., Warter, L., Lanford, R. E., Weinman, S. A., Lemon, S. M., Martin, A., and Li, K. (2007a). GB virus B disrupts RIG-I signaling by NS3/4A-mediated cleavage of the adaptor protein MAVS. *J Virol* 81, 964-976.
- Chen, Z., Rijnbrand, R., Jangra, R. K., Devaraj, S. G., Qu, L., Ma, Y., Lemon, S. M., and Li, K. (2007b). Ubiquitination and proteasomal degradation of interferon regulatory factor-3 induced by Npro from a cytopathic bovine viral diarrhea virus. *Virology* 366, 277-292.

- Cheng, G., Zhong, J., and Chisari, F. V. (2006). Inhibition of dsRNA-induced signaling in hepatitis C virus-infected cells by NS3 protease-dependent and -independent mechanisms. *Proc Natl Acad Sci U S A* *103*, 8499-8504.
- Childs, K. S., Andrejeva, J., Randall, R. E., and Goodbourn, S. (2009). Mechanism of mda-5 Inhibition by paramyxovirus V proteins. *J Virol* *83*, 1465-1473.
- Chisholm, S. T., Coaker, G., Day, B., and Staskawicz, B. J. (2006). Host-microbe interactions: shaping the evolution of the plant immune response. *Cell* *124*, 803-814.
- Choe, J., Kelker, M. S., and Wilson, I. A. (2005). Crystal structure of human toll-like receptor 3 (TLR3) ectodomain. *Science* *309*, 581-585.
- Choo, Q. L., Kuo, G., Weiner, A. J., Overby, L. R., Bradley, D. W., and Houghton, M. (1989). Isolation of a cDNA clone derived from a blood-borne non-A, non-B viral hepatitis genome. *Science* *244*, 359-362.
- Connor, R. J., Kawaoka, Y., Webster, R. G., and Paulson, J. C. (1994). Receptor specificity in human, avian, and equine H2 and H3 influenza virus isolates. *Virology* *205*, 17-23.
- Couceiro, J. N., Paulson, J. C., and Baum, L. G. (1993). Influenza virus strains selectively recognize sialyloligosaccharides on human respiratory epithelium; the role of the host cell in selection of hemagglutinin receptor specificity. *Virus Res* *29*, 155-165.
- Cui, S., Eisenacher, K., Kirchhofer, A., Brzozka, K., Lammens, A., Lammens, K., Fujita, T., Conzelmann, K. K., Krug, A., and Hopfner, K. P. (2008). The C-terminal regulatory domain is the RNA 5'-triphosphate sensor of RIG-I. *Mol Cell* *29*, 169-179.
- De Francesco, R., and Migliaccio, G. (2005). Challenges and successes in developing new therapies for hepatitis C. *Nature* *436*, 953-960.
- Deforges, S., Evlashev, A., Perret, M., Sodoyer, M., Pouzol, S., Scoazec, J. Y., Bonnaud, B., Diaz, O., Paranhos-Baccala, G., Lotteau, V., and Andre, P. (2004). Expression of hepatitis C virus proteins in epithelial intestinal cells in vivo. *J Gen Virol* *85*, 2515-2523.
- Deng, L., Wang, C., Spencer, E., Yang, L., Braun, A., You, J., Slaughter, C., Pickart, C., and Chen, Z. J. (2000). Activation of the IkappaB kinase complex by TRAF6 requires a dimeric ubiquitin-conjugating enzyme complex and a unique polyubiquitin chain. *Cell* *103*, 351-361.
- Devaraj, S. G., Wang, N., Chen, Z., Tseng, M., Barreto, N., Lin, R., Peters, C. J., Tseng, C. T., Baker, S. C., and Li, K. (2007). Regulation of IRF-3-dependent innate immunity by the papain-like protease domain of the severe acute respiratory syndrome coronavirus. *J Biol Chem* *282*, 32208-32221.
- Dias, A., Bouvier, D., Crepin, T., McCarthy, A. A., Hart, D. J., Baudin, F., Cusack, S., and Ruigrok, R. W. (2009). The cap-snatching endonuclease of influenza virus polymerase resides in the PA subunit. *Nature* *458*(7240), 914-918.

- Diebold, S. S., Kaisho, T., Hemmi, H., Akira, S., and Reis e Sousa, C. (2004). Innate antiviral responses by means of TLR7-mediated recognition of single-stranded RNA. *Science* *303*, 1529-1531.
- Doyle, S., Vaidya, S., O'Connell, R., Dadgostar, H., Dempsey, P., Wu, T., Rao, G., Sun, R., Haberland, M., Modlin, R., and Cheng, G. (2002). IRF3 mediates a TLR3/TLR4-specific antiviral gene program. *Immunity* *17*, 251-263.
- Dubois-Dalcq, M. E., Doller, E. W., Haspel, M. V., and Holmes, K. V. (1982). Cell tropism and expression of mouse hepatitis viruses (MHV) in mouse spinal cord cultures. *Virology* *119*, 317-331.
- Edelmann, K. H., Richardson-Burns, S., Alexopoulou, L., Tyler, K. L., Flavell, R. A., and Oldstone, M. B. (2004). Does Toll-like receptor 3 play a biological role in virus infections? *Virology* *322*, 231-238.
- Edwards, K. M., Dupont, W. D., Westrich, M. K., Plummer, W. D., Jr., Palmer, P. S., and Wright, P. F. (1994). A randomized controlled trial of cold-adapted and inactivated vaccines for the prevention of influenza A disease. *J Infect Dis* *169*, 68-76.
- Ehrhardt, C., Wolff, T., Pleschka, S., Planz, O., Beermann, W., Bode, J. G., Schmolke, M., and Ludwig, S. (2007). Influenza A virus NS1 protein activates the PI3K/Akt pathway to mediate antiapoptotic signaling responses. *J Virol* *81*, 3058-3067.
- Eleouet, J. F., Rasschaert, D., Lambert, P., Levy, L., Vende, P., and Laude, H. (1995a). Complete genomic sequence of the transmissible gastroenteritis virus. *Adv Exp Med Biol* *380*, 459-461.
- Eleouet, J. F., Rasschaert, D., Lambert, P., Levy, L., Vende, P., and Laude, H. (1995b). Complete sequence (20 kilobases) of the polyprotein-encoding gene 1 of transmissible gastroenteritis virus. *Virology* *206*, 817-822.
- Enjoji, M., Nakamura, M., Kinukawa, N., Sugimoto, R., Noguchi, K., Tsuruta, S., Iwao, M., Kotoh, K., Iwamoto, H., and Nawata, H. (2000). Beta-lipoproteins influence the serum level of hepatitis C virus. *Med Sci Monit* *6*, 841-844.
- Evans, M. J., von Hahn, T., Tscherne, D. M., Syder, A. J., Panis, M., Wolk, B., Hatzioannou, T., McKeating, J. A., Bieniasz, P. D., and Rice, C. M. (2007). Claudin-1 is a hepatitis C virus co-receptor required for a late step in entry. *Nature*.
- Fan, K., Wei, P., Feng, Q., Chen, S., Huang, C., Ma, L., Lai, B., Pei, J., Liu, Y., Chen, J., and Lai, L. (2004). Biosynthesis, purification, and substrate specificity of severe acute respiratory syndrome coronavirus 3C-like proteinase. *J Biol Chem* *279*, 1637-1642.
- Farcas, G. A., Poutanen, S. M., Mazzulli, T., Willey, B. M., Butany, J., Asa, S. L., Faure, P., Akhavan, P., Low, D. E., and Kain, K. C. (2005). Fatal severe acute respiratory syndrome is associated with multiorgan involvement by coronavirus. *J Infect Dis* *191*, 193-197.

- Fazakerley, J. K., Parker, S. E., Bloom, F., and Buchmeier, M. J. (1992). The V5A13.1 envelope glycoprotein deletion mutant of mouse hepatitis virus type-4 is neuroattenuated by its reduced rate of spread in the central nervous system. *Virology* 187, 178-188.
- Fechter, P., Mingay, L., Sharps, J., Chambers, A., Fodor, E., and Brownlee, G. G. (2003). Two aromatic residues in the PB2 subunit of influenza A RNA polymerase are crucial for cap binding. *J Biol Chem* 278, 20381-20388.
- Feinstone, S. M., Kapikian, A. Z., Purcell, R. H., Alter, H. J., and Holland, P. V. (1975). Transfusion-associated hepatitis not due to viral hepatitis type A or B. *N Engl J Med* 292, 767-770.
- Feld, J. J., and Hoofnagle, J. H. (2005). Mechanism of action of interferon and ribavirin in treatment of hepatitis C. *Nature* 436, 967-972.
- Finkelstein, D. B., Mukatira, S., Mehta, P. K., Obenauer, J. C., Su, X., Webster, R. G., and Naeve, C. W. (2007). Persistent host markers in pandemic and H5N1 influenza viruses. *J Virol* 81, 10292-10299.
- Forton, D. M., Karayiannis, P., Mahmud, N., Taylor-Robinson, S. D., and Thomas, H. C. (2004a). Identification of unique hepatitis C virus quasispecies in the central nervous system and comparative analysis of internal translational efficiency of brain, liver, and serum variants. *J Virol* 78, 5170-5183.
- Forton, D. M., Thomas, H. C., and Taylor-Robinson, S. D. (2004b). Central nervous system involvement in hepatitis C virus infection. *Metab Brain Dis* 19, 383-391.
- Fosmire, J. A., Hwang, K., and Makino, S. (1992). Identification and characterization of a coronavirus packaging signal. *J Virol* 66, 3522-3530.
- Fouchier, R. A., Hartwig, N. G., Bestebroer, T. M., Niemeyer, B., de Jong, J. C., Simon, J. H., and Osterhaus, A. D. (2004). A previously undescribed coronavirus associated with respiratory disease in humans. *Proc Natl Acad Sci U S A* 101, 6212-6216.
- Foy, E., Li, K., Sumpter, R., Jr., Loo, Y. M., Johnson, C. L., Wang, C., Fish, P. M., Yoneyama, M., Fujita, T., Lemon, S. M., and Gale, M., Jr. (2005). Control of antiviral defenses through hepatitis C virus disruption of retinoic acid-inducible gene-I signaling. *Proc Natl Acad Sci U S A* 102, 2986-2991.
- Foy, E., Li, K., Wang, C., Sumpter, R., Jr., Ikeda, M., Lemon, S. M., and Gale, M., Jr. (2003). Regulation of interferon regulatory factor-3 by the hepatitis C virus serine protease. *Science* 300, 1145-1148.
- Fredericksen, B. L., Keller, B. C., Fornek, J., Katze, M. G., and Gale, M., Jr. (2008). Establishment and maintenance of the innate antiviral response to West Nile Virus involves both RIG-I and MDA5 signaling through IPS-1. *J Virol* 82, 609-616.
- Gack, M. U., Albrecht, R. A., Urano, T., Inn, K. S., Huang, I. C., Carnero, E., Farzan, M., Inoue, S., Jung, J. U., and Garcia-Sastre, A. (2009). Influenza A virus NS1 targets the

ubiquitin ligase TRIM25 to evade recognition by the host viral RNA sensor RIG-I. *Cell Host Microbe* 5, 439-449.

Gack, M. U., Kirchhofer, A., Shin, Y. C., Inn, K. S., Liang, C., Cui, S., Myong, S., Ha, T., Hopfner, K. P., and Jung, J. U. (2008). Roles of RIG-I N-terminal tandem CARD and splice variant in TRIM25-mediated antiviral signal transduction. *Proc Natl Acad Sci U S A* 105, 16743-16748.

Gack, M. U., Shin, Y. C., Joo, C. H., Urano, T., Liang, C., Sun, L., Takeuchi, O., Akira, S., Chen, Z., Inoue, S., and Jung, J. U. (2007). TRIM25 RING-finger E3 ubiquitin ligase is essential for RIG-I-mediated antiviral activity. *Nature* 446, 916-920.

Gale, M. J., Jr., Korth, M. J., and Katze, M. G. (1998). Repression of the PKR protein kinase by the hepatitis C virus NS5A protein: a potential mechanism of interferon resistance. *Clin Diagn Virol* 10, 157-162.

Garcia, M. A., Gil, J., Ventoso, I., Guerra, S., Domingo, E., Rivas, C., and Esteban, M. (2006). Impact of protein kinase PKR in cell biology: from antiviral to antiproliferative action. *Microbiol Mol Biol Rev* 70, 1032-1060.

Garlinghouse, L. E., Jr., Smith, A. L., and Holford, T. (1984). The biological relationship of mouse hepatitis virus (MHV) strains and interferon: in vitro induction and sensitivities. *Arch Virol* 82, 19-29.

Gitlin, L., Barchet, W., Gilfillan, S., Celli, M., Beutler, B., Flavell, R. A., Diamond, M. S., and Colonna, M. (2006). Essential role of mda-5 in type I IFN responses to polyribinosinic:polyribocytidyllic acid and encephalomyocarditis picornavirus. *Proc Natl Acad Sci U S A* 103, 8459-8464.

Godet, M., L'Haridon, R., Vautherot, J. F., and Laude, H. (1992). TGEV corona virus ORF4 encodes a membrane protein that is incorporated into virions. *Virology* 188, 666-675.

Gohda, J., Matsumura, T., and Inoue, J. (2004). Cutting edge: TNFR-associated factor (TRAF) 6 is essential for MyD88-dependent pathway but not toll/IL-1 receptor domain-containing adaptor-inducing IFN-beta (TRIF)-dependent pathway in TLR signaling. *J Immunol* 173, 2913-2917.

Gombold, J. L., Hingley, S. T., and Weiss, S. R. (1993). Fusion-defective mutants of mouse hepatitis virus A59 contain a mutation in the spike protein cleavage signal. *J Virol* 67, 4504-4512.

Gorbatenya, A. E., Donchenko, A. P., Koonin, E. V., and Blinov, V. M. (1989). N-terminal domains of putative helicases of flavi- and pestiviruses may be serine proteases. *Nucleic Acids Res* 17, 3889-3897.

Grandvaux, N., Servant, M. J., tenOever, B., Sen, G. C., Balachandran, S., Barber, G. N., Lin, R., and Hiscott, J. (2002). Transcriptional profiling of interferon regulatory factor 3 target genes: direct involvement in the regulation of interferon-stimulated genes. *J Virol* 76, 5532-5539.

- Griffiths, G., and Rottier, P. (1992). Cell biology of viruses that assemble along the biosynthetic pathway. *Semin Cell Biol* 3, 367-381.
- Gu, J., Gong, E., Zhang, B., Zheng, J., Gao, Z., Zhong, Y., Zou, W., Zhan, J., Wang, S., Xie, Z., *et al.* (2005). Multiple organ infection and the pathogenesis of SARS. *J Exp Med* 202, 415-424.
- Guan, Y., Zheng, B. J., He, Y. Q., Liu, X. L., Zhuang, Z. X., Cheung, C. L., Luo, S. W., Li, P. H., Zhang, L. J., Guan, Y. J., *et al.* (2003). Isolation and characterization of viruses related to the SARS coronavirus from animals in southern China. *Science* 302, 276-278.
- Guilligay, D., Tarendreau, F., Resa-Infante, P., Coloma, R., Crepin, T., Sehr, P., Lewis, J., Ruigrok, R. W., Ortin, J., Hart, D. J., and Cusack, S. (2008). The structural basis for cap binding by influenza virus polymerase subunit PB2. *Nat Struct Mol Biol* 15, 500-506.
- Guo, Z., Chen, L. M., Zeng, H., Gomez, J. A., Plowden, J., Fujita, T., Katz, J. M., Donis, R. O., and Sambhara, S. (2007). NS1 protein of influenza A virus inhibits the function of intracytoplasmic pathogen sensor, RIG-I. *Am J Respir Cell Mol Biol* 36, 263-269.
- Guy, J. S., Breslin, J. J., Breuhaus, B., Vivrette, S., and Smith, L. G. (2000). Characterization of a coronavirus isolated from a diarrheic foal. *J Clin Microbiol* 38, 4523-4526.
- Habjan, M., Andersson, I., Klingstrom, J., Schumann, M., Martin, A., Zimmermann, P., Wagner, V., Pichlmair, A., Schneider, U., Muhlberger, E., *et al.* (2008). Processing of genome 5' termini as a strategy of negative-strand RNA viruses to avoid RIG-I-dependent interferon induction. *PLoS ONE* 3, e2032.
- Hacker, H., Redecke, V., Blagoev, B., Kratchmarova, I., Hsu, L. C., Wang, G. G., Kamps, M. P., Raz, E., Wagner, H., Hacker, G., *et al.* (2006). Specificity in Toll-like receptor signalling through distinct effector functions of TRAF3 and TRAF6. *Nature* 439, 204-207.
- Hale, B. G., Barclay, W. S., Randall, R. E., and Russell, R. J. (2008a). Structure of an avian influenza A virus NS1 protein effector domain. *Virology* 378, 1-5.
- Hale, B. G., Randall, R. E., Ortin, J., and Jackson, D. (2008b). The multifunctional NS1 protein of influenza A viruses. *J Gen Virol* 89, 2359-2376.
- Hanson, P. I., and Whiteheart, S. W. (2005). AAA+ proteins: have engine, will work. *Nat Rev Mol Cell Biol* 6, 519-529.
- Harcourt, B. H., Jukneliene, D., Kanjanahaluethai, A., Bechill, J., Severson, K. M., Smith, C. M., Rota, P. A., and Baker, S. C. (2004). Identification of severe acute respiratory syndrome coronavirus replicase products and characterization of papain-like protease activity. *J Virol* 78, 13600-13612.
- Hardarson, H. S., Baker, J. S., Yang, Z., Purejav, E., Huang, C. H., Alexopoulou, L., Li, N., Flavell, R. A., Bowles, N. E., and Vallejo, J. G. (2007). Toll-like receptor 3 is an

- essential component of the innate stress response in virus-induced cardiac injury. *Am J Physiol Heart Circ Physiol* 292, H251-258.
- Hashimoto, G., Wright, P. F., and Karzon, D. T. (1983). Antibody-dependent cell-mediated cytotoxicity against influenza virus-infected cells. *J Infect Dis* 148, 785-794.
- Hayashi, F., Smith, K. D., Ozinsky, A., Hawn, T. R., Yi, E. C., Goodlett, D. R., Eng, J. K., Akira, S., Underhill, D. M., and Aderem, A. (2001). The innate immune response to bacterial flagellin is mediated by Toll-like receptor 5. *Nature* 410, 1099-1103.
- Hegyi, A., Friebel, A., Gorbaleyna, A. E., and Ziebuhr, J. (2002). Mutational analysis of the active centre of coronavirus 3C-like proteases. *J Gen Virol* 83, 581-593.
- Heikkinen, L. S., Kazlauskas, A., Melen, K., Wagner, R., Ziegler, T., Julkunen, I., and Saksela, K. (2008). Avian and 1918 Spanish influenza a virus NS1 proteins bind to Crk/CrkL Src homology 3 domains to activate host cell signaling. *J Biol Chem* 283, 5719-5727.
- Heil, F., Ahmad-Nejad, P., Hemmi, H., Hochrein, H., Ampenberger, F., Gellert, T., Dietrich, H., Lipford, G., Takeda, K., Akira, S., *et al.* (2003). The Toll-like receptor 7 (TLR7)-specific stimulus loxoribine uncovers a strong relationship within the TLR7, 8 and 9 subfamily. *Eur J Immunol* 33, 2987-2997.
- Heil, F., Hemmi, H., Hochrein, H., Ampenberger, F., Kirschning, C., Akira, S., Lipford, G., Wagner, H., and Bauer, S. (2004). Species-specific recognition of single-stranded RNA via toll-like receptor 7 and 8. *Science* 303, 1526-1529.
- Hemmi, H., Kaisho, T., Takeuchi, O., Sato, S., Sanjo, H., Hoshino, K., Horiuchi, T., Tomizawa, H., Takeda, K., and Akira, S. (2002). Small anti-viral compounds activate immune cells via the TLR7 MyD88-dependent signaling pathway. *Nat Immunol* 3, 196-200.
- Hemmi, H., Takeuchi, O., Kawai, T., Kaisho, T., Sato, S., Sanjo, H., Matsumoto, M., Hoshino, K., Wagner, H., Takeda, K., and Akira, S. (2000). A Toll-like receptor recognizes bacterial DNA. *Nature* 408, 740-745.
- Herold, J., Raabe, T., and Siddell, S. (1993a). Molecular analysis of the human coronavirus (strain 229E) genome. *Arch Virol Suppl* 7, 63-74.
- Herold, J., Raabe, T., and Siddell, S. G. (1993b). Characterization of the human coronavirus 229E (HCV 229E) gene 1. *Adv Exp Med Biol* 342, 75-79.
- Hibino, T., Loza-Coll, M., Messier, C., Majeske, A. J., Cohen, A. H., Terwilliger, D. P., Buckley, K. M., Brockton, V., Nair, S. V., Berney, K., *et al.* (2006). The immune gene repertoire encoded in the purple sea urchin genome. *Dev Biol* 300, 349-365.
- Hitotsumatsu, O., Ahmad, R. C., Tavares, R., Wang, M., Philpott, D., Turer, E. E., Lee, B. L., Shiffin, N., Advincula, R., Malynn, B. A., *et al.* (2008). The ubiquitin-editing enzyme A20 restricts nucleotide-binding oligomerization domain containing 2-triggered signals. *Immunity* 28, 381-390.

- Hoffmann, E., Mahmood, K., Yang, C. F., Webster, R. G., Greenberg, H. B., and Kemble, G. (2002). Rescue of influenza B virus from eight plasmids. *Proc Natl Acad Sci U S A* **99**, 11411-11416.
- Hoffmann, E., Neumann, G., Kawaoka, Y., Hobom, G., and Webster, R. G. (2000). A DNA transfection system for generation of influenza A virus from eight plasmids. *Proc Natl Acad Sci U S A* **97**, 6108-6113.
- Hoffmann, E., Stech, J., Guan, Y., Webster, R. G., and Perez, D. R. (2001). Universal primer set for the full-length amplification of all influenza A viruses. *Arch Virol* **146**, 2275-2289.
- Hoffmann, J. A., Kafatos, F. C., Janeway, C. A., and Ezekowitz, R. A. (1999). Phylogenetic perspectives in innate immunity. *Science* **284**, 1313-1318.
- Holmes, K. V. (2003). SARS coronavirus: a new challenge for prevention and therapy. *J Clin Invest* **111**, 1605-1609.
- Honda, K., Ohba, Y., Yanai, H., Negishi, H., Mizutani, T., Takaoka, A., Taya, C., and Taniguchi, T. (2005a). Spatiotemporal regulation of MyD88-IRF-7 signalling for robust type-I interferon induction. *Nature* **434**, 1035-1040.
- Honda, K., Yanai, H., Negishi, H., Asagiri, M., Sato, M., Mizutani, T., Shimada, N., Ohba, Y., Takaoka, A., Yoshida, N., and Taniguchi, T. (2005b). IRF-7 is the master regulator of type-I interferon-dependent immune responses. *Nature* **434**, 772-777.
- Hoofnagle, J. H. (2002). Course and outcome of hepatitis C. *Hepatology* **36**, S21-29.
- Horimoto, T., and Kawaoka, Y. (2005). Influenza: lessons from past pandemics, warnings from current incidents. *Nat Rev Microbiol* **3**, 591-600.
- Ikeda, M., Sugiyama, K., Mizutani, T., Tanaka, T., Tanaka, K., Sekihara, H., Shimotohno, K., and Kato, N. (1998). Human hepatocyte clonal cell lines that support persistent replication of hepatitis C virus. *Virus Res* **56**, 157-167.
- Imai, Y., Kuba, K., Rao, S., Huan, Y., Guo, F., Guan, B., Yang, P., Sarao, R., Wada, T., Leong-Poi, H., et al. (2005). Angiotensin-converting enzyme 2 protects from severe acute lung failure. *Nature* **436**, 112-116.
- Iwamura, T., Yoneyama, M., Yamaguchi, K., Suhara, W., Mori, W., Shiota, K., Okabe, Y., Namiki, H., and Fujita, T. (2001). Induction of IRF-3/-7 kinase and NF-kappaB in response to double-stranded RNA and virus infection: common and unique pathways. *Genes Cells* **6**, 375-388.
- Iwasaki, A., and Medzhitov, R. (2004). Toll-like receptor control of the adaptive immune responses. *Nat Immunol* **5**, 987-995.
- Jackson, D., Hossain, M. J., Hickman, D., Perez, D. R., and Lamb, R. A. (2008). A new influenza virus virulence determinant: the NS1 protein four C-terminal residues modulate pathogenicity. *Proc Natl Acad Sci U S A* **105**, 4381-4386.

- Jefferies, C. A., Doyle, S., Brunner, C., Dunne, A., Brint, E., Wietek, C., Walch, E., Wirth, T., and O'Neill, L. A. (2003). Bruton's tyrosine kinase is a Toll/interleukin-1 receptor domain-binding protein that participates in nuclear factor kappaB activation by Toll-like receptor 4. *J Biol Chem* **278**, 26258-26264.
- Jiang, Z., Zamani-Daryoush, M., Nie, H., Silva, A. M., Williams, B. R., and Li, X. (2003). Poly(I-C)-induced Toll-like receptor 3 (TLR3)-mediated activation of NF $\kappa$ B and MAP kinase is through an interleukin-1 receptor-associated kinase (IRAK)-independent pathway employing the signaling components TLR3-TRAF6-TAK1-TAB2-PKR. *J Biol Chem* **278**, 16713-16719.
- Johnsen, I. B., Nguyen, T. T., Ringdal, M., Tryggestad, A. M., Bakke, O., Lien, E., Espenik, T., and Anthonsen, M. W. (2006). Toll-like receptor 3 associates with c-Src tyrosine kinase on endosomes to initiate antiviral signaling. *Embo J* **25**, 3335-3346.
- Jones, J. D., and Dangl, J. L. (2006). The plant immune system. *Nature* **444**, 323-329.
- Jurk, M., Heil, F., Vollmer, J., Schetter, C., Krieg, A. M., Wagner, H., Lipford, G., and Bauer, S. (2002). Human TLR7 or TLR8 independently confer responsiveness to the antiviral compound R-848. *Nat Immunol* **3**, 499.
- Kadowaki, N., Ho, S., Antonenko, S., Malefyt, R. W., Kastelein, R. A., Bazan, F., and Liu, Y. J. (2001). Subsets of human dendritic cell precursors express different toll-like receptors and respond to different microbial antigens. *J Exp Med* **194**, 863-869.
- Kajita, E., Nishiya, T., and Miwa, S. (2006). The transmembrane domain directs TLR9 to intracellular compartments that contain TLR3. *Biochem Biophys Res Commun* **343**, 578-584.
- Kamitani, W., Narayanan, K., Huang, C., Lokugamage, K., Ikegami, T., Ito, N., Kubo, H., and Makino, S. (2006). Severe acute respiratory syndrome coronavirus nsp1 protein suppresses host gene expression by promoting host mRNA degradation. *Proc Natl Acad Sci U S A* **103**, 12885-12890.
- Kang, D. C., Gopalkrishnan, R. V., Wu, Q., Jankowsky, E., Pyle, A. M., and Fisher, P. B. (2002). mda-5: An interferon-inducible putative RNA helicase with double-stranded RNA-dependent ATPase activity and melanoma growth-suppressive properties. *Proc Natl Acad Sci U S A* **99**, 637-642.
- Kato, H., Sato, S., Yoneyama, M., Yamamoto, M., Uematsu, S., Matsui, K., Tsujimura, T., Takeda, K., Fujita, T., Takeuchi, O., and Akira, S. (2005). Cell type-specific involvement of RIG-I in antiviral response. *Immunity* **23**, 19-28.
- Kato, H., Takeuchi, O., Sato, S., Yoneyama, M., Yamamoto, M., Matsui, K., Uematsu, S., Jung, A., Kawai, T., Ishii, K. J., et al. (2006). Differential roles of MDA5 and RIG-I helicases in the recognition of RNA viruses. *Nature* **441**, 101-105.
- Kato, N., Ikeda, M., Mizutani, T., Sugiyama, K., Noguchi, M., Hirohashi, S., and Shimotohno, K. (1996). Replication of hepatitis C virus in cultured non-neoplastic human hepatocytes. *Jpn J Cancer Res* **87**, 787-792.

- Kato, T., Date, T., Miyamoto, M., Furusaka, A., Tokushige, K., Mizokami, M., and Wakita, T. (2003). Efficient replication of the genotype 2a hepatitis C virus subgenomic replicon. *Gastroenterology* *125*, 1808-1817.
- Kawai, T., and Akira, S. (2006a). Antiviral signaling through pattern recognition receptors. *J Biochem (Tokyo)*.
- Kawai, T., and Akira, S. (2006b). Innate immune recognition of viral infection. *Nat Immunol* *7*, 131-137.
- Kawai, T., Sato, S., Ishii, K. J., Coban, C., Hemmi, H., Yamamoto, M., Terai, K., Matsuda, M., Inoue, J., Uematsu, S., *et al.* (2004). Interferon-alpha induction through Toll-like receptors involves a direct interaction of IRF7 with MyD88 and TRAF6. *Nat Immunol* *5*, 1061-1068.
- Kawai, T., Takahashi, K., Sato, S., Coban, C., Kumar, H., Kato, H., Ishii, K. J., Takeuchi, O., and Akira, S. (2005). IPS-1, an adaptor triggering RIG-I- and Mda5-mediated type I interferon induction. *Nat Immunol* *6*, 981-988.
- Keskinen, P., Nyqvist, M., Sareneva, T., Pirhonen, J., Melen, K., and Julkunen, I. (1999). Impaired antiviral response in human hepatoma cells. *Virology* *263*, 364-375.
- Kim, Y. M., Brinkmann, M. M., Paquet, M. E., and Ploegh, H. L. (2008). UNC93B1 delivers nucleotide-sensing toll-like receptors to endolysosomes. *Nature* *452*, 234-238.
- Kiso, M., Mitamura, K., Sakai-Tagawa, Y., Shiraihi, K., Kawakami, C., Kimura, K., Hayden, F. G., Sugaya, N., and Kawaoka, Y. (2004). Resistant influenza A viruses in children treated with oseltamivir: descriptive study. *Lancet* *364*, 759-765.
- Klumperman, J., Locker, J. K., Meijer, A., Horzinek, M. C., Geuze, H. J., and Rottier, P. J. (1994). Coronavirus M proteins accumulate in the Golgi complex beyond the site of virion budding. *J Virol* *68*, 6523-6534.
- Kochs, G., Garcia-Sastre, A., and Martinez-Sobrido, L. (2007). Multiple anti-interferon actions of the influenza A virus NS1 protein. *J Virol* *81*, 7011-7021.
- Komatsu, T., Takeuchi, K., and Gotoh, B. (2007). Bovine parainfluenza virus type 3 accessory proteins that suppress beta interferon production. *Microbes Infect* *9*, 954-962.
- Kopecky-Bromberg, S. A., Martinez-Sobrido, L., Frieman, M., Baric, R. A., and Palese, P. (2007). Severe acute respiratory syndrome coronavirus open reading frame (ORF) 3b, ORF 6, and nucleocapsid proteins function as interferon antagonists. *J Virol* *81*, 548-557.
- Kopecky-Bromberg, S. A., Martinez-Sobrido, L., and Palese, P. (2006). 7a protein of severe acute respiratory syndrome coronavirus inhibits cellular protein synthesis and activates p38 mitogen-activated protein kinase. *J Virol* *80*, 785-793.
- Kovacsics, M., Martinon, F., Micheau, O., Bodmer, J. L., Hofmann, K., and Tschopp, J. (2002). Overexpression of Helicard, a CARD-containing helicase cleaved during apoptosis, accelerates DNA degradation. *Curr Biol* *12*, 838-843.

- Krug, A., French, A. R., Barchet, W., Fischer, J. A., Dziona, A., Pingel, J. T., Orihuela, M. M., Akira, S., Yokoyama, W. M., and Colonna, M. (2004a). TLR9-dependent recognition of MCMV by IPC and DC generates coordinated cytokine responses that activate antiviral NK cell function. *Immunity* 21, 107-119.
- Krug, A., Luker, G. D., Barchet, W., Leib, D. A., Akira, S., and Colonna, M. (2004b). Herpes simplex virus type 1 activates murine natural interferon-producing cells through toll-like receptor 9. *Blood* 103, 1433-1437.
- Krug, R. M., Bouloy, M., and Plotch, S. J. (1980a). RNA primers and the role of host nuclear RNA polymerase II in influenza viral RNA transcription. *Philos Trans R Soc Lond B Biol Sci* 288, 359-370.
- Krug, R. M., Broni, B. A., LaFiandra, A. J., Morgan, M. A., and Shatkin, A. J. (1980b). Priming and inhibitory activities of RNAs for the influenza viral transcriptase do not require base pairing with the virion template RNA. *Proc Natl Acad Sci U S A* 77, 5874-5878.
- Kuba, K., Imai, Y., Rao, S., Gao, H., Guo, F., Guan, B., Huan, Y., Yang, P., Zhang, Y., Deng, W., et al. (2005). A crucial role of angiotensin converting enzyme 2 (ACE2) in SARS coronavirus-induced lung injury. *Nat Med* 11, 875-879.
- Kuiken, T., Fouchier, R., Rimmelzwaan, G., and Osterhaus, A. (2003a). Emerging viral infections in a rapidly changing world. *Curr Opin Biotechnol* 14, 641-646.
- Kuiken, T., Fouchier, R. A., Schutten, M., Rimmelzwaan, G. F., van Amerongen, G., van Riel, D., Laman, J. D., de Jong, T., van Doornum, G., Lim, W., et al. (2003b). Newly discovered coronavirus as the primary cause of severe acute respiratory syndrome. *Lancet* 362, 263-270.
- Kumar, A., Zhang, J., and Yu, F. S. (2006). Toll-like receptor 3 agonist poly(I:C)-induced antiviral response in human corneal epithelial cells. *Immunology* 117, 11-21.
- Kumar, M. V., Nagineni, C. N., Chin, M. S., Hooks, J. J., and Detrick, B. (2004). Innate immunity in the retina: Toll-like receptor (TLR) signaling in human retinal pigment epithelial cells. *J Neuroimmunol* 153, 7-15.
- Lai, M. M., and Cavanagh, D. (1997). The molecular biology of coronaviruses. *Adv Virus Res* 48, 1-100.
- Lai, M. M., Patton, C. D., Baric, R. S., and Stohlman, S. A. (1983). Presence of leader sequences in the mRNA of mouse hepatitis virus. *J Virol* 46, 1027-1033.
- Lanford, R. E., Bigger, C., Bassett, S., and Klimpel, G. (2001). The chimpanzee model of hepatitis C virus infections. *Ilar J* 42, 117-126.
- Latz, E., Schoenemeyer, A., Visintin, A., Fitzgerald, K. A., Monks, B. G., Knetter, C. F., Lien, E., Nilsen, N. J., Espevik, T., and Golenbock, D. T. (2004a). TLR9 signals after translocating from the ER to CpG DNA in the lysosome. *Nat Immunol* 5, 190-198.

- Latz, E., Visintin, A., Espevik, T., and Golenbock, D. T. (2004b). Mechanisms of TLR9 activation. *J Endotoxin Res* 10, 406-412.
- Latz, E., Visintin, A., Lien, E., Fitzgerald, K. A., Monks, B. G., Kurt-Jones, E. A., Golenbock, D. T., and Espevik, T. (2002). Lipopolysaccharide rapidly traffics to and from the Golgi apparatus with the toll-like receptor 4-MD-2-CD14 complex in a process that is distinct from the initiation of signal transduction. *J Biol Chem* 277, 47834-47843.
- Le Goffic, R., Pothlichet, J., Vitour, D., Fujita, T., Meurs, E., Chignard, M., and Si-Tahar, M. (2007). Cutting Edge: Influenza A virus activates TLR3-dependent inflammatory and RIG-I-dependent antiviral responses in human lung epithelial cells. *J Immunol* 178, 3368-3372.
- Lee, H. J., Shieh, C. K., Gorbalyena, A. E., Koonin, E. V., La Monica, N., Tuler, J., Bagdzhadzhyan, A., and Lai, M. M. (1991). The complete sequence (22 kilobases) of murine coronavirus gene 1 encoding the putative proteases and RNA polymerase. *Virology* 180, 567-582.
- Leifer, C. A., Kennedy, M. N., Mazzoni, A., Lee, C., Kruhlak, M. J., and Segal, D. M. (2004). TLR9 is localized in the endoplasmic reticulum prior to stimulation. *J Immunol* 173, 1179-1183.
- Leonard, J. N., Ghirlando, R., Askins, J., Bell, J. K., Margulies, D. H., Davies, D. R., and Segal, D. M. (2008). The TLR3 signaling complex forms by cooperative receptor dimerization. *Proc Natl Acad Sci U S A* 105, 258-263.
- Li, K., Chen, Z., Kato, N., Gale, M., Jr., and Lemon, S. M. (2005a). Distinct poly(I-C) and virus-activated signaling pathways leading to interferon-beta production in hepatocytes. *J Biol Chem* 280, 16739-16747.
- Li, K., Foy, E., Ferrecon, J. C., Nakamura, M., Ferrecon, A. C., Ikeda, M., Ray, S. C., Gale, M., Jr., and Lemon, S. M. (2005b). Immune evasion by hepatitis C virus NS3/4A protease-mediated cleavage of the Toll-like receptor 3 adaptor protein TRIF. *Proc Natl Acad Sci U S A* 102, 2992-2997.
- Li, M. L., Rao, P., and Krug, R. M. (2001). The active sites of the influenza cap-dependent endonuclease are on different polymerase subunits. *Embo J* 20, 2078-2086.
- Li, W., Moore, M. J., Vasilieva, N., Sui, J., Wong, S. K., Berne, M. A., Somasundaran, M., Sullivan, J. L., Luzuriaga, K., Greenough, T. C., et al. (2003). Angiotensin-converting enzyme 2 is a functional receptor for the SARS coronavirus. *Nature* 426, 450-454.
- Li, X. D., Sun, L., Seth, R. B., Pineda, G., and Chen, Z. J. (2005c). Hepatitis C virus protease NS3/4A cleaves mitochondrial antiviral signaling protein off the mitochondria to evade innate immunity. *Proc Natl Acad Sci U S A* 102, 17717-17722.
- Liew, F. Y., Xu, D., Brint, E. K., and O'Neill, L. A. (2005). Negative regulation of toll-like receptor-mediated immune responses. *Nat Rev Immunol* 5, 446-458.

- Lin, R., Heylbroeck, C., Pitha, P. M., and Hiscott, J. (1998). Virus-dependent phosphorylation of the IRF-3 transcription factor regulates nuclear translocation, transactivation potential, and proteasome-mediated degradation. *Mol Cell Biol* 18, 2986-2996.
- Lin, R., Yang, L., Nakhaei, P., Sun, Q., Sharif-Askari, E., Julkunen, I., and Hiscott, J. (2006). Negative regulation of the retinoic acid-inducible gene I-induced antiviral state by the ubiquitin-editing protein A20. *J Biol Chem* 281, 2095-2103.
- Lindenbach, B. D., Evans, M. J., Syder, A. J., Wolk, B., Tellinghuisen, T. L., Liu, C. C., Maruyama, T., Hynes, R. O., Burton, D. R., McKeating, J. A., and Rice, C. M. (2005). Complete replication of hepatitis C virus in cell culture. *Science* 309, 623-626.
- Lindenbach, B. D., and Rice, C. M. (2005). Unravelling hepatitis C virus replication from genome to function. *Nature* 436, 933-938.
- Lindenbach, B. D., Thiel, H.-J., and Rice, C. M. (2006). Flaviviridae: The Viruses and Their Replication. In *Fields Virology*, D. M. Knipe, and P. M. Howley, eds. (Lippincott Williams & Wilkins), pp. 1101-1152.
- Lindner, H. A., Fotouhi-Ardakani, N., Lytvyn, V., Lachance, P., Sulea, T., and Menard, R. (2005). The papain-like protease from the severe acute respiratory syndrome coronavirus is a deubiquitinating enzyme. *J Virol* 79, 15199-15208.
- Liu, D. X., Cavanagh, D., Green, P., and Inglis, S. C. (1991). A polycistronic mRNA specified by the coronavirus infectious bronchitis virus. *Virology* 184, 531-544.
- Liu, L., Botos, I., Wang, Y., Leonard, J. N., Shiloach, J., Segal, D. M., and Davies, D. R. (2008). Structural basis of toll-like receptor 3 signaling with double-stranded RNA. *Science* 320, 379-381.
- Lomniczi, B. (1977). Biological properties of avian coronavirus RNA. *J Gen Virol* 36, 531-533.
- Loo, Y. M., Fornek, J., Crochet, N., Bajwa, G., Perwitasari, O., Martinez-Sobrido, L., Akira, S., Gill, M. A., Garcia-Sastre, A., Katze, M. G., and Gale, M., Jr. (2008). Distinct RIG-I and MDA5 signaling by RNA viruses in innate immunity. *J Virol* 82, 335-345.
- Loo, Y. M., Owen, D. M., Li, K., Erickson, A. K., Johnson, C. L., Fish, P. M., Carney, D. S., Wang, T., Ishida, H., Yoneyama, M., et al. (2006). Viral and therapeutic control of IFN-beta promoter stimulator 1 during hepatitis C virus infection. *Proc Natl Acad Sci U S A* 103, 6001-6006.
- Ludwig, S., and Wolff, T. (2009). Influenza A virus TRIMs the type I interferon response. *Cell Host Microbe* 5, 420-421.
- Lund, J., Sato, A., Akira, S., Medzhitov, R., and Iwasaki, A. (2003). Toll-like receptor 9-mediated recognition of Herpes simplex virus-2 by plasmacytoid dendritic cells. *J Exp Med* 198, 513-520.

- Lund, J. M., Alexopoulou, L., Sato, A., Karow, M., Adams, N. C., Gale, N. W., Iwasaki, A., and Flavell, R. A. (2004). Recognition of single-stranded RNA viruses by Toll-like receptor 7. *Proc Natl Acad Sci U S A* *101*, 5598-5603.
- Machamer, C. E., Grim, M. G., Esquela, A., Chung, S. W., Rolls, M., Ryan, K., and Swift, A. M. (1993). Retention of a cis Golgi protein requires polar residues on one face of a predicted alpha-helix in the transmembrane domain. *Mol Biol Cell* *4*, 695-704.
- Machamer, C. E., Mentone, S. A., Rose, J. K., and Farquhar, M. G. (1990). The E1 glycoprotein of an avian coronavirus is targeted to the cis Golgi complex. *Proc Natl Acad Sci U S A* *87*, 6944-6948.
- Machamer, C. E., and Rose, J. K. (1987). A specific transmembrane domain of a coronavirus E1 glycoprotein is required for its retention in the Golgi region. *J Cell Biol* *105*, 1205-1214.
- MacNaughton, M. R. (1978). The genomes of three coronaviruses. *FEBS Lett* *94*, 191-194.
- Marra, M. A., Jones, S. J., Astell, C. R., Holt, R. A., Brooks-Wilson, A., Butterfield, Y. S., Khattra, J., Asano, J. K., Barber, S. A., Chan, S. Y., et al. (2003). The Genome sequence of the SARS-associated coronavirus. *Science* *300*, 1399-1404.
- Martin, K., and Helenius, A. (1991). Transport of incoming influenza virus nucleocapsids into the nucleus. *J Virol* *65*, 232-244.
- Martina, B. E., Haagmans, B. L., Kuiken, T., Fouchier, R. A., Rimmelzwaan, G. F., Van Amerongen, G., Peiris, J. S., Lim, W., and Osterhaus, A. D. (2003). Virology: SARS virus infection of cats and ferrets. *Nature* *425*, 915.
- Masters, P. S. (1992). Localization of an RNA-binding domain in the nucleocapsid protein of the coronavirus mouse hepatitis virus. *Arch Virol* *125*, 141-160.
- Masters, P. S., Koetzner, C. A., Kerr, C. A., and Heo, Y. (1994). Optimization of targeted RNA recombination and mapping of a novel nucleocapsid gene mutation in the coronavirus mouse hepatitis virus. *J Virol* *68*, 328-337.
- Matlin, K. S., Reggio, H., Helenius, A., and Simons, K. (1981). Infectious entry pathway of influenza virus in a canine kidney cell line. *J Cell Biol* *91*, 601-613.
- Matsumoto, M., Funami, K., Tanabe, M., Oshiumi, H., Shingai, M., Seto, Y., Yamamoto, A., and Seya, T. (2003). Subcellular localization of Toll-like receptor 3 in human dendritic cells. *J Immunol* *171*, 3154-3162.
- Matsumoto, M., Kikkawa, S., Kohase, M., Miyake, K., and Seya, T. (2002). Establishment of a monoclonal antibody against human Toll-like receptor 3 that blocks double-stranded RNA-mediated signaling. *Biochem Biophys Res Commun* *293*, 1364-1369.

- Matsuzawa, A., Tseng, P. H., Vallabhapurapu, S., Luo, J. L., Zhang, W., Wang, H., Vignali, D. A., Gallagher, E., and Karin, M. (2008). Essential cytoplasmic translocation of a cytokine receptor-assembled signaling complex. *Science* *321*, 663-668.
- Mazzulli, T., Farcas, G. A., Poutanen, S. M., Willey, B. M., Low, D. E., Butany, J., Asa, S. L., and Kain, K. C. (2004). Severe acute respiratory syndrome-associated coronavirus in lung tissue. *Emerg Infect Dis* *10*, 20-24.
- McCartney, S. A., Thackray, L. B., Gitlin, L., Gilfillan, S., Virgin, H. W., and Colonna, M. (2008). MDA-5 recognition of a murine norovirus. *PLoS Pathog* *4*, e1000108.
- McHutchison, J. G., Manns, M., Patel, K., Poynard, T., Lindsay, K. L., Trepo, C., Dienstag, J., Lee, W. M., Mak, C., Garaud, J. J., and Albrecht, J. K. (2002a). Adherence to combination therapy enhances sustained response in genotype-1-infected patients with chronic hepatitis C. *Gastroenterology* *123*, 1061-1069.
- McHutchison, J. G., Poynard, T., Esteban-Mur, R., Davis, G. L., Goodman, Z. D., Harvey, J., Ling, M. H., Garaud, J. J., Albrecht, J. K., Patel, K., *et al.* (2002b). Hepatic HCV RNA before and after treatment with interferon alone or combined with ribavirin. *Hepatology* *35*, 688-693.
- Medzhitov, R., and Janeway, C., Jr. (2000a). Innate immune recognition: mechanisms and pathways. *Immunol Rev* *173*, 89-97.
- Medzhitov, R., and Janeway, C., Jr. (2000b). Innate immunity. *N Engl J Med* *343*, 338-344.
- Medzhitov, R., and Janeway, C., Jr. (2000c). The Toll receptor family and microbial recognition. *Trends Microbiol* *8*, 452-456.
- Medzhitov, R., and Janeway, C. A., Jr. (1997). Innate immunity: the virtues of a nonclonal system of recognition. *Cell* *91*, 295-298.
- Medzhitov, R., and Janeway, C. A., Jr. (2000d). How does the immune system distinguish self from nonself? *Semin Immunol* *12*, 185-188; discussion 257-344.
- Meylan, E., Curran, J., Hofmann, K., Moradpour, D., Binder, M., Bartenschlager, R., and Tschopp, J. (2005). Cardif is an adaptor protein in the RIG-I antiviral pathway and is targeted by hepatitis C virus. *Nature* *437*, 1167-1172.
- Mibayashi, M., Martinez-Sobrido, L., Loo, Y. M., Cardenas, W. B., Gale, M., Jr., and Garcia-Sastre, A. (2007). Inhibition of retinoic acid-inducible gene I-mediated induction of beta interferon by the NS1 protein of influenza A virus. *J Virol* *81*, 514-524.
- Mullooly, J. P., and Barker, W. H. (1982). Impact of type A influenza on children: a retrospective study. *Am J Public Health* *72*, 1008-1016.
- Muruve, D. A., Petrilli, V., Zaiss, A. K., White, L. R., Clark, S. A., Ross, P. J., Parks, R. J., and Tschopp, J. (2008). The inflammasome recognizes cytosolic microbial and host DNA and triggers an innate immune response. *Nature* *452*, 103-107.

- Nakabayashi, H., Taketa, K., Miyano, K., Yamane, T., and Sato, J. (1982). Growth of human hepatoma cells lines with differentiated functions in chemically defined medium. *Cancer Res* 42, 3858-3863.
- Naviaux, R. K., Costanzi, E., Haas, M., and Verma, I. M. (1996). The pCL vector system: rapid production of helper-free, high-titer, recombinant retroviruses. *J Virol* 70, 5701-5705.
- Neumann, A. U., Lam, N. P., Dahari, H., Gretch, D. R., Wiley, T. E., Layden, T. J., and Perelson, A. S. (1998). Hepatitis C viral dynamics in vivo and the antiviral efficacy of interferon-alpha therapy. *Science* 282, 103-107.
- Ng, M. L., Tan, S. H., See, E. E., Ooi, E. E., and Ling, A. E. (2003). Early events of SARS coronavirus infection in vero cells. *J Med Virol* 71, 323-331.
- Nishiya, T., and DeFranco, A. L. (2004). Ligand-regulated chimeric receptor approach reveals distinctive subcellular localization and signaling properties of the Toll-like receptors. *J Biol Chem* 279, 19008-19017.
- Nishiya, T., Kajita, E., Miwa, S., and DeFranco, A. L. (2005). TLR3 and TLR7 are targeted to the same intracellular compartments by distinct regulatory elements. *J Biol Chem* 280, 37107-37117.
- Obenauer, J. C., Denson, J., Mehta, P. K., Su, X., Mukatira, S., Finkelstein, D. B., Xu, X., Wang, J., Ma, J., Fan, Y., et al. (2006). Large-scale sequence analysis of avian influenza isolates. *Science* 311, 1576-1580.
- Oganesyan, G., Saha, S. K., Guo, B., He, J. Q., Shahangian, A., Zarnegar, B., Perry, A., and Cheng, G. (2006). Critical role of TRAF3 in the Toll-like receptor-dependent and -independent antiviral response. *Nature* 439, 208-211.
- Opitz, B., Rejaibi, A., Dauber, B., Eckhard, J., Vinzing, M., Schmeck, B., Hippenstiel, S., Suttorp, N., and Wolff, T. (2007). IFN $\beta$  induction by influenza A virus is mediated by RIG-I which is regulated by the viral NS1 protein. *Cell Microbiol* 9, 930-938.
- Oshiumi, H., Matsumoto, M., Funami, K., Akazawa, T., and Seya, T. (2003a). TICAM-1, an adaptor molecule that participates in Toll-like receptor 3-mediated interferon-beta induction. *Nat Immunol* 4, 161-167.
- Oshiumi, H., Sasai, M., Shida, K., Fujita, T., Matsumoto, M., and Seya, T. (2003b). TIR-containing adapter molecule (TICAM)-2, a bridging adapter recruiting to toll-like receptor 4 TICAM-1 that induces interferon-beta. *J Biol Chem* 278, 49751-49762.
- Paul, A. V., Peters, J., Mugavero, J., Yin, J., van Boom, J. H., and Wimmer, E. (2003). Biochemical and genetic studies of the VPg uridylylation reaction catalyzed by the RNA polymerase of poliovirus. *J Virol* 77, 891-904.
- Pear, W. S., Nolan, G. P., Scott, M. L., and Baltimore, D. (1993). Production of high-titer helper-free retroviruses by transient transfection. *Proc Natl Acad Sci U S A* 90, 8392-8396.

- Peiris, J. S. (2003). Severe Acute Respiratory Syndrome (SARS). *J Clin Virol* 28, 245-247.
- Peiris, J. S., Guan, Y., and Yuen, K. Y. (2004). Severe acute respiratory syndrome. *Nat Med* 10, S88-97.
- Peiris, J. S., Yuen, K. Y., Osterhaus, A. D., and Stohr, K. (2003). The severe acute respiratory syndrome. *N Engl J Med* 349, 2431-2441.
- Perlman, S., and Dandekar, A. A. (2005). Immunopathogenesis of coronavirus infections: implications for SARS. *Nat Rev Immunol* 5, 917-927.
- Perry, A. K., Chen, G., Zheng, D., Tang, H., and Cheng, G. (2005). The host type I interferon response to viral and bacterial infections. *Cell Res* 15, 407-422.
- Pewe, L., Zhou, H., Netland, J., Tangudu, C., Olivares, H., Shi, L., Look, D., Gallagher, T., and Perlman, S. (2005). A severe acute respiratory syndrome-associated coronavirus-specific protein enhances virulence of an attenuated murine coronavirus. *J Virol* 79, 11335-11342.
- Pichlmair, A., Schulz, O., Tan, C. P., Naslund, T. I., Liljestrom, P., Weber, F., and Reis e Sousa, C. (2006). RIG-I-mediated antiviral responses to single-stranded RNA bearing 5'-phosphates. *Science* 314, 997-1001.
- Pietschmann, T., Kaul, A., Koutsoudakis, G., Shavinskaya, A., Kallis, S., Steinmann, E., Abid, K., Negro, F., Dreux, M., Cosset, F. L., and Bartenschlager, R. (2006). Construction and characterization of infectious intragenotypic and intergenotypic hepatitis C virus chimeras. *Proc Natl Acad Sci U S A* 103, 7408-7413.
- Pileri, P., Uematsu, Y., Campagnoli, S., Galli, G., Falugi, F., Petracca, R., Weiner, A. J., Houghton, M., Rosa, D., Grandi, G., and Abrignani, S. (1998). Binding of hepatitis C virus to CD81. *Science* 282, 938-941.
- Pirher, N., Ivicak, K., Pohar, J., Bencina, M., and Jerala, R. (2008). A second binding site for double-stranded RNA in TLR3 and consequences for interferon activation. *Nat Struct Mol Biol* 15, 761-763.
- Pisitkun, P., Deane, J. A., Difilippantonio, M. J., Tarasenko, T., Satterthwaite, A. B., and Bolland, S. (2006). Autoreactive B cell responses to RNA-related antigens due to TLR7 gene duplication. *Science* 312, 1669-1672.
- Ploss, A., Evans, M. J., Gaysinskaya, V. A., Panis, M., You, H., de Jong, Y. P., and Rice, C. M. (2009). Human occludin is a hepatitis C virus entry factor required for infection of mouse cells. *Nature* 457, 882-886.
- Plotch, S. J., Bouloy, M., Ulmanen, I., and Krug, R. M. (1981). A unique cap(m7GpppXm)-dependent influenza virion endonuclease cleaves capped RNAs to generate the primers that initiate viral RNA transcription. *Cell* 23, 847-858.
- Poltorak, A., Smirnova, I., He, X., Liu, M. Y., Van Huffel, C., McNally, O., Birdwell, D., Alejos, E., Silva, M., Du, X., et al. (1998). Genetic and physical mapping of the Lps

locus: identification of the toll-4 receptor as a candidate gene in the critical region. *Blood Cells Mol Dis* 24, 340-355.

Risco, C., Anton, I. M., Enjuanes, L., and Carrascosa, J. L. (1996). The transmissible gastroenteritis coronavirus contains a spherical core shell consisting of M and N proteins. *J Virol* 70, 4773-4777.

Roach, J. C., Glusman, G., Rowen, L., Kaur, A., Purcell, M. K., Smith, K. D., Hood, L. E., and Aderem, A. (2005). The evolution of vertebrate Toll-like receptors. *Proc Natl Acad Sci U S A* 102, 9577-9582.

Rota, P. A., Oberste, M. S., Monroe, S. S., Nix, W. A., Campagnoli, R., Icenogle, J. P., Penaranda, S., Bankamp, B., Maher, K., Chen, M. H., *et al.* (2003). Characterization of a novel coronavirus associated with severe acute respiratory syndrome. *Science* 300, 1394-1399.

Roth-Cross, J. K., Bender, S. J., and Weiss, S. R. (2008). Murine coronavirus mouse hepatitis virus is recognized by MDA5 and induces type I interferon in brain macrophages/microglia. *J Virol* 82, 9829-9838.

Rothenfusser, S., Goutagny, N., DiPerna, G., Gong, M., Monks, B. G., Schoenemeyer, A., Yamamoto, M., Akira, S., and Fitzgerald, K. A. (2005). The RNA helicase Lgp2 inhibits TLR-independent sensing of viral replication by retinoic acid-inducible gene-I. *J Immunol* 175, 5260-5268.

Rudd, B. D., Burstein, E., Duckett, C. S., Li, X., and Lukacs, N. W. (2005). Differential role for TLR3 in respiratory syncytial virus-induced chemokine expression. *J Virol* 79, 3350-3357.

Rudd, B. D., Smit, J. J., Flavell, R. A., Alexopoulou, L., Schaller, M. A., Gruber, A., Berlin, A. A., and Lukacs, N. W. (2006). Deletion of TLR3 alters the pulmonary immune environment and mucus production during respiratory syncytial virus infection. *J Immunol* 176, 1937-1942.

Saito, T., Hirai, R., Loo, Y. M., Owen, D., Johnson, C. L., Sinha, S. C., Akira, S., Fujita, T., and Gale, M., Jr. (2007). Regulation of innate antiviral defenses through a shared repressor domain in RIG-I and LGP2. *Proc Natl Acad Sci U S A* 104, 582-587.

Saitoh, T., Yamamoto, M., Miyagishi, M., Taira, K., Nakanishi, M., Fujita, T., Akira, S., Yamamoto, N., and Yamaoka, S. (2005). A20 is a negative regulator of IFN regulatory factor 3 signaling. *J Immunol* 174, 1507-1512.

Sarkar, S. N., Peters, K. L., Elco, C. P., Sakamoto, S., Pal, S., and Sen, G. C. (2004). Novel roles of TLR3 tyrosine phosphorylation and PI3 kinase in double-stranded RNA signaling. *Nat Struct Mol Biol* 11, 1060-1067.

Schmidt, K. N., Leung, B., Kwong, M., Zaremba, K. A., Satyal, S., Navas, T. A., Wang, F., and Godowski, P. J. (2004). APC-independent activation of NK cells by the Toll-like receptor 3 agonist double-stranded RNA. *J Immunol* 172, 138-143.

- Schochetman, G., Stevens, R. H., and Simpson, R. W. (1977). Presence of infectious polyadenylated RNA in coronavirus avian bronchitis virus. *Virology* 77, 772-782.
- Schwandner, R., Dziarski, R., Wesche, H., Rothe, M., and Kirschning, C. J. (1999). Peptidoglycan- and lipoteichoic acid-induced cell activation is mediated by toll-like receptor 2. *J Biol Chem* 274, 17406-17409.
- Seth, R. B., Sun, L., Ea, C. K., and Chen, Z. J. (2005). Identification and characterization of MAVS, a mitochondrial antiviral signaling protein that activates NF-kappaB and IRF 3. *Cell* 122, 669-682.
- Seto, W. H., Tsang, D., Yung, R. W., Ching, T. Y., Ng, T. K., Ho, M., Ho, L. M., and Peiris, J. S. (2003). Effectiveness of precautions against droplets and contact in prevention of nosocomial transmission of severe acute respiratory syndrome (SARS). *Lancet* 361, 1519-1520.
- Sharma, S., tenOever, B. R., Grandvaux, N., Zhou, G. P., Lin, R., and Hiscott, J. (2003). Triggering the interferon antiviral response through an IKK-related pathway. *Science* 300, 1148-1151.
- Shieh, C. K., Soe, L. H., Makino, S., Chang, M. F., Stohlman, S. A., and Lai, M. M. (1987). The 5'-end sequence of the murine coronavirus genome: implications for multiple fusion sites in leader-primed transcription. *Virology* 156, 321-330.
- Sochorova, K., Horvath, R., Rozkova, D., Litzman, J., Bartunkova, J., Sediva, A., and Spisek, R. (2007). Impaired Toll-like receptor 8-mediated IL-6 and TNF-alpha production in antigen-presenting cells from patients with X-linked agammaglobulinemia. *Blood* 109, 2553-2556.
- Spaan, W., Delius, H., Skinner, M., Armstrong, J., Rottier, P., Smeekens, S., van der Zeijst, B. A., and Siddell, S. G. (1983). Coronavirus mRNA synthesis involves fusion of non-contiguous sequences. *Embo J* 2, 1839-1844.
- Spiegel, M., Pichlmair, A., Martinez-Sobrido, L., Cros, J., Garcia-Sastre, A., Haller, O., and Weber, F. (2005). Inhibition of Beta interferon induction by severe acute respiratory syndrome coronavirus suggests a two-step model for activation of interferon regulatory factor 3. *J Virol* 79, 2079-2086.
- Spiegel, M., Pichlmair, A., Muhlberger, E., Haller, O., and Weber, F. (2004). The antiviral effect of interferon-beta against SARS-coronavirus is not mediated by MxA protein. *J Clin Virol* 30, 211-213.
- Stauber, R., Pfleiderer, M., and Siddell, S. (1993). Proteolytic cleavage of the murine coronavirus surface glycoprotein is not required for fusion activity. *J Gen Virol* 74 (Pt 2), 183-191.
- Stegmann, T., Booy, F. P., and Wilschut, J. (1987a). Effects of low pH on influenza virus. Activation and inactivation of the membrane fusion capacity of the hemagglutinin. *J Biol Chem* 262, 17744-17749.

- Stegmann, T., Morselt, H. W., Scholma, J., and Wilschut, J. (1987b). Fusion of influenza virus in an intracellular acidic compartment measured by fluorescence dequenching. *Biochim Biophys Acta* *904*, 165-170.
- Stertz, S., Reichelt, M., Spiegel, M., Kuri, T., Martinez-Sobrido, L., Garcia-Sastre, A., Weber, F., and Kochs, G. (2007). The intracellular sites of early replication and budding of SARS-coronavirus. *Virology* *361*, 304-315.
- Stohlman, S. A., Baric, R. S., Nelson, G. N., Soe, L. H., Welter, L. M., and Deans, R. J. (1988). Specific interaction between coronavirus leader RNA and nucleocapsid protein. *J Virol* *62*, 4288-4295.
- Sturman, L. S., Holmes, K. V., and Behnke, J. (1980). Isolation of coronavirus envelope glycoproteins and interaction with the viral nucleocapsid. *J Virol* *33*, 449-462.
- Sturman, L. S., Ricard, C. S., and Holmes, K. V. (1985). Proteolytic cleavage of the E2 glycoprotein of murine coronavirus: activation of cell-fusing activity of virions by trypsin and separation of two different 90K cleavage fragments. *J Virol* *56*, 904-911.
- Subbarao, K. (1999). Influenza vaccines: present and future. *Adv Virus Res* *54*, 349-373.
- Subbarao, K., and Roberts, A. (2006). Is there an ideal animal model for SARS? *Trends Microbiol* *14*, 299-303.
- Subramaniam, S., Stansberg, C., and Cunningham, C. (2004). The interleukin 1 receptor family. *Dev Comp Immunol* *28*, 415-428.
- Sulea, T., Lindner, H. A., Purisima, E. O., and Menard, R. (2005). Deubiquitination, a new function of the severe acute respiratory syndrome coronavirus papain-like protease? *J Virol* *79*, 4550-4551.
- Sulea, T., Lindner, H. A., Purisima, E. O., and Menard, R. (2006). Binding site-based classification of coronaviral papain-like proteases. *Proteins* *62*, 760-775.
- Sumpter, R., Jr., Loo, Y. M., Foy, E., Li, K., Yoneyama, M., Fujita, T., Lemon, S. M., and Gale, M., Jr. (2005). Regulating intracellular antiviral defense and permissiveness to hepatitis C virus RNA replication through a cellular RNA helicase, RIG-I. *J Virol* *79*, 2689-2699.
- Suzuki, N., Suzuki, S., and Yeh, W. C. (2002). IRAK-4 as the central TIR signaling mediator in innate immunity. *Trends Immunol* *23*, 503-506.
- Tabeta, K., Georgel, P., Janssen, E., Du, X., Hoebe, K., Crozat, K., Mudd, S., Shamel, L., Sovath, S., Goode, J., et al. (2004). Toll-like receptors 9 and 3 as essential components of innate immune defense against mouse cytomegalovirus infection. *Proc Natl Acad Sci U S A* *101*, 3516-3521.
- Tabeta, K., Hoebe, K., Janssen, E. M., Du, X., Georgel, P., Crozat, K., Mudd, S., Mann, N., Sovath, S., Goode, J., et al. (2006). The Unc93b1 mutation 3d disrupts exogenous antigen presentation and signaling via Toll-like receptors 3, 7 and 9. *Nat Immunol* *7*, 156-164.

- Taguchi, F., Ikeda, T., Saeki, K., Kubo, H., and Kikuchi, T. (1993). Fusogenic properties of uncleaved spike protein of murine coronavirus JHMV. *Adv Exp Med Biol* 342, 171-175.
- Takahasi, K., Yoneyama, M., Nishihori, T., Hirai, R., Kumeta, H., Narita, R., Gale, M., Jr., Inagaki, F., and Fujita, T. (2008). Nonself RNA-sensing mechanism of RIG-I helicase and activation of antiviral immune responses. *Mol Cell* 29, 428-440.
- Takaoka, A., Wang, Z., Choi, M. K., Yanai, H., Negishi, H., Ban, T., Lu, Y., Miyagishi, M., Kodama, T., Honda, K., et al. (2007). DAI (DLM-1/ZBP1) is a cytosolic DNA sensor and an activator of innate immune response. *Nature* 448, 501-505.
- Takaoka, A., Yanai, H., Kondo, S., Duncan, G., Negishi, H., Mizutani, T., Kano, S., Honda, K., Ohba, Y., Mak, T. W., and Taniguchi, T. (2005). Integral role of IRF-5 in the gene induction programme activated by Toll-like receptors. *Nature* 434, 243-249.
- Takeuchi, O., and Akira, S. (2007). [Pathogen recognition by innate immunity]. *Arerugi* 56, 558-562.
- Takeuchi, O., Hoshino, K., Kawai, T., Sanjo, H., Takada, H., Ogawa, T., Takeda, K., and Akira, S. (1999a). Differential roles of TLR2 and TLR4 in recognition of gram-negative and gram-positive bacterial cell wall components. *Immunity* 11, 443-451.
- Takeuchi, O., Kawai, T., Sanjo, H., Copeland, N. G., Gilbert, D. J., Jenkins, N. A., Takeda, K., and Akira, S. (1999b). TLR6: A novel member of an expanding toll-like receptor family. *Gene* 231, 59-65.
- Theofilopoulos, A. N., Baccala, R., Beutler, B., and Kono, D. H. (2005). Type I interferons (alpha/beta) in immunity and autoimmunity. *Annu Rev Immunol* 23, 307-336.
- Thiel, V., Ivanov, K. A., Putics, A., Hertzog, T., Schelle, B., Bayer, S., Weissbrich, B., Snijder, E. J., Rabenau, H., Doerr, H. W., et al. (2003). Mechanisms and enzymes involved in SARS coronavirus genome expression. *J Gen Virol* 84, 2305-2315.
- Ting, J. P., Lovering, R. C., Alnemri, E. S., Bertin, J., Boss, J. M., Davis, B. K., Flavell, R. A., Girardin, S. E., Godzik, A., Harton, J. A., et al. (2008). The NLR gene family: a standard nomenclature. *Immunity* 28, 285-287.
- Tohyama, M., Dai, X., Sayama, K., Yamasaki, K., Shirakata, Y., Hanakawa, Y., Tokumaru, S., Yahata, Y., Yang, L., Nagai, H., et al. (2005). dsRNA-mediated innate immunity of epidermal keratinocytes. *Biochem Biophys Res Commun* 335, 505-511.
- Tooze, J., Tooze, S., and Warren, G. (1984). Replication of coronavirus MHV-A59 in sac- cells: determination of the first site of budding of progeny virions. *Eur J Cell Biol* 33, 281-293.
- Tooze, J., and Tooze, S. A. (1985). Infection of AtT20 murine pituitary tumour cells by mouse hepatitis virus strain A59: virus budding is restricted to the Golgi region. *Eur J Cell Biol* 37, 203-212.

- Treanor, J. J., Hayden, F. G., Vrooman, P. S., Barbarash, R., Bettis, R., Riff, D., Singh, S., Kinnersley, N., Ward, P., and Mills, R. G. (2000). Efficacy and safety of the oral neuraminidase inhibitor oseltamivir in treating acute influenza: a randomized controlled trial. US Oral Neuraminidase Study Group. *Jama* *283*, 1016-1024.
- Tscherne, D. M., Jones, C. T., Evans, M. J., Lindenbach, B. D., McKeating, J. A., and Rice, C. M. (2006). Time- and temperature-dependent activation of hepatitis C virus for low-pH-triggered entry. *J Virol* *80*, 1734-1741.
- Twu, K. Y., Noah, D. L., Rao, P., Kuo, R. L., and Krug, R. M. (2006). The CPSF30 binding site on the NS1A protein of influenza A virus is a potential antiviral target. *J Virol* *80*, 3957-3965.
- van der Hoek, L., Pyrc, K., Jebbink, M. F., Vermeulen-Oost, W., Berkhout, R. J., Wolthers, K. C., Wertheim-van Dillen, P. M., Kaandorp, J., Spaargaren, J., and Berkhout, B. (2004). Identification of a new human coronavirus. *Nat Med* *10*, 368-373.
- van der Most, R. G., Bredenbeek, P. J., and Spaan, W. J. (1991). A domain at the 3' end of the polymerase gene is essential for encapsidation of coronavirus defective interfering RNAs. *J Virol* *65*, 3219-3226.
- Venkataraman, T., Valdes, M., Elsby, R., Kakuta, S., Caceres, G., Saijo, S., Iwakura, Y., and Barber, G. N. (2007). Loss of DExD/H box RNA helicase LGP2 manifests disparate antiviral responses. *J Immunol* *178*, 6444-6455.
- Vennema, H., Godeke, G. J., Rossen, J. W., Voorhout, W. F., Horzinek, M. C., Opstelten, D. J., and Rottier, P. J. (1996). Nucleocapsid-independent assembly of coronavirus-like particles by co-expression of viral envelope protein genes. *Embo J* *15*, 2020-2028.
- Wagner, H. (2004). The immunobiology of the TLR9 subfamily. *Trends Immunol* *25*, 381-386.
- Wakita, T., Pietschmann, T., Kato, T., Date, T., Miyamoto, M., Zhao, Z., Murthy, K., Habermann, A., Krausslich, H. G., Mizokami, M., et al. (2005). Production of infectious hepatitis C virus in tissue culture from a cloned viral genome. *Nat Med* *11*, 791-796.
- Wang, C., Deng, L., Hong, M., Akkaraju, G. R., Inoue, J., and Chen, Z. J. (2001). TAK1 is a ubiquitin-dependent kinase of MKK and IKK. *Nature* *412*, 346-351.
- Wang, Y., Zhang, H. X., Sun, Y. P., Liu, Z. X., Liu, X. S., Wang, L., Lu, S. Y., Kong, H., Liu, Q. L., Li, X. H., et al. (2007). Rig-I-/- mice develop colitis associated with downregulation of G alpha i2. *Cell Res* *17*, 858-868.
- Wang, Y. Y., Li, L., Han, K. J., Zhai, Z., and Shu, H. B. (2004). A20 is a potent inhibitor of TLR3- and Sendai virus-induced activation of NF-kappaB and ISRE and IFN-beta promoter. *FEBS Lett* *576*, 86-90.
- Wang, Z., Choi, M. K., Ban, T., Yanai, H., Negishi, H., Lu, Y., Tamura, T., Takaoka, A., Nishikura, K., and Taniguchi, T. (2008). Regulation of innate immune responses by DAI

(DLM-1/ZBP1) and other DNA-sensing molecules. *Proc Natl Acad Sci U S A* **105**, 5477-5482.

Watanabe, T., Watanabe, S., Shinya, K., Kim, J. H., Hatta, M., and Kawaoka, Y. (2009). Viral RNA polymerase complex promotes optimal growth of 1918 virus in the lower respiratory tract of ferrets. *Proc Natl Acad Sci U S A* **106**, 588-592.

Webster, R. G., Bean, W. J., Gorman, O. T., Chambers, T. M., and Kawaoka, Y. (1992). Evolution and ecology of influenza A viruses. *Microbiol Rev* **56**, 152-179.

Wesley, R. D., Woods, R. D., and Cheung, A. K. (1991). Genetic analysis of porcine respiratory coronavirus, an attenuated variant of transmissible gastroenteritis virus. *J Virol* **65**, 3369-3373.

Whittaker, G. R., and Helenius, A. (1998). Nuclear import and export of viruses and virus genomes. *Virology* **246**, 1-23.

Williams, R. K., Jiang, G. S., and Holmes, K. V. (1991). Receptor for mouse hepatitis virus is a member of the carcinoembryonic antigen family of glycoproteins. *Proc Natl Acad Sci U S A* **88**, 5533-5536.

Wong, R. S., Wu, A., To, K. F., Lee, N., Lam, C. W., Wong, C. K., Chan, P. K., Ng, M. H., Yu, L. M., Hui, D. S., *et al.* (2003). Haematological manifestations in patients with severe acute respiratory syndrome: retrospective analysis. *Bmj* **326**, 1358-1362.

Wong, T. W., and Tam, W. W. (2005). Handwashing practice and the use of personal protective equipment among medical students after the SARS epidemic in Hong Kong. *Am J Infect Control* **33**, 580-586.

Woo, K., Joo, M., Narayanan, K., Kim, K. H., and Makino, S. (1997). Murine coronavirus packaging signal confers packaging to nonviral RNA. *J Virol* **71**, 824-827.

Woo, P. C., Lau, S. K., Chu, C. M., Chan, K. H., Tsui, H. W., Huang, Y., Wong, B. H., Poon, R. W., Cai, J. J., Luk, W. K., *et al.* (2005a). Characterization and complete genome sequence of a novel coronavirus, coronavirus HKU1, from patients with pneumonia. *J Virol* **79**, 884-895.

Woo, P. C., Lau, S. K., Huang, Y., Tsui, H. W., Chan, K. H., and Yuen, K. Y. (2005b). Phylogenetic and recombination analysis of coronavirus HKU1, a novel coronavirus from patients with pneumonia. *Arch Virol* **150**, 2299-2311.

Xu, L. G., Wang, Y. Y., Han, K. J., Li, L. Y., Zhai, Z., and Shu, H. B. (2005). VISA is an adapter protein required for virus-triggered IFN-beta signaling. *Mol Cell* **19**, 727-740.

Yamamoto, M., and Akira, S. (2004). [TIR domain-containing adaptors regulate TLR-mediated signaling pathways]. *Nippon Rinsho* **62**, 2197-2203.

Yamamoto, M., Takeda, K., and Akira, S. (2004). TIR domain-containing adaptors define the specificity of TLR signaling. *Mol Immunol* **40**, 861-868.

- Yang, H., Lin, C. H., Ma, G., Baffi, M. O., and Wathelet, M. G. (2003). Interferon regulatory factor-7 synergizes with other transcription factors through multiple interactions with p300/CBP coactivators. *J Biol Chem* 278, 15495-15504.
- Yang, H., Ma, G., Lin, C. H., Orr, M., and Wathelet, M. G. (2004). Mechanism for transcriptional synergy between interferon regulatory factor (IRF)-3 and IRF-7 in activation of the interferon-beta gene promoter. *Eur J Biochem* 271, 3693-3703.
- Yang, K., Puel, A., Zhang, S., Eidenschenk, C., Ku, C. L., Casrouge, A., Picard, C., von Bernuth, H., Senechal, B., Plancoulaine, S., *et al.* (2005). Human TLR-7-, -8-, and -9-mediated induction of IFN-alpha/beta and -lambda Is IRAK-4 dependent and redundant for protective immunity to viruses. *Immunity* 23, 465-478.
- Yi, M., Ma, Y., Yates, J., and Lemon, S. M. (2007). Compensatory mutations in E1, p7, NS2, and NS3 enhance yields of cell culture-infectious intergenotypic chimeric hepatitis C virus. *J Virol* 81, 629-638.
- Yi, M., Villanueva, R. A., Thomas, D. L., Wakita, T., and Lemon, S. M. (2006). Production of infectious genotype 1a hepatitis C virus (Hutchinson strain) in cultured human hepatoma cells. *Proc Natl Acad Sci U S A* 103, 2310-2315.
- Yoneyama, M., and Fujita, T. (2004a). [RIG-I: critical regulator for virus-induced innate immunity]. *Tanpakushitsu Kakusan Koso* 49, 2571-2578.
- Yoneyama, M., and Fujita, T. (2004b). [Virus-induced expression of type I interferon genes]. *Uirusu* 54, 161-167.
- Yoneyama, M., and Fujita, T. (2009). RNA recognition and signal transduction by RIG-I-like receptors. *Immunol Rev* 227, 54-65.
- Yoneyama, M., Kikuchi, M., Natsukawa, T., Shinobu, N., Imaizumi, T., Miyagishi, M., Taira, K., Akira, S., and Fujita, T. (2004). The RNA helicase RIG-I has an essential function in double-stranded RNA-induced innate antiviral responses. *Nat Immunol* 5, 730-737.
- Yount, B., Roberts, R. S., Sims, A. C., Deming, D., Frieman, M. B., Sparks, J., Denison, M. R., Davis, N., and Baric, R. S. (2005). Severe acute respiratory syndrome coronavirus group-specific open reading frames encode nonessential functions for replication in cell cultures and mice. *J Virol* 79, 14909-14922.
- Yu, I. T., Li, Y., Wong, T. W., Tam, W., Chan, A. T., Lee, J. H., Leung, D. Y., and Ho, T. (2004). Evidence of airborne transmission of the severe acute respiratory syndrome virus. *N Engl J Med* 350, 1731-1739.
- Yu, X., Bi, W., Weiss, S. R., and Leibowitz, J. L. (1994). Mouse hepatitis virus gene 5b protein is a new virion envelope protein. *Virology* 202, 1018-1023.
- Yuan, P., Bartlam, M., Lou, Z., Chen, S., Zhou, J., He, X., Lv, Z., Ge, R., Li, X., Deng, T., *et al.* (2009). Crystal structure of an avian influenza polymerase PA(N) reveals an endonuclease active site. *Nature* 458(7240), 909-913.

- Zak, D. E., and Aderem, A. (2009). Systems biology of innate immunity. *Immunol Rev* 227, 264-282.
- Zhang, S. Y., Jouanguy, E., Ugolini, S., Smahi, A., Elain, G., Romero, P., Segal, D., Sancho-Shimizu, V., Lorenzo, L., Puel, A., *et al.* (2007). TLR3 deficiency in patients with herpes simplex encephalitis. *Science* 317, 1522-1527.
- Zhirnov, O. P., and Klenk, H. D. (2007). Control of apoptosis in influenza virus-infected cells by up-regulation of Akt and p53 signaling. *Apoptosis* 12, 1419-1432.
- Zhong, J., Gastaminza, P., Cheng, G., Kapadia, S., Kato, T., Burton, D. R., Wieland, S. F., Uprichard, S. L., Wakita, T., and Chisari, F. V. (2005). Robust hepatitis C virus infection in vitro. *Proc Natl Acad Sci U S A* 102, 9294-9299.
- Zhou, H., and Perlman, S. (2007). Mouse hepatitis virus does not induce Beta interferon synthesis and does not inhibit its induction by double-stranded RNA. *J Virol* 81, 568-574.
- Ziebuhr, J. (2004). Molecular biology of severe acute respiratory syndrome coronavirus. *Curr Opin Microbiol* 7, 412-419.
- Ziebuhr, J. (2005). The coronavirus replicase. *Curr Top Microbiol Immunol* 287, 57-94.
- Ziebuhr, J. (2006). The coronavirus replicase: insights into a sophisticated enzyme machinery. *Adv Exp Med Biol* 581, 3-11.

## **BIOSKETCH (VITA)**

Santhana Gowri Thangavelu Devaraj (Gowri) was born in Chitoor, Southern India on March 24, 1974 to Kasturi and Devaraj Pillai. Gowri earned her bachelor's and Master's degrees from Sri Venkateswara University, Tirupathi specializing in virology. She worked on nucleocapsid assembly of Morbilli virus (PPRV) with Prof. M.S. Sheila at Indian Institute of science (IISC) Bangalore as part of her master's dissertation project. During this time she met her husband Lokesh Rao. Gowri came to Galveston with her husband and her daughter Yogapriya and continued her research interests with Dr. Andres Oberhauser at UTMB. She joined the graduate school of UTMB in 2004. She worked on innate immune evasion mediated by Severe Acquired Respiratory Syndrome Virus (SARS-CoV) and Hepatitis C Virus (HCV) under the supervision of Dr. Kui Li. Gowri joined Dr. Erich Hoffmann's Lab at Galveston National Laboratory after her supervisor moved to Memphis and she now continues her studies on innate immune evasion mediated by influenza. Her Ph.D dissertation discusses the molecular mechanisms by which viruses can evade host innate immune response. During her graduate study at UTMB, She has received travel awards from McLaughlin endowment fund (2007) and annual meeting travel award from the American society for Virology (2008).

### Education

B.S., 1993-1996, Sri Venkateswara University Tirupathi INDIA  
M.S., 1996-1998, Sri Venkateswara University Tirupathi INDIA

### Publications

**Devaraj SG**, Wang N, Chen Z, Chen Z, Tseng M, Barreto N, Lin R, Peters CJ, Tseng CT, Baker SC, Li K. *Regulation of IRF3-dependent innate immunity by the papain-like protease domain of the severe acute respiratory syndrome coronavirus*. J Biol Chem. 2007 Nov 2; 282(44):32208-21.

Chen Z, Rijnbrand R, Jangra RK, **Devaraj SG**, Qu L, Ma Y, Lemon SM, Li K. *Ubiquitination and proteasomal degradation of interferon regulatory factor-3 induced by Npro from a cytopathic bovine viral diarrhea virus*. Virology. 2007 Sep 30;366(2):277-92.

Anindya R, Joseph J, **Gowri TD**, Savithri HS. *Complete genomic sequence of Pepper vein banding virus (PVBV): a distinct member of the genus Potyvirus.* Arch Virol. 2004 Mar;149(3):625-32.

Sangita V, Parthasarathy S, Toma S, Lokesh GL, **Gowri T.D.** Satheshkumar PS, Savithri HS, Murthy MRN. *Determination of the structure of the recombinant T=1 capsid of Sesbania mosaic virus.* Curr Sci. 2002; 82(9):1123-31.

Lokesh GL, **Gowri TD**, Satheshkumar PS, Murthy MR, Savithri HS. [A molecular switch in the capsid protein controls the particle polymorphism in an icosahedral virus.](#) Virology. 2002 Jan 20; 292(2):211-23.

#### SUMMARY OF DISSERTATION

One of the first and fast line of defense launched by mammalian hosts to counter virus infection is production of type I interferon (IFN), an innate immune response that generates antiviral state to prevent virus replication and spread by expressing several IFN-stimulated genes. Type I interferon response depends on a set of germ-line encoded receptors called pattern recognition receptors (PRRs) that initiate antiviral signaling upon recognizing distinct pathogen associated molecular patterns (PAMPs). TLR3, RIG-I and MDA5, trigger complex intertwined signaling pathways in response to viral dsRNA leading to the activation of interferon regulatory transcription factors IRF3, IRF7 and NF- $\kappa$ B. These transcription factors mediate inflammatory process to clear virus infection. Viruses can evade host antiviral defenses by using several strategies. SARS coronavirus (SARS-CoV), a highly contagious causative agent of severe acute respiratory syndrome does not induce interferon response suggesting an unknown immune evasive mechanism. My experiments demonstrate that papain-like protease (PLpro) encoded by SARS-CoV is a potent interferon antagonist that functions independent of its protease activity. PLpro directly interacts with IRF-3 preventing its phosphorylation, dimerization, nuclear translocation and thus inhibits type I interferon response triggered by TLR3/RIG-I pathways. Hepatitis C virus is a major blood borne pathogen responsible for 100,000 deaths worldwide annually due to chronic liver cirrhosis. In cell culture normal human hepatocytes are not permissive to HCV replication due to intact TLR3/RIG-I/MDA5 antiviral signaling pathways. However, human hepatoma cells defective in antiviral signal pathways are found to permit HCV replication. My experiments involving reconstitution of functional TLR3 signaling pathways in human heptoma cells demonstrate that TLR3 plays a major role in HCV cellular permissiveness. Finally, my studies with influenza virus NS1 protein demonstrate that NS1 antagonizes the IFN response by blocking RIG-I activation in a strain specific manner. In conclusion, I have made an attempt to understand the complex antiviral signaling pathways at the cellular level in context to three distinct single strand RNA viruses namely, SARS-CoV, HCV and Influenza virus. Though, these viruses are detected by the same set of PRRs to trigger

antiviral signaling, the mechanism by which they evade antiviral response appears to be distinct.

Permanent address: 1003 Ash Pointe League City Texas 77573

This dissertation was typed by Santhana G. T. Devaraj.